REGIONALIZATION OF THE DEVELOPING MOUSE TELENCEPHALON:

CELLULAR AND MOLECULAR MECHANISMS

Dissertation der Fakultät für Biologie der Ludwig-Maximilian-Universität München
Eingereicht am 25. März 2002

Gutachter:

Prof. G. Boyan
Dr. M. Götz

Mündliche Prüfung am 01.Oktober 2002

TABLE OF CONTENTS

		Page
SUMMARY		5
INTRODUCTION		6
MATERIALS AND METHODS		13
	Animals	13
	EGFP-adenovirus injections	14
	Migration analysis	14
	Dissociated cell cultures and immuncytochemistry	14
	Immunohistochemistry	15
	Time-lapse study	15
	In vitro transplantations	16
	Plasmid preparation and in vitro transcription	16
	X-Gal histochemistry	18
	In-situ hybridization	19
	Gap junctions filling	21
RESULTS		
I-	Asymmetric migration across the cortico-striatal boundary in wild type mice	22
	I-A- EGFP-adenovirus injections in cortex and GE	22
	I-A-1 Control experiments and slice morphology	22
	I-A-2 Restriction of cortical cell migration	24
	I-A-3 Migration of GE cells into the cortex	24
	Tables 1-3	24
	I-B- Time-lapse study	27
	I-C- Transplantation experiments	29
II-	Enhanced migration across the cortico-striatal boundary in the *Pax6* mutant	34
	II-A- Enhanced cell migration from the GE into the cortex	34
	II-B- Tangential migration in vivo	35
	II-C- Enhanced migration of cortical cells	36
	II-D- Molecular changes affecting the *Sey/Sey* boundary	37
III-	Enhanced dorsal to ventral Migration across the cortico-striatal boundary in the *Ngn*2 mutant	39
	III-A- Ectopic cells in the GE of homozygous *Ngn2* ^{LacZ} mice	39
	III-B- Dorso-ventral cell migration from the cortex into the GE in homozygous *Ngn2*^{LacZ} mice	41
	III-C- Cellular and molecular changes at the boundary between cortex and GE in homozygous *Ngn2* ^{LacZ} mice	43
	III-D- Non-cell autonomous effects on cell migration in the *Ngn2-/-* telencephalon	44

III-E- Fate change of ectopic cells in the GE of *Ngn2*^{LacZ} mice 45

IV- Comparison between *Pax6* mutant and *Ngn2* mutant 47

V- Gap junction uncoupling at the cortico-striatal boundary: another aspect of regionalization 49
IV-A- Control experiments 49
IV-B- Uncoupling of cells in the cortico-striatal boundary 50
IV-C- No uncoupling in the Small-eye mutant boundary 51

FIGURE APPENDIX (Fig.1- Fig.17)

DISCUSSION 53

ACKNOWLEDGMENTS 61

REFERENCES 62

CURRICULUM VITAE 67

SUMMARY

This work is concerned with the delineation of two adjacent regions within the developing telencephalon: the dorsally located cerebral cortex and the ventrally located ganglionic eminence (abbreviated GE). The GE gives rise to the mature striatum and other basal ganglia. During embryonic development, the cortex and the GE express distinct transcription factors, creating a sharp gene expression border between them. This is the emergence of the so-called cortico-striatal boundary. Since other boundaries in the embryo have the property to hinder the migration of cells, we have studied the permeability of the cortico-striatal boundary to the migration of cortical and GE cells. In the first part of this study we have found that the cortico-striatal boundary restricts cell migration in an asymmetrical way, preventing cortical cells from entering into the GE while enabling many cells to migrate from GE into the cortex. In the following parts of this work, we sought to understand the molecular mechanisms promoting this asymmetry. For this we studied two mouse mutants where a transcription factor specifically expressed in the cortex and in the boundary region was missing. In the Neurogenin2 mutant mouse, the migration of cortical cells into the GE was increased in a non-cell-autonomous way, revealing a role for *Ngn2* in making the boundary impermeable to cortical cells. In the *Pax6* mutant Small-eye, where Neurogenin2 is absent, both the migration of cortical cells and the migration of GE cells across the boundary were increased. The enhanced migration from the GE into the cortex hence revealed a role of *Pax6* in partially restricting the migration of GE cells. The comparison of both mutants and their diverse molecular alterations allowed us to draw some conclusions about the nature of the signals promoting the asymmetry of migration across the boundary. These are developed in the discussion. Finally, the fifth part of this study deals with another feature of developmental boundaries, concerning the coupling of cells via gap junctions and their uncoupling at boundaries. We showed that the cortico-striatal boundary interrupts cell coupling, whereas in the *Pax6* mutant, cells between the cortex and the GE retain their communication via gap junctions.

INTRODUCTION

Regionalization is a process that occurs during the embryonic phase of development throughout the embryo, allowing distinct compartments to arise next to each other, in order to give rise to neighboring organs. This phenomenon of regionalization requires the formation of boundaries at the interface between groups of cells. It involves several molecular and cellular mechanisms that have been partly studied in different animal models and different parts of the body. In order to understand the context of this study, it is important to first consider the partial conservation of those mechanisms at the different boundaries along the body and throughout evolution. Six examples will be next briefly introduced.

-1- In the drosophila embryo, 14 segments arise along the antero-posterior axis of the body that are subdivided in anterior and posterior compartments. The formation of boundaries between segments involves segment polarity genes being expressed distinctly in anterior and posterior compartment cells. The transcription factor Engrailed (En) is expressed in posterior cells of a segment, driving the expression of the signaling molecule Hedgehog (Hh). Posterior cells themselves cannot respond to Hh as a result of the repression by En of a transcription factor mediating the response to Hh, Cubitus interruptus (Ci). In contrast, anterior compartment cells express Ci and respond to Hh by first activating Ci and then expressing other signaling molecules, such as Decapentaplegic (Dpp) and Wingless (Wg). The differential transcriptional activity of Ci and En on both sides of the border results in an affinity boundary, where cells from both segments segregate from each other. A mechanism achieving this cell segregation has been proposed, in which the opposing transcriptional activities of En and Ci would regulate a single cell adhesion molecule. (Dahmann and Basler, 2000).

-2- The drosophila embryo is also compartimentalized along its dorso-ventral axis, as for example in the wing imaginal disc. The mechanisms acting at this dorso-ventral boundary, involving the Notch signaling pathway, are very similar to the one governing the positioning of the apical ectodermal ridge (AER) in vertebrates, which separates the presumptive dorsal and ventral side of the limb bud. Fringe is a secreted glycosyltransferase that modulates the activity of the Notch receptor (Moloney et al., 2000, Bruckner et al., 2000) by rendering Notch more sensitive to its ligand Delta and less sensitive to its ligand Serrate (Panin et al., 1997). In Drosophila, the dorsal expression of Fringe and serrate, and the ventral expression of Delta creates a

restricted territory of Notch signaling within a narrow band of cells at the dorso-ventral boundary. As a result, boundary cells are specified to express Wingless and organize the wing growth and patterning. Furthermore, by positioning a Notch signaling stripe, the activity of Fringe creates a boundary of cell segregation (Rauskolb et al., 1999). However, two transmembrane proteins expressed dorsally, Capricious and Tartan, have also been shown to be responsible for the specific affinity of dorsal cells and their segregation from the ventral compartment (Milan et al. 2001). In vertebrates as well, R-Fringe, expressed by dorsal cells, has a positioning function of the dorso-ventral boundary of the limb bud. The AER has been shown to form wherever a tissue expressing Fringe abuts a tissue not expressing Fringe (Rodriguez-Esteban et al., 1997, Laufer et al., 1997). Unlike at the drosophila wing dorso-ventral boundary, but like in the drosophila posterior compartment cells, the transcription factor Engrailed-1 is expressed by ventral cells lining the vertebrate AER, where it represses Fringe expression. As a result of the molecular interactions, the AER is a cell lineage boundary, preventing cells from the dorsal and ventral compartment to intermingle (Kimmel et al., 2000, Altabef et al.,2000).

-3- Segmentation of the mesoderm along the antero-posterior axis in vertebrates gives rise to the somites, transient structures that will later give rise to the vertebrae and skeletal muscles. As for the AER and the dorso-ventral drosophila wing margin, the mechanisms of segmentation of the presomitic mesoderm involve signaling interactions through the Notch pathway. The Notch modulating molecule L-fringe is expressed within the border between two somites and is required for their proper segmentation (Zhang and Gridley, 1998). Other molecular interactions of the Notch pathway allowing this segmentation to occur have been identified. For instance the basic Helix-Loop-Helix (bHLH) transcription factor Mesp2 is expressed anteriorly in the presumptive somites, and inhibits the transcription of the Notch ligand Delta-like-1 (Dll1), by inhibiting the Presenillin mediated Notch signaling pathway. (Presenilin is an intracellular membrane bound protein allowing the translocation of Notch to the nucleus). In posterior cells, presenilin is active and Dll1 is expressed (Takahashi et al., 2000). Thus, signaling activity of Notch and the distinct molecular cascades used in the presumptive anterior and posterior halves of the somite play a role in the segmentation of the presomitic mesoderm. Additionally, the Notch signaling pathway also regulates the expression of cell adhesion molecules in the forming somites. For example PAPC, a member of the protocadherin family of cell adhesion molecules, is expressed anteriorly under the control of Mesp2 (Kim et. al., 2000). The Eph receptor tyrosine

kinase EphA4 is as well expressed anteriorly under the control of Notch pathway molecules, whereas ephrinB2 is expressed posteriorly (Barrantes et al., 1999; Durbin et al., 2000). The differential expression of Eph receptors and their ephrin ligands in neighboring compartments has been indeed shown to promote the segregation of cell groups (Mellitzer et al., 1999).

Besides the different boundaries segmenting the vertebrate body, the brain itself is also segmented and contains boundaries that delineate several regions along the antero-posterior and the ventro-dorsal axis.

-4- The mid-hindbrain boundary (MHB) separates the developing hindbrain from the developing midbrain. At early neural plate stages, this boundary is visible as a switch between the expression of the transcription factors Otx2 in the midbrain, and Gbx2 in the hindbrain. The expression of molecules such as Pax2, En1, Wnt1 and FGF8 is induced at the interface between Otx2 and Gbx2 expressing cells and these molecules in turn organize the development of both adjacent regions (Rhinn and Brand, 2001; Wurst and Bally-Cuif, 2001). Hence, the mid-hindbrain boundary is also called mid-hindbrain organizer. The interface between Otx2 and Gbx2 expressing cells is a sharp border. However, cells in the two adjacent compartments have revealed no difference in adhesive properties, and the boundary does not restrict cell migration, as shown by an in vitro aggregation assay and by cell lineage analysis (Jungbluth et al., 2001). Instead of a restricted migration, cells are believed to be able to change their fate rapidly when they cross the mid-hindbrain boundary.

-5- In the diencephalon, the Zona Limitans Intrathalamica (ZLI) appears at early developmental stages as a wide territory, detectable as a region negative for L-fringe expression, at the junction between prechordal and epichordal neuraxis. This territory later narrows and becomes a thin boundary between the ventral and the dorsal thalamus. On each side of the ZLI, cells are lineage restricted within their compartment (Figdor and Stern, 1993). The expression of L-fringe on both sides, but not inside the ZLI, has been shown to prevent the mixing of ZLI cells with the surrounding cells, probably as a result of the Notch pathway activation. (Zeltser et al., 2001).

-6- The hindbrain is divided into 7 rhombomeres separated on the antero-posterior axis by the inter-rhombomeric boundaries. These boundaries have been very well studied and several cellular and molecular mechanisms have been described in those

regions. At early developmental stages, the differential expression of transcription factors in odd and even rhombomeres induces directly the expression of different cell adhesion molecules. For exemple the zinc-finger transcription factor Krox20 in rhombomeres 3 and 5 induces the expression of EphA4 (Theil et al., 1998). As a consequence, the interaction of Eph receptors and their ligands in alternating rhombomeres promotes cell segregation at the borders by a mechanism of repulsion (Mellitzer et al., 1999; Xu et al., 1999, Xu and Wilkinson, 1997). Within the boundary region, the cells reveal the particularity of dividing slower than the cells inside the rhombomeres (Guthrie et al., 1991). These boundary cells specialize into radial glia cells, whose fibers form a fascicle. The presence of this fascicle is however not crucial for the segregation of the cells at the border (Nittenberg et al., 1997). Finally, despite a strong level of cell segregation at the borders between rhombomeres, a small percentage of cells is still able to migrate from one rhombomere into the next (Birgbauer and Fraser, 1994). Another mechanism involved in the delineation of the adjacent rhombomeres is the reduction of intercellular communication through gap junction: cells within rhombomeres are coupled via gap junctions, allowing the passage of mRNA and calcium ions for example, however, this communication is interrupted at boundaries (Martinez et al., 1992).

These examples reveal that the same molecules and signaling pathways come into play at the diverse boundaries segmenting embryos. Molecules of the Notch pathway promote the exact positioning of cell-cell signaling at borders. The interaction between the Notch receptor and the ligands Delta and Serrate mediates both cell adhesion and cell-cell signaling, inducing for example the expression of Wnt signaling molecules that control the growth of the tissues. The Notch signaling pathway can also induce the expression of cell adhesion molecules, such as PAPC or Eph receptors. Notch signaling pathway is implicated in the dorso-ventral wing margin, in the apical ectodermal ridge, in the somite borders, at the ZLI and also at the rhombomere boundaries (where Fringe is expressed, Johnston et al., 1997) and thus seems to be a universal mechanism acting at boundary formation. The organization of the abutting regions controlled by Wnt signaling is also found in most of the boundaries, also independently of Notch, like in the antero-posterior compartmentalization of the drosophila embryo or at the mid-hindbrain boundary. Eph receptor tyrosine kinases and the ephrin receptors, which operate as signaling molecules and cell adhesion molecules at the same time, also seem to be involved in the formation of several boundaries, promoting the segregation of cells (for example at the somite and

rhombomere boundaries). Thus, boundaries seem to use common molecular mechanisms that allow common cellular mechanisms to take place, such as restriction of cell migration and growth of the abutting tissues. Signaling activity at borders and/or distinct affinity properties between groups of cells seem to promote at almost every boundary the segregation of cells into the distinct regions.

In this work, we focused our attention on a particular dorso-ventral boundary in the developing murine forebrain: the cortico-striatal boundary. This boundary delineates the developing cerebral cortex, dorsally located, from the developing ganglionic eminence (GE), ventrally located. The GE comprises the medial ganglionic eminence (MGE) and the lateral ganglionic eminence (LGE). As the GE will later give rise to the basal ganglia, and in particular the LGE to the striatum (Olsson et al., 1995), the boundary is called cortico-striatal boundary. Both regions, cortex and GE, are located in the telencephalon which is part of the forebrain and is the anteriormost part of the vertebrate brain. The mature cortex will be involved in information processing, and the mature striatum in the control of movements. Both regions are endowed with different neuronal cell type composition, and different cytoarchitecture. The cortex contains 80% of excitatory glutamatergic projecting neurons and 20% of inhibitory gabaergic interneurons (Peters and Jones 1984), and the neurons are ordered in 6 layers, from the ventricular surface to the pial surface. On the other side of the boundary, the striatum contains mostly inhibitory gabaergic neurons (Gerfen, 1992) that are organized in nuclei instead of layers. It is therefore interesting to study how the cortex and striatum are delineated, and how they acquire their different phenotype during development.

At around embryonic day 9 (E9), before neurogenesis starts in the telencephalic vesicle, the cortico-striatal boundary appears as a gene expression border. Transcription factors like *Pax6*, *Otx1* and -2, *Emx1* and -2, *Ngn1* and -*2* are expressed within the cortex, with a sharp border to the negative GE. Conversly, transcription factors like *Dlx1*, -*2* and -*5*, *Mash1* are expressed in the GE but not in the cortex. Other genes, coding for cell adhesion molecules, are also expressed in a region specific manner, like R-cadherin in the cortex. From around embryonic day 13, the cortico-striatal boundary is then also characterized by a fascicle of radial glial cells, which spans from the sulcus, at the surface of the ventricle, to the pial surface. Figure 1A illustrates the above description, depicting an E14 coronal section through the telencephalon, with the cortex, the GE, and the cortico-striatal boundary in between.

The expression territory of several transcription factors is represented in color. Figure1B shows the radial glia fascicle of the cortico-striatal boundary, stained by a monoclonal antibody that recognizes specifically these cells.

As described above, a mechanism often involved in the delineation of adjacent regions is the restriction of cell migration. We were therefore interested to study the regionalization of the telencephalon under the aspect of cell migration, and first verified whether the cortico-striatal boundary represents a migrational restriction boundary as well. A previous study had shown that cells isolated from both regions segregate from each other in a short-term aggregation assay (Götz et al. 1996). It had been also shown that ventricular zone cells of the cortex do not migrate across the boundary into the GE (Fishell et al., 1993). In contrast, other studies had shown in a different culture system that GE cells could enter into the cortex (Anderson et al., 1997; Tamamaki et al., 1997). But the migration across the cortico-striatal boundary had not been studied in both directions in a single assay.

In the first part of this work, we showed that the migration across the cortico-striatal boundary in wild type mice is asymmetrical, allowing GE cells to enter the cortex, but hindering cortical cells to enter into the GE. For this, we used several experimental paradigms. First, injections of green fluorescent protein (GFP) containing adenovirus in telencephalic slices allowed the tracing of a small group of cells and the analysis of their migration over 48 hours in culture. These experiments revealed the strong restriction of cortical cell migration, and a certain degree of restriction of the GE cells in their migration into the cortex. Then, time-lapse recording experiments were performed, using transgenic mice that express GFP in neurons, in order to study the movements of the cells approaching the cortico-striatal boundary. Finally, transplantations in slice culture were performed in order to examine whether the ability to cross the cortico-striatal boundary is cell autonomous, or substrate dependent.

In order to further understand which molecular mechanisms make the boundary asymmetric in its permeability, we studied two mouse mutants in which transcription factors expressed specifically in the cortex and in the boundary were missing. The second part of this work hence describes the study of the Small-Eye mouse, a naturally occurring mutant in which the paired- homeodomain transcription factor *Pax6* is non-functional. It had been shown before that in this mutant, the radial glia fascicle of the cortico-striatal boundary is disrupted, and that cells from cortex and GE intermingle in

vitro in a higher proportion than they do in wild type (Stoykova et al. 1997). This work shows a massive increase in cell migration from the GE into the cortex in the Small-eye mutant. Thus, it reveals an important role of *Pax6* in restricting GE cells to their own region. Cells coming from the cortex also cross the boundary in a higher amount in the Small-eye mutant. Further, the expression pattern of several adhesion- or signaling molecules known to play a role in cell migration was examined in this mutant, revealing two new candidates that could account for the restriction of migration at the boundary.
The third part of this work is concerned with the migration across the cortico-striatal boundary in a mutant for the basic Helix-Loop-Helix transcription factor *Ngn2*. In contrast to the *Pax6* mutant, where several ventral genes are up-regulated in the cortex, the absence of Neurogenin2 leads to the only up-regulation of *Mash1* in the cortex. This upregulation was shown to arise by mis-specification of the mutant cortical cells rather than by a migration of ventral cells into the cortex (Fode et al., 2000). We were interested to examine what happens to the mis-specified dorsal cells that express a ventral gene. We found in this mutant an increase of cortical cell migration into the GE. Cellular and molecular defects within the mutant boundary, and transplantation experiments revealed a non-cell-autonomous cause for this defect. These results reveal a role for *Ngn2* in restricting cortical cells within the cortex.

The last part of this work is concerned with another aspect of boundary formation which involves the coupling and uncoupling of cells via gap junctions. Within organs, or developing organs, cells are connected via channels called gap junctions that allow the passage of ions and small molecules, like messenger RNA molecules. Gap junctions are made of connexin units that are transmembrane proteins. Depending on the pH, on calcium ionic concentration, or on the phosphorylation level of the connexins, gap junctions can be opened or closed. In certain boundary regions, for example in the drosophila wing imaginal disc (Weir and Lo, 1985) or at rhombomere boundaries (Martinez et al., 1992), the communication via gap junctions is interrupted. Within the developing telencephalon, progenitor cells in the cortical ventricular zone are connected via gap junctions and form columnar clusters (LoTurco et al., 1991). This coupling is regulated for example during the different phases of the cell cycle (Bittman et al., 1997; Owens and Kriegstein, 1998). We were interested to know whether the cortico-striatal boundary is a zone where the coupling is interrupted. We showed by the use of an electrophysiological method that cells are indeed uncoupled in the cortico-striatal boundary. Furthermore we compared wild type animals to small-eye mutant, and found that this boundary feature was lost in the Small-eye mutant.

MATERIALS AND METHODS

Animals

The wild type mice used in this work are C56BL6 mice (Charles River company).

The *Pax-6* mutant mice used in this work carry the *Sey* allele on a C56BL6/6J x DBA/2J background. This naturally occurring point mutation in the *Pax6* gene leads to the expression of a truncated non-functional protein (Hill et al., 1991). Heterozygous *Sey/+* mice, recognized by their eye phenotype, were crossed to obtain homozygous, heterozygous and wild type embryos. In this study we used only wild type and homozygous *Sey/Sey* littermates, recognized by the lack of eyes (Hill et al., 1991).

The $Ngn2^{LacZKI}$ mice (*KI*= knock-in) contain the *LacZ* reporter in the coding sequences of the *Ngn2* bHLH domain (Fode et al., 2000). Embryos were obtained by crossing two heterozygous $Ngn2^{LacZKI}$ parents. The litters contained wild type ($Ngn2^{WT}/Ngn2^{WT}$), heterozygous ($Ngn2^{WT}/Ngn2^{LacZKI}$) and homozygous mutant ($Ngn2^{LacZKI}/Ngn2^{LacZKI}$). In control experiments an EGFP knock-in mouse ($Ngn2^{GFPKI}$, Gerard Gradwohl and Francois Guillemot, unpublished data) was crossed to a $Ngn2^{LacZKI}$ mouse in order to obtain null mutants with only one *LacZ* copy.

Genotyping of mice was performed by PCR on genomic DNA extracted from tails (Laird et al., 1991) Genotyping of the $Ngn2^{lacZKI}$ allele was performed with primers situated in the upper (CCAGCTGGCGTAATAGCGAA) and lower (CGCCCGTTGCACCACAGATG) strands of the bacterial ß-galactosidase sequence. The $Ngn2^{WT}$ allele was detected using an upper primer in the 5´untranslated region of the gene (GGACATTCCCGGACACACAC) and a lower primer in the coding sequence (AGATGTAATTGTGGGCGAAG) which generates an 813 bp product. PCR conditions were 30 cycles of 94°C/1min; 60°C/1min; 72°C/1min (Fode et al., 2000). The genotype of the $Ngn2^{GFPKI}$ allele was revealed at the fluorescence microscope. All experiments were performed blind and the genotype was only revealed after analysis of the experiment.

Tau^{GFPKI} mice: For the time-lapse migration study, a mouse containing EGFP in the Tau locus was used. (Tucker et al., 2000).

Green mice: For in vitro transplantation experiments, mice expressing the EGFP (enhanced green fluorescent protein) transgene under the actin promotor were used. (Okabe et al., 1997)

Wistar rats were used as well for transplantation experiments.

For all animals used in this work, the day of vaginal plug was considered as embryonic day 0 (E0) and the experiments were performed at embryonic day (E) 13 to 17 (The total gestational time for mice and rats is 19 days). Mice were anesthetized with ether or with CO_2, killed by cervical dislocation, embryos were removed, placed in Hanks Balanced Salt Solution (HBSS) on ice, decapitated and dissected immediately.

EGFP-adenovirus injections

The Adenovirus construct used was made by Annette Gärtner. This adenovirus lacks the E1 region and is thus replication incompetent. The EGFP transgene is under the control of the CMV promotor and has been inserted into the viral vector by homologous recombination.

Frontal sections of the telencephalon were cut at 250-300µm thickness using a tissue chopper (McIlwain). The slices were collected in HBSS (Hank´s Balanced Salt Solution) containing 5mM HEPES, and transferred to Millipore inserts (Millicell-CM 0.4µm, 30mm diameter) in 6-well plates. They were cultured in 1.5 ml Dulbecco´s modified medium (DMEM) with 10% foetal calf serum (FCS) for two days at 37°C and 5% CO_2. The injections were performed immediately after preparation of the slices: EGFP adenovirus was pressure injected focally onto the surface of the slice through a glass pipette with a 10µm opening diameter, with a Pneumatic PicoPump PV820 (WPI). Injections were placed either in the cortex or in the ganglionic eminence (GE). Usually, about 10 to 100 cells were infected in an area ranging from 200-400µm.

In order to monitor the passive diffusion of the viral vectors, cytochalasin-D was added to the culture medium. Cytochalasin-D blocks actin polymerisation and thereby cell migration (Cooper 1987). The remaining spread of green fluorescent cells under this condition reflects the amount of passive virus diffusion. The 2mg/ml cytochalasin-D stock solution in DMSO was diluted in culture medium to final concentrations of 2µg/ml to 8µg/ml and added immediately after the adenovirus injections.

Migration analysis

In order to follow the migration of green fluorescent cells, the infected slices were photographed at three time points after the injection (at 16/17, 25/26 and 44/45 hours) at the fluorescence microscope (Zeiss Axiophot) using the 10X objective. The distribution of green fluorescent cells was drawn from these photos for each time point and the drawings were superimposed. With increasing time a higher number of cells was detected further away from the injection site. The cells outside the injection site after 25 and 45 hours were considered as migrating and their number and distance from the injection site was quantified. The maximum distance was measured as the distance between the injection site and the furthest cell from the injection site after 25 and 45 hours. When cells were already located outside the injection spot after 16 hours we used their location as the zero value instead of the rim of the injection site to measure the distance of migration. The mean distance of migration was calculated as the average distance of all migrating cells in a respective slice.

Dissociated cell cultures and immuncytochemistry

The cerebral cortex and the GE of brains from E14 mice were dissected in cold HBSS and incubated 15 minutes at 37°C in trypsin-EDTA (Gibco). The cells were dissociated using a fire-polished Pasteur pipette and washed three times in DMEM with 10%FCS. Cells were plated at 10^6 cells/ml in DMEM/FCS (0,5ml/well) in a 24-well plate on poly-D-lysine coated coverslips.

After 24 hours in culture (37°C, 5% CO_2) cells were fixed in 4% paraformaldehyde in phosphate buffered saline (PBS) for 15 minutes. Infection with 1µl GFP-adenovirus per coverslip was performed one hour after plating of the cells. Cultures were fixed after one day and immunostained as described below. Neurons were detected by a monoclonal antibody (mAb) directed against β-III-Tubulin (IgG2b, 1:100, Sigma), and precursor cells by a mAb against nestin (IgG1, 1:4, Developmental Studies Hybridoma Bank).

Immunohistochemistry

Forebrains of were dissected and fixed in 2% paraformaldehyde (PFA) in PBS at 4°C for 6 hours. For GABA stainings brains were fixed in 4% PFA with 0.2% glutaraldehyde at 4°C for 8 hours. After fixing, brains were embedded in 3% agarose in PBS, and 100µm thick coronal sections were cut on a vibratom (Campden Instruments LTD). Alternatively, 12µm thick cryostate sections were used. Sections of both kinds were stained by incubation in the primary antiserum over night at 4°C (diluted in PBS with 0.5%tritonX100 and 10% normal goat serum (NGS)), followed by three washings in PBS. Subsequently, dissociated cells or slices were incubated in fluorescently tagged (usually Cy2 or Cy3, from Dianova) secondary antisera (1:200 in PBS) for 45 minutes at room temperature. Washings were performed in PBS and the sections were mounted in Aqua Polymount (Polysciences Inc) and analyzed at a Zeiss Axiophot or Leitz confocal microscope. Following antibodies have been used:

Anti-calbindin and anti-calretinin: polyclonal rabbit antibodies (Swant), diluted 1:500;

Anti-GABA: polyclonal rabbit antibody (Sigma), 1:1000;

RC2: mouse IgM (P.Leprince, University of Liège, Belgium), 1:500;

Anti-BLBP: polyclonal rabbit antibody (N. Heintz, Rockefeller University, New York, USA), 1:5000;

9-4: monoclonal rat antiserum (T.Hirata, Kyoto University, Japan), 1:10.

Time-lapse study

Brains were dissected, embedded in 1% agarose in PBS, and frontal slices of 160µm thickness were cut immediately on a vibratome in ice cold ACSF (Artificial Cerebrospinal Fluid, see Gap Junctions). One slice was laid in the flow chamber of an Axiovert microscope and fixed to the bottom with a transparent millicell membrane glued to a platine ring (1cm diameter). Oxygenated ACSF at room temperature constantly flew through the chamber. Fluorescence pictures were taken at the 40X objective every 10 minutes with a digital CCD camera driven by the Metaview software. Analysis of the cell movements was achieved by measuring in Metaview the x,y position of a cell in each plane of the recorded stack. The distances and rates of migrations were then calculated in the Excel program.

In vitro transplantations

Telencephali of E14 mice or E16 rats were isolated, sectioned and cultured as for the adenovirus injection assay. When the slices had been placed in the millicell inserts, a small piece (about 300x300µm) of cortex from the green mice (Okabe et al., 1997) or from wild type mice was cut with a scalpel and laid onto the host slice with the help of forceps. (green mouse onto WT mouse slice, or WT mouse onto rat slice). The slices with transplants were cultured for 24 hours. Slices were fixed in 4% PFA for 20 minutes, and rat slices were subsequently stained with M2 and M6 antisera (C.Lagenaur) diluted 1:50 in PBS with10% normal goat serum over night at 4°C. The secondary antibody anti-rat-Cy3 (Dianova) was diluted 1:200 and incubated for 30 minutes at room temperature. Slices were mounted in Acqua Polymount embedding medium (Polysciences) and examined at the confocal microscope.

Plasmid preparation and in vitro transcription

Plasmids were transformed in XL-1 Blue E.Coli bacteria by electroporation after the Maniatis protocol, with following parameters: 0.2 mm electroporation cuvettes, 2.2kV, 25µF, 400Ω. After recovering of the bacteria for 1 hour in the incubator, 50 µl were plated on ampicilin containing (50µg/ml) LB-agar plates and incubated at 37°C over night. One colony was picked the next day and grown for around 4 hours in 3ml LB-ampicillin medium. One ml of this culture was given to 100ml LB-ampicilin and shuttled over night at 37°C. The plasmid was harvested following the Quiagen midiprep protocol, through a midi Tip100 column. The DNA pellet was dissolved in 200µl ddH_2O.

20µg plasmid were linearized with the appropriate enzyme (40 units) in a total volume of 50 to 60µl for 2.5 hours at 37°C. The plasmid was then

phenol extracted:

-Add up the volume to 200µl with pure water

-Add 200µl phenol/chloroform/isoamylalcohol (50:49:1) under the hood

-Vortex strongly for 1 minute

-Centrifuge for 5 minutes in a table centrifuge a maximal speed

-Recover the waterphase (on the top)

-Add 1/10 vol. (20µl) sodium acetate 3M and 0.7 vol. Isopropanol

-Let precipitate for 10 minutes at room temperature

-Centrifuge at maximum speed for15 minutes

-Wash the pellet quickly with 70% ethanol

-Resuspend in 18µl TE pH8, RNAase-free.

The linearized plasmid was ready for in-vitro transcription, and stable for about one year at –20°C.

in-vitro transcription: The following compounds were mixed:

1µl (about 1µg) plasmid

2µl NTP mix containing digoxigenin labeled UTP (DIG-UTP, Boehringer Mannheim)

4µl 5X transcription buffer (Stratagene)

1µl RNAase inhibitor (Boehringer Mannheim)
1µl T3, T7 or SP6 RNA-polymerase (Stratagene, 50U/µl).
Add up to 20µl with pure H_2O.
Incubate at 37°C for 2 hours.
Add 2µl 0.2M EDTA to stop the reaction
Add 2.5µl 4M LiCl and 75µl pure Ethanol to precipitate the RNA
Incubate at –20°C over night, or-80°C for two hours
centrifuge at 4°C for 7 minutes
Dissolve the pellet in 22.5µl ddH_2O for 30 minutes at 37°C
Add 2.5µl 4MliCl and 75µl EtOH 100%
Incubate 2 hours at -20°C, or until the probe is needed
Centrifuge 7 minutes at 4°C
Resuspend in 20µl H_2O and 200µl Hybridization buffer.

Hybridization buffer:
-1X salt solution
-50% formamide
-10% dextran sulfate (Sigma)
-1mg/ml wheat germ tRNA (Sigma, R7876)
-1X Denhardt´s solution (Sigma, D2532)
-ddH_2O
The RNA concentration should be then around 100ng/µl.
Following probes were prepared:
Dlx5: Plasmid from Malin Parmar, Lund, Denmark. Vector pCRII, insert full length. Antisense RNA probe: Digest with BamH1, transcribe with T7.
Cadherin6: Plasmid from M. Takeichi, Japan. Vector: pBluescriptII, insert full length. Antisense RNA probe: digest with SmaI, transcribe with T3.
Cadherin8: Plasmid from Christoph Redies, Essen, Germany. Vector: BluescriptII SK(+). Insert: 1.6kb in the 5´ region. Antisense RNA probe: digest with HindIII, transcribe with T3.
Cadherin11: Plasmid from M. Takeichi, Japan. Vector: pSP73, insert 0,8kb. Antisense RNA probe: digest with EcoRI, transcribe with T7.
R-Cadherin: plasmid from Andrea Wizenman, Würzburg, Germany. Vector: pBluescript-SK+; Insert: full length minus sacI fragment:400-500 first bp. Antisense RNA probe: digest with HindIII, transcribe with T3.
EphA3: Own Plasmid. Vector pCRII, insert 0,4kb. Antisense RNA probe: digest with Pme1, transcribe with T7.
EphA5: Plasmid from Lothar Lindeman, Basel, Switzerland. Vector pCRII, insert 0,3kb. Antisense RNA probe: digest with Not1, transcribe with SP6.
EphrinA5: Plasmid from Lothar Lindeman, Basel, Switzerland. Vector pCRII, insert 0,6kb. Antisense RNA probe: digest with BamH1, transcribe with T7.

EphrinB1: Plasmid from Rüdiger Klein, Martinsried, Germany. Vector pGEM-T, insert 2,1kb. Antisense RNA probe: digest with NcoI, transcribe with SP6.

EphrinB2: Plasmid from Rüdiger Klein, Martinsried, Germany. Vector pGEM-3Z, insert 0,9kb. Antisense RNA probe: digest with BamH1, transcribe with SP6.

EphrinB3: Plasmid from Rüdiger Klein, Martinsried, Germany. Vector pGEM-T, insert full length (1,1kb). Antisense RNA probe: digest with BamH1, transcribe with T7.

Ngn2: Plasmid from Francois Guillemot, Strasbourg, France. *(Gradwohl et al., 1996)*. Vector: pGEM-3, Insert: 1.5kb. Antisense RNA probe: digest with BamHI, transcribe with T7.

LacZ: Plasmid from Francesco Cecconi, Göttingen, Germany. Vector: pBluescript-SK+; Insert: 0,9kb. Antisense RNA probe: digest with EcoRV, transcribe with T7.

Mash1: Plasmid from Francois Guillemot, Strasbourg, France. Vector pGEM7, insert full length cDNA. Antisense RNA probe: digest with XbaI, transcribe with SP6.

Math2: Plasmid from Francois Guillemot, Strasbourg, France

Pax6: *Pax6*sc32, Plasmid from Claudia Walther, Göttingen, Germany. Vector: pBluescript-SK+; Insert: EcoRI / NheI cDNA fragement, 260bp. Antisense RNA probe: digest with HindIII, transcribe with T7.

rROBO1: Plasmid from Y. Rao. Vector: pBluescript-SK+; Insert: full length. Antisense RNA probe: digest with HindIII, transcribe with T7.

rROBO2: Plasmid from Katja Brose, USA. Vector: pBluescript-SK+, Insert: portion of the extracellular domain, 1.7kb. Antisense RNA probe: digest with NotI, transcribe with T7.

mSlit1: Plasmid from Y. Rao. Vector: pGEM, insert: (nt1036-2508 of mSL1DO), 1.5kb. Antisense RNA probe: digest with BamHI, transcribe with T7.

mSlit2: Plasmid from Y. Rao. Vector: pGEM; Insert: (nt361-1687 of mSL2DO), 1.3kb. Antisense RNA probe: digest with NcoI, transcribe with SP6.

mSlit3: Plasmid from Y. Rao. Vector: pBluescript-SK; Insert: (nt2056-3300 of mSL1DO), 1.3kb. Antisense RNA probe: digest with HindIII, transcribe with T3.

SFRP2: Plasmid from Samuel Pleasure, USA. Vector pBluescript II, insert 2kb. Antisense RNA probe: Digest with EcoR1, transcribe with T7.

Wnt7b: plasmid constructed by Gwen Wong, Nutley, USA. Vector: pBluescript II SK; Insert: complete cDNA sequence, 1.5kb. Antisense RNA probe: digest with ApaI, transcribe with T3.

X-Gal histochemistry

Frontal slices of 300µm thickness where cut on a tissue chopper and fixed for 15 minutes at room temperature or 30 minutes at 4°C.

Fixative:

-0.5% Glutaraldehyde

-2mM $MgCl_2$

-1.25mM EGTA

A 10X fixative can be stored for several months at 4°C.

Slices were washed twice in PBS and incubated over night at 37°C in X-Gal staining solution:

-20mM potassium ferrocyanide,
-20mM potassium ferricyanide,
-2mM $MgCl_2$,
-0.01% sodium desoxycholate,
-0.02% NP-40,
-1mg/ml 5-Bromo-4-chloro-3-indolyl ß-D-galactopyranoside
in PBS.
Alternatively whole telencephali were fixed, stained, and subsequently cut in 100µm sections with a vibratome (Campden).

For the combination of X-gal staining with in situ hybridization, (described in Houzelstein and Tajbakshs, 1999) telencephali were fixed in 4% paraformaldehyde (PFA) for 1,5 hours at 4°C, incubated in 20%sucrose in PBS overnight, embedded in Tissue-Tek and frozen on dry ice. They were conserved at –80°C or immediately cut. 12µm sections were cut on a cryostat and recover on gelatin coated slides. The slides were stained at 30°C, for several hours (or over night) in the following solution:
-0,1% PFA
-0,4mg/ml X-Gal (stock solution 100mg/ml in DMSO)
-4mM $K_3Fe(CN)_6$
-4mM K_4 $Fe(CN)_6$
-1mM $MgCl_2$
-0.02% tween
in PBS
Slides were then washed three times in PBS and hybridized as described below.

In situ hybridization
Treatment of slides: For the recovering of the cryostat sections, slides were coated with gelatin: The solution containing 0.5% gelatin and 0.1% potassium-chrome(III)sulfate was heated at 65°C about 30 minutes and filtered. Slides were drained in the gelatin solution at room temperature, dried over night at room temperature, and dried in the oven at 120°C for 3 hours.
Cryostat sections were cut at 12 µm, conserved at –80°C, or immediately processed for X-Gal staining and in-situ hybridization, or directly in-situ hybridization.
Non-radioactive in-situ hybridization:
The RNA-antisense probe was diluted in hybridization buffer (see recipe in the in-vitro transcription protocol).
1 liter 10X salt solution contained:
-114g NaCl
-14.04g Tris HCl, pH7.5
-1.34g Tris base
-7,8g NaH_2PO_4

-7.1g $Na_2H\ PO_4$

-100ml 0.5M EDTA

-ddH_2O

The diluted probe was heated at 70°C for 5 minutes in order to denature the RNA.120µl were applied on one defrost slide, and a clean coverslip was put on the top. Slides were incubated over night at 65°C in a sealed box with whatmann paper wetted with 1XSSC in 50% formamide. (20X SSC: 3M NaCl, 0,3M sodium citrate)

Slides were washed in prewarmed washing solution at 65°C (Washing solution: 1XSSC, 50% formamide, 0,1% tween-20). First wash:10 minutes at 65°C to allow the coverslips to fall off, then 2 to 3 washes at 65°C for 30 minutes.

Slides were washed twice in MABT at room temperature for 30 minutes.

5X MABT:

-500mM maleic acid

-750mM NaCl, pH7.5

-0.1% tween-20

To prepare 2 liters of 5X MABT:

Dissolve first 116.08g maleic acid. Adjust the pH to 7.5 with about 100ml 10N NaOH. Add 87.76g NaCl and 20ml 10% Tween-20 and fill up to 2 liters with H_2O.

Slides were blocked at room temperature for at least one hour in MABT with 2% blocking reagent (Boehringer Mannheim) and 20% heat inactivated sheep serum (Sigma, G6767). Anti-digoxigenin Fab fragments coupled to alkaline phosphatase were diluted 1:2500 in blocking solution and 150µl per slide were applied. slides were covered with parafilm. The antibody staining was performed at room temperature over night in a humid chamber.

Slides were washed in MABT at room temperature 4 to 5 times for 20 minutes, and rinced twice in staining buffer minus NBT and BCIP for 10 minutes at room temperature rocking.

Alkaline-phosphatase staining buffer:

-100mM NaCl

-50mM $MgCl_2$

-100mM Tris pH9.5

-0.1% tween-20

-1mM levamisole

In 1ml staining solution 3.5µl 100mg/ml NBT (Boehringer Mannheim) and 3.5µl 50mg/ml BCIP (Boehringer Mannheim) were added.

When the staining was strong enough (after about 12 to 24 hours) it was stopped by rinsing in staining buffer and shortly in water. Slides were dried for several hours at the air and mounted under a coverslip in acqua-polymount (Polysciences).

Gap junctions filling

Brains were dissected on ice, embedded in 1% agarose in PBS at 37°C, and frontal slices of 300µm thickness were immediately cut on a vibratome (Leica), in ice cold ACSF solution (in mM: NaCl 124; KCl 3; KH_2PO_4 1.25; $MgSO_4.7H_2O$ 2; $NaHCO_3$ 26; $CaCl_2$ 2.5; d-glucose 10). Slices were then incubated 2 hours in oxygenated ACSF at room temperature, then laid in a flow chamber with oxygenated ACSF at 32°C mounted on a Zeiss IM35 microscope and equilibrated for 10 minutes before patching. The recording pipette was filled with internal solution (in mM: K-gluconat 136.5; KCl 17.5; NaCl 9; $MgCl_2.6H_2O$ 1; Hepes 10; EGTA 0.2) with an addition of 2% neurobiotin). Positive pressure was applied to the back of the pipette which was then driven onto the slice, into the first two to three cell layers of the ventricular zone. Small voltage steps were applied, and a decrease in the current deflection signaled that the electrode tip was approaching a cell. Negative pressure was then applied to the electrode, resulting in a tight seal onto the cell membrane. A stronger negative pressure allowed breaking the membrane, and making a contact between cytosol and pipette solution. The cell was filled with neurobiotin for 10 minutes. Neurobiotin was allowed to enter the cell without applying any current pulses. (Cell clusters connected by gap junctions were entirely filled by neurobiotin, as the molecule is small enough to pass through gap junctions). The electrode was then gently removed from the slice. Slices remained 10 minutes more in the chamber before being fixed in 4% PFA for 30 minutes. After 3 washings in PBS, slices were incubated over night in avidin-biotin-HRP (A B kit solution, Vector Labs) in PBS+0,5% triton. Slices were washed and stained with DAB reagent for a few minutes. Slices were mounted in aqua polymount on slides, and the number of cells per cluster was counted at the microscope. In order to control whether cells would be filled by neurobiotin when the tissue is just injured by the pipette, control experiments were performed whereby the recording pipette was driven into the slice without making a patch, and left there for 10 minutes.

RESULTS

I- ASYMMETRIC MIGRATION ACROSS THE CORTICO-STRIATAL BOUNDARY IN WILD TYPE MICE

In order to study the extent to which cell migration is restricted across the cortico-striatal boundary between the cortex and the ganglionic eminence (GE), we developed several assays that focussed on different aspects of this migration. The aim of the first approach was to trace the cells in slice culture and to analyze their migration by infecting the slices focally with an EGFP (Enhanced Green Fluorescent Protein) containing adenovirus. This assay revealed over a time course of two days the direction and speed of migration, and the degree of migrational restriction on both sides of the boundary. In the second approach we followed the migration of cells in slices with the help of time-lapse video microscopy in order to observe the behavior of cells when they approach the boundary. For this purpose we used a mouse that expresses the green fluorescence protein in neurons. The third approach consisted in transplanting small pieces of cortex or GE onto a host slice. The comparison between homotypic (cortex on cortex, or GE on GE) and heterotypic transplants (cortex on GE, or GE on cortex) allowed conclusions about the cell-autonomous or non-cell-autonomous (environment dependent) mechanisms that regulate the migration at the boundary.

I-A EGFP-adenovirus injections in cortex and GE.

In order to analyze cell migration we performed focal injections of adenoviral vectors containing EGFP. Small groups of cells (10 to 100 cells) thus expressed EGFP and could be photographed at several time points after infection under the fluorescence microscope. Figure 2A depicts schematically the experimental paradigm, and Fig. 2B shows an example of a slice with a focal injection in the GE that has been photographed 16 hours, 26 hours and 41 hours after the injection. After 41 hours of culture the infected cells have spread beyond the injection site.

I-A-1 Control experiments and slice morphology

We first evaluated the use of GFP-adenovirus to analyze cell migration in slices of mouse telencephalon. The following control experiments have shown that the

adenovirus was a suitable tool for tracing the cells in slice culture and studying their migration.

We examined first whether all cell types in the telencephalon were equally well infected by the EGFP-adenovirus. When dissociated cell cultures of embryonic day 14 (E14) cortex and GE were infected with the GFP-adenovirus, 44% of the GFP-fluorescent cells were ßIII-tubulin immunoreactive neurons and 43% were nestin-positive precursor cells after one day in vitro. Thus, the cell types present at this developmental stage are equally well infected.

Secondly, in order to ascertain whether the apparent spread of GFP-expressing cells, as shown in Fig.2B, was due to migration or to passive diffusion of adenoviral particles, we blocked cell migration by addition of cytochalasin-D, which inhibits the actin polymerisation (Cooper, 1987). Cytochalasin-D was applied at 2-8µg/ml after the injection with GFP-adenovirus. No GFP expressing cell could be found outside the injection spot under these conditions up to 45 hours, as shown in Fig. 2C. Thus, the spread of infective virus particles seems to be very restricted in this preparation, indicating that the fluorescent cells outside the injection site observed under normal conditions are migrating from the injection site. Indeed these cells exhibit the morphology typical for migrating cells, with a small ovoid cell soma and a longer leading process, as shown in Fig. 2B(c´).

Since the radial glia fascicle that indicates the cortico-striatal boundary spans the region from the sulcus to further ventral positions, we used the sulcus as a suitable ‘landmark’. From there, the cortico-striatal boundary extends in a latero-ventral direction, as visible in phase contrast (Fig. 2B,a,b,c). This landmark was maintained over two days of culture. The position of the boundary was confirmed by staining for the radial glia fascicle, which also persisted during the two days in vitro (data not shown). Thus, the boundary structure is maintained in this culture system.

In order to verify that the cells were able to reach the boundary, we confirmed that the maximum distance of migration exceeded the distance of the injection site to the boundary. The latter distance was 364µm (±36, n=19) in the GE and 222µm (±39, n=12) in cortical injections. Since cells labelled in the GE migrated a maximum distance of 928µm, and cells labelled in the cortex a maximum of 526µm (Table 1, 2, p.25), at least some cells should be able to cross the boundary from both sides. The

quantification of migration distance showed that 57% of cortical and 39% of GE cells migrated over a distance exceeding that to the boundary. Hence, we therefore consider this preparation to be an appropriate system for examining the restriction of migration between cortex and GE.

I-A-2 Restriction of cortical cell migration

When GFP-adenovirus was injected on the cortical side of the boundary, fluorescent cells were observed to migrate radially and laterally within the cortex, but hardly any cell crossed the boundary into the GE during the two days of observation. Very few cells (0.8 per slice) were found in the GE, and only 23% of all slices injected into the cortex showed cells in the GE. We also noted that in about 50% of all cortical injections, cells only migrated away from the boundary, as in the example in Fig. 3A. Often, the cells were distributed in a mushroom-like shape, with little spreading at the ventricular zone and more tangential movement in the cortical plate at the pial side (Fig. 3A). Interestingly, the few cells that crossed the boundary into the GE did not migrate as far as those migrating within the cortex did (Table 1). Taken together, these results show that in slice preparations, cortical cells hardly migrate into the GE at all. This result is in agreement with the work of Fishell et al. (1993) and Neyt et al.(1997), which shows that cells in the ventricular zone of the cortex in flat mounted preparation of the telencephalon stop their movements at the cortico-striatal boundary.

I-A-3 Migration from the GE into the cortex

In contrast to the cortical injections, a substantial number of cells were observed to migrate in the opposite direction, from the GE into the cortex, consistent with previous observations (Anderson et al., 1997; Tamamaki et al., 1997; Sussel et al., 1999; Wichterle et al., 1999). Fig.3B depicts an example of cells labeled in the GE with some cells in the cortex after 43 hours in vitro. Hardly any cells had crossed the boundary to the cortex after 25 hours, but a mean of 13 cells per slice had migrated into the cortex in almost every culture (89%, Table 3) 45 hours after injection into the GE. Most of the cells that migrated from the GE were found in the lateral cortex (see Fig.2B(c´), 3B), and some were also detected in more dorsal areas of the cortex (arrows in Fig.3B). Interestingly, for cells migrating into the cortex, the maximum distance of migration from the injection site was almost double the distance migrated by cells within the GE (Table 3). This is in contrast to the behavior of cortical cells that migrated less far

towards and across the boundary than in other directions. Thus, there is a marked difference in the behavior of cells around the boundary, depending on their side of origin.

In order to examine the cells crossing the boundary more closely, we quantified cells moving towards and away from the boundary, as depicted in Fig.4A. The GE was divided into two segments by a line through the injection site parallel to the boundary (Fig.4A). The proportion of cells migrating towards (56%) and away from (44%, n=257) the boundary were similar. Moreover, the mean distance of migration was comparable for cells migrating in both directions (197±14, n=72; 235±14, n=112). In fact, half of the cells migrating towards the boundary crossed into the cortex. As depicted in Fig.4B, there was an obvious trough in the number of cells that migrate as far as the boundary. Few cells were found in the region of the boundary. This paucity of cells is reminiscent of that of TUJ1-positive neurons in the boundary region previously observed by Neyt et al., 1997. This observation suggests a certain degree of migrational restriction also for cells from the GE.

Table1: EGFP-adenovirus injections in the cortex

	Proportion of slices with cells in the GE 45h	Mean number of cells/slice in the GE 45h	Maximum distance of migration within the cortex (µm) 25h	45h	Maximum distance of migration to the GE (µm) 45h
WT	**23%** (n=26)	**0.8**	**331** ±83(n=14)	**526** ±82(n=13)	**322** ±52(n=3)
SEY	**35%** (n=26)	**1.3**	**227** ±57(n=14)	**529** ±76(n=15)	**336** ±128(n=3)

Table2: Mean distances of migration (at 45hours, in µm)

	Cortex INJECTIONS		**GE INJECTIONS**	
	cells in the cortex	cells in the GE	cells in the GE	cells in the cortex
WT	**228** +/-15(n=125)	**202** +/-54(n=5)	**220** +/-10(n=182)	**645** +/-28(n=73)
SEY	**238** +/-15(n=125)	**288** +/-78(n=4)	**306** +/-10(n=301)	**606** +/-13(n=264)

Table3: EGFP-adenovirus injections in the GE

	Proportion of slices with cells in the cortex 25h	45h	Mean number of cells/slice in the cortex 25h	45h	Maximum distance of migration within the GE (µm) 25h	45h	Maximum distance of migration to the cortex (µm) 45h
WT	**22%** (n=27)	**89%**	**1**	**13**	**238** ±34(n=19)	**525** ±40(n=19)	**928** ±65(n=18)
SEY	**57%** (n=26)	**85%**	**3**	**21**	**303** ±59(n=13)	**571** ±48(n=19)	**997** ±53(n=16)

Tables 1-3
Quantitative analysis of migration in slices injected with EGFP-adenovirus into the cortex or GE. The number of slices analysed is depicted in Table 1 and 3 as 'n', whereas in table 2 n indicates the number of analysed cells. The standard error of the mean is depicted as ±. For details, see Methods.

I-B Time-lapse study

In order to analyze more closely the restriction of migration at the boundary and to understand for example how the trough in the distribution of GE migrating cells is created around the boundary, we aimed to analyze the movements and the speed of the cells when they approach the boundary. For this purpose we used mice expressing EGFP in neurons (Tucker et al. 2000). In these mice, the gene coding for EGFP has been inserted into the Tau locus. Tau is an intermediate filament expressed specifically by neurons, and the absence of this gene does not impair the maturation and functioning of the neurons (Harada et al., 1994). The use of mice where neurons are labeled is an appropriate system to study the migration of cells around the cortico-striatal boundary, since migrating cells were identified as neurons. Indeed, tangentially migrating cells within the cortex have been shown to be immunoreactive for TuJ1, an antibody recognizing the neuron specific ßIII-tubulin isoform (O´Rourke et al., 1997). Further, these TuJ1 positive cells in the cortex have been observed to respect the boundary region (Neyt et al., 1997). Finally, on the other side of the boundary, cells migrating out of the GE have also been shown to be TuJ1 positive (Tamamaki et al., 1997, Zhu et al., 1999).

We imaged living slices of E14 telencephali in a flow chamber under a fluorescence microscope, with time intervals of 10 minutes, over a period of 24 hours. Fig. 5A first depicts the distribution of the GFP expressing neurons, which are very sparse in the ventricular zone (VZ), and start to appear in the more differentiated subventricular zone (SVZ) and mantle zones of the GE and cerebral cortex. The images were taken at the cortico-striatal boundary in the VZ and SVZ in two fields of view (A and B). The cells were migrating in the direction pointed by their leading process, and we were able to follow 50 migrating cells. Many more cells in these images were migrating, however, often they where suddenly appearing or disappearing out of the plane of focus, so that some of them were visible only for a short time.

The analysis of the image sequences revealed first that the cells could be classified in several groups, according their direction of migration. This classification is represented in Fig. 5C, and reveals the asymmetrical property of the cortico-striatal boundary. The proportion of cells migrating from the GE in the direction of the cortex was 76% in field A, and 36% in field B. Thus, a high proportion of migrating cells followed a ventral to dorsal direction. Some of these cells changed their plane of focus so that their further

path when arriving into the boundary could not be followed. They may have continued their migration in another plane of focus, or stopped, or changed their direction of migration. Cells that were tracked all the way from the GE into the cortex represented a proportion of 40% in A, and 16% in B, in agreement with the earlier observation that GE cells are able to enter into the cortex. A second group of migrating cells took a direction from the cortex to the GE. Cells migrating in this direction represented only 4% of all recorded cells in field A, and 8 % in field B. In B, all these cells where also observed to enter into the GE, whereas in A, no cell was observed to cross the boundary into the GE. However, it was not clear if they had stopped their migration, or if we lost their path.

Thus, we found a much higher proportion of cells crossing the boundary from the GE to the cortex, than in the opposite direction, in agreement with the results of the injection experiments. This asymmetry was stronger in the field A (in the SVZ) than in the field B (in the VZ). This difference might be explained by the location of the recording field in respect to the ventricular zone. GE cells crossing the boundary should be more numerous in the subventricular zone (SVZ) than in the VZ, according to data suggesting that these cells express the transcription factors *Dlx*2, *Dlx*5 and *Lhx*6. The expression pattern of these transcription factors reveals a main stream of GE cells entering the cortex that is located in the SVZ (Anderson et al., 1997; Lavdas et al., 1999 and Stühmer et al., 2002).

Apart from the majority of the cells migrating in the orientation GE-cortex, some other directions were taken by smaller groups of cells: within the GE inwardly from the VZ to the mantle zone, on the boundary itself in ventral direction, or in dorsal direction, or they migrated within the cortex towards the marginal zone. This last type of migration is known as radial migration, allowing mature neurons to reach their final position within the cortical layers (Angevine and Sidman, 1961).

The next observation we made concerned the mode of migration of cells. Analyzing the sequence of images revealed that cells migrated in a stop-and-go way, whereby the cell soma remained at the same location for about 20 to 60 minutes, during this time just changing its shape and extending in one direction. The cell soma then suddenly shot into the direction of the leading process. Changes of direction were also observed in some cases (as for the cell circled in blue in Fig.5B): cells could make a 90° turn, by first sending their leading process in the new direction. The rates of migration could

reach maxima of 150 µm/hour, and the average was 25 µm/hour. This rate of migration is similar to the one observed by O´Rourke et al. (1992; 30µm/h) in cells migrating tangentially within the cortex. The variations in speed of migration were analyzed and are depicted for two examples in Fig. 5D. The depicted cell migrating within the cortex (circled in blue) became slower before making a 90° turn when it approached the boundary. However, in general it was difficult to observe any particular behavior at the boundary, for example whether the cells arriving around the boundary become slower or quicker. This difficulty may be explained by the fact that the field of view was small compared to the width of the boundary, so that a large part of the field observed included the boundary itself. The observation of a wider field of view should reveal more information about the speed of migration when cells approach the boundary.

Overall, the imaging experiments confirm the results seen in the injection experiments, concerning the asymmetry of migration on both sides of the boundary. Only a few cells enter the GE coming from the cortex, whereas a high proportion of migrating cells from the GE enter the cortex. However the mechanisms regulating migration across the boundary are not immediately apparent. We could not observe any repulsion mechanism when the cells encountered the boundary. The cells we observed crossing the boundary might already be selected to enter into the neighboring region and migrate without difficulty.

I-C Transplantation experiments

The migration of a population of cells across the cortico-striatal boundary, as opposed to the restriction of the adjacent population of cells, could be achieved by different mechanisms. This asymmetry could arise as the result of the specification of selected cells that would be allowed to cross the boundary, where other cells would remain restricted. Alternatively, this asymmetry could be achieved by the existence of directional cues that would drive the migration of cells in one direction. A mechanism involving directional cues, attractant or repellant molecules in given territories, would mean that the location of the cells would direct their migration independently of their identity. In this case, GE cells placed onto the cortex should be restricted in their migration within the cortex and should not cross the boundary. The alternative mechanism involving distinct cell populations being endowed with a distinct migratory

capacity would imply that GE cells placed onto the cortex would still be able to migrate across the boundary.

In order to assess which mechanisms drive cell migration across the boundary, whether migrational restriction and permeability is a cell autonomous mechanism (achieved by receptors on the cells), or a non-cell-autonomous (environment dependent) mechanism, we performed transplantations in slice culture. We transplanted cortical cells in a GE environment, or GE cells in a cortical environment and then examined whether migration occurred following the “rule” of the host region, or following the rule of the transplanted cells.

In order to perform the experiment, we needed to visualize the transplanted cells on the host slice. We tested two approaches, as shown in the scheme 6A: one approach was to place mouse cells onto a rat telencephalic slice, and stain the transplanted cells with a mouse specific antiserum called M2M6 (Malatesta et al., 2000). As the M2M6 antiserum recognizes a membrane-bound epitope, cell processes were strongly stained and cell somata weakly stained and not easily recognizable. Hence, the quantification of migrating cells was impaired. However, some of the slices were clear enough to be analyzed. In the second approach we used the green mouse, which expresses GFP under the actin promotor, and therefore in all cells (Okabe et al., 1997). In this case, the cytoplasmic staining of the transplanted cells allowed them to be easily recognizable.

In a first step, we performed homotypical transplants, in order to test the validity of the assay: Cortical cells were transplanted onto the cortex, and GE cells were transplanted onto the GE. In this configuration, we detected after 24 hours many cells migrating out of the transplants. Furthermore, we observed that cortical transplanted cells migrated mostly within the cortex, and very few of them cross the boundary (see table 4 and 5 and Fig. 6B). Many GE cells, in contrast, crossed the boundary into the cortex (Fig. 6C). This experimental paradigm thus reflects the typical asymmetrical restriction at the cortico-striatal boundary.

In order to test for the cell autonomous, or non-cell-autonomous regulation of migration, we performed heterotypic transplants. When GE transplants were placed onto the cortex, the cells revealed a stronger ability to migrate into the GE than cells of a cortical transplant. The mean number of cells crossing the boundary increased 14 fold, both in

mouse-on-rat and in green mouse-on-mouse transplants (see table 4 and 5). There are two possibilities to explain this difference between cortex- and GE transplanted cells. First, the restriction of cortical cells within the cortex could be a cell autonomous phenomenon, involving cell surface properties of cortex cells. Second, the migration of GE cells across the boundary could also be a cell autonomous phenomenon. Both possible mechanisms could act simultaneously.

When we transplanted cortical cells onto the GE, they crossed the boundary 7 times less than GE cells do. This and the former comparison suggest that GE cells on both substrates have a higher ability to cross the boundary than cortex cells. Thus, it seems that the migration of GE cells across the boundary is allowed by a cell autonomous mechanism. On the other hand, there was also a slight increase in boundary crossings when GE cells were placed onto the GE substrate, as compared to the cortex substrate (a 1,3 and 2,3 fold increase, in both experimental paradigms). This result also implies a dependence on the substrate for the ability of GE cells to cross the boundary. However, GE cells crossed the boundary in high numbers in both directions. The substrate seems therefore to play a less important role for their migration across the boundary than the identity of the GE cells.

Cortex cells placed onto the GE crossed the boundary 4.5 times more often than when they were placed on the opposite side of the boundary. This result suggests that the restriction of cortical cells in their own territory is achieved by the substrate of migration. In other words, there is a non-cell autonomous mechanism restricting the migration of cortical cells. Nevertheless, the comparison to the GE cells, that migrate across the boundary in both directions more often than cortex cells do, suggests that cortical cell restriction also has a cell-autonomous component. Molecules in the cortex and the boundary may be recognized by receptors present only on cortical cells and may not be detected by GE cells.

All together the transplantation experiments do not give evidence of a mechanism where directional cues within the telencephalon would lead the migration of cells in one direction. Instead, these results suggest a mechanism where GE cells are specified to enter the neighboring region, whereas cortical cells recognize signals preventing them from crossing the boundary.

Table 4:

E14 mouse on E16 rat; number of cells having migrated into the adjacent territory

Substrate / Transplant	**Cortex**	**Ganglionic eminence**	
Cortex	2.8±4.8, n=9	12.7±6.4, n=3	x 4.5
Ganglionic eminence	39.0±21.5, n=3	88.5±51.8, n=10	x 2.3
	x 14	x 7	

Table 5:

E14 GFP mouse on E14 mouse; number of cells having migrated into the adjacent territory

Substrate / Transplant	**Cortex**	**Ganglionic eminence**	
Cortex	5.3± 7.6 n=44	not done	
Ganglionic eminence	73.3±11.5, n=3	96.2±6.3, n=4	x 1.3
	x 14		

Table 4 and 5: The type of transplanted tissue is given vertically and the region onto which it was transplanted is given horizontally. The corresponding cells in the table show the number of cells (± standard deviation) that have crossed the boundary into the adjacent region.

The three experimental approaches used in the first part of this study have all revealed the asymmetric character of the cortico-striatal boundary that permits the cells from the cortex and cells from the GE to have distinct migratory capacities. While only a very small number of cortical cells is able to cross the boundary without migrating far away into the adjacent GE, many GE cells migrate long distances into the cortex. The distinct characteristics of both cell populations had been described in independent studies using different experimental paradigms, but the evidence for a real asymmetry could only be found by assaying cells from both regions in single assays. These experiments have also revealed other properties of the migration across the cortico-striatal boundary. We have found that some GE cells encounter a barrier of migration at the boundary, as the distribution of migrating GE cells reveals a trough at the boundary. Furthermore, transplantation experiments have suggested the capacity of GE cells to enter the cortex to be cell autonomous, whereas the restriction of cortical cells appeared to be non-cell autonomous. In order to understand better the molecular mechanisms governing the migration across the cortico-striatal boundary, we have

examined the role of two transcription factors expressed in the cortex and in the boundary in the following parts of the study.

II- ENHANCED MIGRATION ACROSS THE CORTICO-STRIATAL BOUNDARY IN THE PAX6 MUTANT

The first event leading to the delineation of distinct regions within the embryo is the regionalized expression of transcription factors. This patterned expression precedes the restriction of cell migration. One example is the early expression of the transcription factor Krox20 in rhombomeres r3 and r5 in the hindbrain, which directly induces the expression of EphA4 (Theil et al., 1998) that in turn mediates the segregation of cells at rhombomere boundaries. In the developing telencephalon several transcription factors are expressed in a patterned manner, either dorsally or ventrally. One of these genes is the paired homeobox transcription factor *Pax6*, expressed dorsally, in the cortex and in the boundary. Small-eye is a naturally occurring mutant of the Pax6 gene, in which a point mutation in *Pax6* leads to a non-functional truncated protein (Hill et al., 1991). This causes the heterozygous mice to have a phenotype with small eyes. Previous analysis has shown that in the Small-eye homozygous mutant (*Sey/Sey*) the cortex-specific expression of R-cadherin, as well as the region-specific segregation of cells from the cortex and the GE are lost (Stoykova et al., 1997). In addition, the boundary formed by a radial glia fascicle extending between GE and cortex fails to develop in the *Pax6* mutant (Stoykova et al., 1997), as shown by the 9-4 immunostaining (see Fig.7A). These results suggest that *Pax6* might be involved in restricting cell movements between these regions since both selective adhesion and boundary formation are disturbed. Furthermore, *Dlx*1 expression that is normally restricted to the GE gradually spreads into the developing cortex in this mutant (Stoykova et al., 1996). This raises the question of whether this is due to cell migration or to the ectopic up-regulation of a ventral gene. We therefore studied the migration at the cortico-striatal boundary in the Small-eye mutant mouse embryos (*Sey/Sey*) and their wild type littermates (WT), using the adenovirus injection assay described above.

II-A Enhanced cell migration from the GE into the cortex

When we injected EGFP-adenovirus in the GE of E14 *Sey/Sey* mice, we found a significant increase in cells migrating into the cortex, as compared to WT littermates (Table 3, p.25). As observed in WT GE injections, cells mostly migrated to the lateral part of the cortex. An example showing a massive migration of cells from the GE into the *Sey/Sey* mutant cortex is depicted in Fig. 7B. Increased migration into the cortex

was already observed after 27 hours. Cells crossed the boundary in 57% of all slices from *Sey/Sey*, as compared with 22% in WT slices. Although few cells were found in the mutant cortex 27 hours after injection (a mean of 3 cells per slice), this number increased within 43 hours to a mean of 21 cells per slice, as compared to 13 cells per slice in WT slices (Table 3). We noted, however, that also the total number of cells labeled in the *Sey/Sey* GE (100±12, n=18) was higher than in WT LGE injections (82±8, n=23), and therefore quantified the proportion of labeled cells that crossed into the cortex. In *Sey/Sey* slices, 46% of all migrating GE cells (n=263, analyzed in 9 slices) crossed the boundary into the cortex, whereas this was the case for only 28% of WT GE cells. This represents a 1.6-fold increase in cell migration from the GE into the cortex in *Sey/Sey* telencephalic slices. We also took care that the injections were not closer to the boundary in *Sey/Sey* slices (383± 35µm, n=14, *Sey/Sey* GE; 364± 36µm, n=19, WT GE) and verified that GE cells in *Sey/Sey* slices did not migrate faster than in WT (Table 2,3). The analysis of migrating cells revealed furthermore a continuous distribution of cells in the boundary region of the *Pax6*-mutant, compared to the prominent trough observed in WT slices (Fig. 5B/C). Thus, while in WT, cells from the GE were restricted to some extent in their migration into the cortex, the increased number of cells entering the *Pax6* mutant cortex and their continuous distribution across the boundary suggest that GE cells are free to move into the *Pax6*-mutant cortex. Hence, this result demonstrates that *Pax6* is required to restrict the migration of cells from the GE into the cortex.

II-B Tangential migration in vivo

The injection experiments described above reveal an enhanced migration from the GE into the cortex in the Small-eye mutant. In order to exclude the possibility of an in vitro artefact, we verified whether this migration is reflected by an increased number of ventral cells in dorsal territories. Cells migrating from the GE into the cortex have previously been shown to contain *Dlx*, GAD 67, GABA, calbindin and calretinin (DeDiego et al., 1994; Anderson et al., 1997; Lavdas et al., 1998; Sussel et al., 1999). This prompts the prediction that the enhanced ventro-dorsal cell migration in *Sey/Sey* mice should be reflected by an increase of GABA-immunoreactive cells in the cortex. Indeed, the lateral cortex of *Pax6*-mutants contains a dense accumulation of calbindin-positive cells (Fig. 8A and B). A quantification of GABA-, calbindin-, and calretinin-immunoreactive cells revealed that about twice as many immunoreactive cells were

located in the lateral cortex of *Pax6*-mutants as compared to WT littermates (Fig. 8B). This increase is comparable to the value obtained in our migrational analysis in slice preparations. Interestingly, we also noted the complete absence of calretinin- and calbindin-positive fibers in the intermediate zone of the cortex in the *Pax6*-mutant (Fig. 8Ac/f) most likely representing the absence of thalamocortical projections in the *Pax6*-mutant (Kawano et al., 1999).

Since GABAergic cells are also generated in the cortex, the increase of GABAergic cells in *Pax6*-mutant mice could also be explained by a misspecification of cortical neurons. Therefore, we also quantified the number of GABAergic cells in the cortical plate of the dorsal cortex, i.e., a different cortical region of the same section (Fig. 8A, B). Since similar numbers of GABA-/calbindin- and calretinin-positive cells were found in the cortical plate of the dorsal cortex of WT and *Sey/Sey* mice at E15, their specification does not seem to be impaired in the *Pax6*-mutant. These results strongly suggest that the increase of GABAergic cells in the lateral cortex of *Sey/Sey* mice is due to an enhanced migration from the GE.

When we analyzed sections at later stages, at E17, we still observed the higher number of calbindin-positive cells in the lateral cortex of *Sey/Sey* mice as compared to WT (2.2 fold increase; Fig. 8B). Interestingly, the number of calbindin-positive cells at this stage was also increased in the cortical plate of the dorsal cortex in *Sey/Sey* mice, although to a lesser extent (1.4x). Thus, the increase of immunoreactive cells in *Pax6*-mutant mice seems to spread from the lateral to the dorsal cortex. These findings suggest that the ongoing cell migration from the GE into the cortex in *Pax6*-mutant mice leads to an ever-increasing number of GABAergic cells in the cortex.

II-C Enhanced migration of cortical cells

In order to observe the migration of cortical cells, we injected EGFP-adenovirus into the *Sey/Sey* cortex at E14 (Fig.7C). Cells in *Sey/Sey* cortex migrated for distances comparable to those observed in the WT cortex (Table 1 and 3). Nevertheless, we noted some differences in the distribution of green fluorescent cells in slices from *Sey/Sey* compared with these from WT. In the *Pax6* mutant cortex, cells rarely migrated in radial columns as described above for the WT, but appeared to migrate in a less organized fashion (Fig.7C). The less radially directed migration within the *Sey/Sey*

cortex might account for the decrease in the net radial movement observed in BrdU-birthdating studies (Caric et al. 1997). These defects are likely to be related to alterations in the radial glia cells of the *Pax6*-mutant cortex (Götz et al., 1998). The distance of the injection site from the boundary in *Sey/Sey* cortex (277±47µm, n=12) was comparable to the WT cortex (222±47µm, n=12), as was the distance of migration (table 1). The number of cortical cells that migrated into the GE was slightly increased, compared to the wild type, and the percentage of slices with cells crossing the boundary was higher. These results indicate an increased permeability of the Small-eye boundary in the dorsal to ventral direction as well.

II-D Molecular changes affecting the *Sey/Sey* boundary

Which are the molecules that are altered in the Small-eye mutant and are responsible for the increased migration across the boundary? In the absence of *pax6*, the expression of some cell adhesion molecules or extracellular matrix molecules must be changed, provoking the enhanced migration at the cortico-striatal boundary. The cell adhesion molecule R-cadherin, normally expressed throughout the cortex and in the boundary, is in this region absent in the *Sey/Sey* mutant (Stoykova et al., 1997). The signaling molecule Wnt7a, normally expressed in the boundary and in the abutting lateral cortex, and its inhibitor Sfrp-2 (soluble frizzled related protein), normally expressed strongly in the VZ in the boundary region, are both missing in the *Sey/Sey* mutant. (Fig.9; See also Kim et al., 2000). However, the *Sey/Sey* mutant cortex reveals many defects, and it is likely that other molecules generally involved in boundary formation would also show an altered expression pattern in this mutant, and hence could play a role in the restriction of migration at the cortico-striatal boundary. We therefore observed in the Small-eye mutant the expression pattern of molecules known to play a role in cell segregation. We performed non-radioactive in-situ hybridizations on telencephalic cryosections of *Sey/Sey* and WT littermates and used dig-labeled antisense RNA probes coding for: EphrinB1, EphrinB2, EphrinB3, EphA3, EphA5, Robo1, Robo2, Slit1, Slit2 and Slit3, Cadherin6, Cadherin8 and Cadherin11. Among all the Eph and ephrin molecules tested, ephrinB2 revealed an interesting change in its expression pattern: the lateral cortex normally containing this molecule was negative in the *Sey/Sey* mutant, as depicted by the arrows in Fig.9C, G. As ephrin molecules exert repellent activities in cell migration, this could explain why in the Small-eye GE cells invade the lateral cortex very strongly. The secreted Slit signaling molecules have also

been shown to be repellent for migrating cells. Interestingly, Slit2 was also missing in the *Sey/Sey* cortex, as depicted by the arrow in Fig.9D, H. Thus, a possible mechanism would be that the expression of ephrinA2 and slit2 on cortical cells would hinder the entrance of GE cells into the cortex. Additional changes were noticed in the expression pattern of other molecules. They are summarized in table 10. Thus, several molecules (R-cadherin, Sfrp2, Wnt7a, ephrinB2, Slit2) are likely to promote the restriction cells on both sides of the cortico-striatal boundary.

III- ENHANCED DORSAL TO VENTRAL MIGRATION ACROSS THE CORTICO-STRIATAL BOUNDARY IN THE NGN2 MUTANT

In the Small-eye mutant, the enhanced migration across the cortico-striatal boundary is accompanied by severe patterning defects of the telencephalon. Several ventral transcription factors, such as *Mash1* and *Dlx*1, are upregulated dorsally, while a dorsal transcription factor, Neurogenin2 (*Ngn2*), is absent in the *Sey/Sey* cortex (Stoykova et al., 2000; Toresson et al., 2000). In the absence of *Ngn2* itself in the *Ngn2* mutant, *Mash1* is also upregulated in the cortex while most other ventral transcription factors do not expand into the cortex (Fode et al., 2000). Hence, we were interested to examine the behaviour of cortical cells in the *Ngn2* mutant, that, like in the *Sey/Sey* mutant, lack *Ngn2* and overexpress a ventral gene, in an environment that however does not contain as many patterning defects as in the *Sey/Sey* mutant. We studied a mouse mutant for *Ngn*2, in order to see whether the loss of *Ngn2* and the acquisition of *Mash1* allows the spread of cortical cells into ventral regions.

III-A Ectopic cells in the GE of homozygous *Ngn2* ^{LacZ} mice

To trace cells from the cortex, and examine a possible role of *Ngn2* in their restriction, we used a mutant containing the *LacZ* gene in the *Ngn2* locus. We used X-gal histochemistry to first analyze the distribution of ß-galactosidase positive cells in mice heterozygous ($Ngn2^{WT}/Ngn2^{LacZ}$) and homozygous ($Ngn2^{LacZ}/Ngn2^{LacZ}$) for a knock-in allele of *Ngn2* in which coding sequences have been replaced by the *LacZ* gene. Mice with only one mutant allele have previously been reported to show no phenotype (Fode et al. 2000). Consistent with this, the pattern of ß-galactosidase staining in the telencephalon of $Ngn2^{WT}/Ngn2^{LacZ}$ mice at embryonic day 14 closely resembled the expression pattern of *Neurogenin2* with a strong signal in the cortex and a sharp limit at the border to the unstained GE (Fig.10A). As previously reported (Fode et al., 2000), X-gal staining was present not only in the ventricular zone (VZ) of the cortex, where *Ngn2*-expressing precursor cells are located (Gradwohl et al., 1996), but also in post-mitotic neurons of the cortical plate that do not normally express *Ngn2*. The persistence of ß-galactosidase activity in comparison to the endogenous protein is explained by the relatively long half-life of the enzyme (see also Nieto et al. 2001).

A similar pattern of X-gal staining was detected in homozygous mutant littermates (*Ngn2*^{LacZ}/*Ngn2*^{LacZ}), with a sharp border between the ß-galactosidase-positive cortex and the negative GE. However, in contrast to the heterozygous situation, a large number of ectopic X-Gal positive cells were scattered in the GE of *Ngn2*^{LacZ}/*Ngn2*^{LacZ} mice (Fig.10B; 50±19 cells per section, n=10), with most ectopic X-gal positive cells located in the rostral half of the telencephalon, and few in the caudal half. A further difference observed between heterozygous and homozygous embryos was the intensity of X-gal staining. In heterozygous mice (Fig. 10A), ß-galactosidase activity was weaker in the cortical plate (CP) than in the ventricular zone (VZ), whereas it was equally strong throughout the cortex of homozygous mutants (Fig. 10B). Given that the increased intensity of X-gal staining in homozygous mutant embryos may account for the visualisation of ectopic X-gal positive cells in the GE of only homozygous and not heterozygous mutant embryos, we examined whether ectopic cells were also observed in homozygous *Ngn2*-mutants carrying only one *LacZ* allele. Heterozygous *Ngn2*^{WT}/*Ngn2*^{LacZ} and heterozygous *Ngn2*^{WT}/*Ngn2*^{GFP} mice were crossed to generate *Ngn2*^{GFP}/*Ngn2*^{LacZ} homozygous mutant embryos carrying only one *LacZ* allele. Interestingly, also in the *Ngn2*^{LacZ}/*Ngn2*^{GFP} mutant telencephalon, ectopic cells were detected in the GE to a similar extent than in *Ngn2*^{LacZ}/*Ngn2*^{LacZ} mice (Fig. 10D). The increased X-gal activity in the cortical plate compared to *Ngn2*^{WT}/*Ngn2*^{LacZ} was also confirmed in the *Ngn2*^{LacZ}/*Ngn2*^{GFP} telencephalon. Thus, the appearance of ectopic X-gal positive cells in the GE and increased signal in the CP is not due to the increased copy number of *LacZ* in homozygous embryos, but to the loss of *Ngn2* function.

In order to test whether the cause for the ectopic location of cortical cells is their up-regulation of *Mash1*, we crossed the *Ngn2*^{LacZ} mice to *Mash1* knock out mice. We found in the double mutant embryos lacking both *Ngn2* and *Mash1* that the ectopic cells were still present (Fig. 10E). Thus, the up-regulation of a ventral gene is not the cause for for the wrong location of dorsal cells in ventral positions.

If the ectopic cells in the GE were due to migrational spread from the cortex, one might expect their accumulation over time. We therefore analyzed *Ngn2*^{LacZ} mice three days later, at E17. Indeed, the number of ectopic cells in the GE of *Ngn2*^{LacZ}/*Ngn2*^{LacZ} mice (95±19 cells per section, n=10) was almost double the number observed at E14 (50±19 cells per section, n=10; =1.9 fold increase). We also observed that cells had spread deeper into the GE at E17 than at E14 and ectopic cells were also located in the ventricular zone of the GE at E17 where no cells were detected at E14 (Fig. 10G). This

increase in ß-galactosidase-positive cells in the GE during development suggests that more and more cells of cortical origin become located in the GE where they accumulate in the absence of *Ngn2* function. Indeed, an additional hint for an unusual cell migration from the cortex into the GE in the $Ngn2^{LacZ}/Ngn2^{LacZ}$ mice is that many ß-galactosidase positive cells in GE exhibit the morphology of migrating cells, with an elongated cell body and a leading process (Fig. 10H).

III-B Dorso-ventral cell migration from the cortex into the GE in homozygous *Ngn2* ^{LacZ} mice

To directly examine if the loss of *Ngn2* function affects cell migration, we used focal injections of EGFP-expressing adenovirus into telencephalic slices. Cortical slices from E14 WT and *Ngn2* mutant littermates were cut at 300µm and infected focally close to the cortico-striatal border with an EGFP-adenovirus as depicted in Fig.11. As observed previously, few cells infected in the cortex of E14 WT mice crossed the boundary into the GE 18 or 45 hours post-infection (Fig. 11A), with ectopic cells found in the GE in only 17% of slices and a mean number of 0.3 cells crossing the border per slice (Table 6). In contrast, many labeled cells were observed to migrate within the cortex, confirming that infected cells retained their migratory capacity (Fig. 11A).

EGFP-adenovirus infection of slices from the telencephalon of *Ngn2* homozygous mutant embryos revealed an increased capacity for mutant cells to migrate from the cortex into the GE. In the example shown in Fig. 11B, four infected cortical cells migrated into the GE 45 hours after infection. A quantification of this effect in several embryos indicated that migration from the cortex into the GE was doubled in *Ngn2*-homozygous mutants compared to WT littermates (0.8 versus 0.3 ectopic cells/slice) as depicted in Table 6. However, as the total number of cortical cells infected and migrating into the GE was low in these experiments, the significance of the differences was difficult to evaluate. To overcome this problem we increased the number of infected cells and thus the probability of observing cells crossing the boundary by placing several injections on the cortical side of the boundary. In these high density infections, 51% of wild-type slices had cells crossing the boundary, a number which was further increased to 71% in slices obtained from homozygous mutant littermates. Moreover, the mean number of cells crossing the cortico-striatal boundary increased 1.8 fold in *Ngn2* mutant compared to WT slices. In contrast, the migration distance into

the GE was comparable (WT: 315±39µm; *Ngn2*-/-: 371±45µm respectively). Thus, as suggested by the low density viral infections, there is a significant increase in the dorso-ventral migration of cortical cells in *Ngn2*-mutant slices.

We also examined whether the boundary in the *Ngn2*-mutant telencephalon is more permeable to cells from the GE, by injecting EGFP-adenovirus in the GE of E14 WT and *Ngn2-/-* telencephalic slices. As previously observed, GE cells migrate into the cortex much more frequently than cortical cells migrate into the GE. In most of the injected slices (79%) cells from the GE had migrated into the cortex two days after labeling and no difference was detected in telencephalic slices from homozygous *Ngn2* mutants (GE cells migrated into the cortex in 89% of slices, see Table 7). Thus, the absence of *Ngn2* does not affect cell migration from the GE into the cortex, but only from the cortex into the GE.

Taken together, these data suggest either that *Ngn2* mutant cortical cells have an increased migratory capacity, or that the boundary delineating the cortex and GE is more permeable to cortical cells in the absence of *Ngn2* function.

Table 6: Adenovirus injections in the cortex

single injections in the cortex	% of slices with cells in the GE	Mean number of cells in the GE	**several injections in the cortex**	% of slices with cells in the GE	Mean number of cells in the GE
Ngn2 +/+	17%, n=29	0.3±0.1	**Ngn2 +/+**	51%, n=39	1.4±0.4
Ngn2 -/-	33%, n=30	0.8±0.4	**Ngn2 -/-**	72%, n=19	2.3±0.6
Normalized to WT	x 1.9	x 2.7	**Normalized to WT**	x 1.4	x 1.6

Table 7: Adenovirus injections in the GE

single injections in the ganglionic eminence	% of slices with cells in the cortex	Mean number of cells in the cortex
Ngn2 **+/+**	79%, n=19	5.5
Ngn2 **-/-**	89%, n=9	6
Normalized to WT	x 1.1	x 1.1

III-C Cellular and molecular changes at the boundary between cortex and GE in homozygous *Ngn2* ^{LacZ} mice

Because cortical cells in *Ngn2*-deficient brains are able to cross the boundary into the GE in a higher proportion than in the wild type telencephalon, we tested whether this boundary in the mutant is affected in its cellular composition or molecular properties. A prominent radial glial fascicle delineates the cortex and the GE from E12 onwards (Edwards et al., 1990; Stoykova et al., 1997). To detect this fascicle, we performed immuno-stainings for RC2 and BLBP (Stoykova et al., 1997; Hartfuss et al., 2001) on sections of WT and homozygous *Ngn2*-mutant telencephali. While the characteristic fasciculation of RC2- and BLBP-immunoreactive radial glial fibers was present, it was less tight in the homozygous *Ngn2*-mutant telencephalon compared to WT littermates (Fig. 12A-D). This was seen throughout the rostrocaudal extent of the boundary. Similarly, immunostaining of the 9-4 antigen, a marker for boundary radial glial cells (T. Hirata) also revealed a certain defasciculation of radial glia fibers at the boundary in the homozygous *Ngn2*-mutant telencephalon (Fig. 12E, F). Thus, in the absence of *Ngn2* the radial glia fascicle present at the border between cortex and GE, is less well fasciculated, suggesting that mechanical defects may account to some extent for the enhanced cell migration observed at the border in *Ngn2* mutants.

We also examined whether molecular changes in border cells had occurred in *Ngn2* mutants. Interestingly, a molecular marker of the boundary region, the soluble frizzled related protein 2 (SFRP2; Kim et al., 2001) also showed a broader expression domain in the *Ngn2-/-* telencephalon compared to WT littermates (Fig. 12G, H). In WT embryos, Sfrp2 is most strongly expressed in the VZ of the ventral pallium, the border region extending from the GE to the cortico-striatal sulcus (arrow in Fig. 12G). In the *Ngn2-/-* telencephalon, however, the Sfrp2 expression domain spreads above the sulcus into the cortex (Fig. 12H). This enlargement of Sfrp2-expression in *Ngn2*-mutants was observed at all rostrocaudal levels of the cortex. In contrast, expression of Wnt7b*,* the Sfrp2 ligand, was not affected in the lateral cortex of *Ngn2* mutants (data not shown, analyzed at E14 and 17). Similarly, we did not see any changes in the expression patterns of Slit1, 2, 3 or ROBO1, 2 (data not shown), secreted molecules and their receptors that were previously suggested to play a role in tangential cell migration in the telencephalon (Zhu et al., 1999). In particular Slit2 has a prominent expression domain along the boundary between the cortex and GE at E16, a pattern that is not affected in *Ngn2* mutant mice (not shown). Cadherin-mediated cell adhesion

has also been implicated in restricting the intermingling of cells from the cortex and the GE (Götz et al, 1996; Inoue et al., 2001), but no changes were observed in the expression of R-Cadherin, Cadherin 6, 8 and 11 in the *Ngn2-/-* telencephalon (data not shown). Likewise, the expression patterns of ephrins (ephrin A5, B1, B2 and B3) and Eph receptors (Eph A5 and A3) were unaffected in *Ngn2-/-* telencephalon (data not shown). Thus, no defects were observed in the expression of cell surface and signaling molecules known to regulate cell adhesion and migration in the developing telencephalon of *Ngn2-/-* mice, except a broadening of the boundary between the cortex and the GE at cellular and molecular level.

III-D Non-cell autonomous effects on cell migration in *Ngn2-/-* telencephalon

Two explanations might account for the migrational defects observed in the absence of *Ngn*2 function. Either alterations occur in the substrate of migration, as suggested by the molecular and cellular changes observed in the cortico-striatal boundary in *Ngn2* mutants or *Ngn*2-deficient cortical cells acquire ventral surface properties, e.g. by up-regulation of *Mash*1, allowing only the mutant cells to cross into the GE. The first possibility predicts that the migration defects observed in *Ngn2* mutants are non-cell autonomous and the migration of WT cells should also be affected on a *Ngn2*-/- telencephalic substrate. In contrast, if the second possibility were correct, only *Ngn2*-mutant should be able to spread into the GE. To test this idea, we used the same in vitro transplantation approach which was used in the first part of this work. We transplanted small pieces of cortex or GE from 'green mice', a transgenic line that expresses EGFP ubiquitously in all cells (Okabe et al., 1997), onto slices of *Ngn2-/-* or WT telencephali.

When we transplanted pieces of green fluorescent cortex onto the cortex of slices from *Ngn2-/-* telencephalon (Fig. 13A) we observed a clear increase in the number of cortical cells crossing into the GE compared to transplants placed on slices from WT littermates. While on a WT cortex a mean number of 3.2±1.2 (n=42) green cortical cells had entered the GE after 1 day in vitro, more than fivefold the number of cells (16.0±3.3; n=28) had crossed the boundary on a *Ngn2-/-* substrate. Thus, WT cortical cells can spread to a larger extent into the GE on a *Ngn2-/-* versus a WT substrate. Two possible mechanisms could lead to this result: first, migration is enhanced on the *Ngn2-/-* telencephalon, or, second, the mutant boundary is more permissive for cortical

cells to enter the GE. Despite a comparable size of the transplants (see Materials and Methods for details), we noted that a higher number of cells migrated out of transplants placed on *Ngn2-/-* telencephalic slices compared to WT slices (1.6 fold increase, Fig. 13B), suggesting that the mutant cortex is a more permissive substrate for migration than the wild type cortex. Nevertheless, taking this difference into account by normalizing the proportion of cells entering the GE to the total number of migrating cells, there were still more cells crossing the boundary on a mutant substrate (3.7%±0.7%) than on a WT substrate (1.2%±0.5%; Fig. 13C; 3.1 fold increase on *Ngn2-/-* substrate). This suggests that the boundary between the cortex and the GE has become more permissive for cortical cells in the absence of *Ngn2* and that the loss of *Ngn2* is not required in the migrating cells since also WT cells react to the substrate changes of *Ngn2*-/- slices.

Table 8: migration out of cortical transplants

GFP-cortex transplants	Transplant area (mm^2)	Mean number of migrating cells in the cortex	Mean Number of migrating cells in the GE	GE cells/ total number of cells
WT	0.364	266±62	3±1.2	1.1%
Ngn2 -/-	0.406	424±57	16±4.9	3.7%
Normalized to WT	X1.1	X1.6	X5.3	X3.4

III-E Fate change of ectopic cells in the GE of *Ngn2^{LacZ}* mice

The results shown above strongly support the interpretation that the X-Gal-positive cells detected in the GE of *Ngn2*^{LacZ} mice are indeed cortical cells having crossed the cortico-striatal border. These cells therefore can be used to ask whether cortical cells in a GE environment retain a cortical identity or whether they acquire the identity of GE cells. To answer this question we examined the expression of several transcription factors specific for dorsal or ventral regions in the developing telencephalon. First, we analyzed whether X-Gal positive cells still express *Ngn2* transcripts (using a *Neurogenin2* riboprobe, which hybridizes to a region still present in the mutated gene) or the *LacZ* gene at ectopic positions. In the cortex, as expected, most of the X-Gal positive cells express the *LacZ* mRNA (Fig. 14A). In contrast, the X-Gal positive cells in the GE did not contain detectable levels of *LacZ* (Fig. 14A) or *Ngn2* transcripts (data not shown). Thus, expression from the *Ngn2*-locus seems to be down regulated after

cortical cells have crossed the boundary into the GE. Interestingly, the same was observed for expression of the transcription factor *Pax6*, which is expressed in many cortical precursors, but only at very low levels in the GE. Indeed, most ß-galactosidase positive cells in the cortex express *Pax6*, while most ectopic cells in the GE did not. Interestingly, the few X-gal-positive cells that retained *Pax6* transcripts were located still close to the boundary (data not shown). We also examined the expression of *Math2*, a bHLH transcription factor expressed in postmitotic neurons of the cortex, but not the GE (Bartholomä and Nave, 1994; Fode et al., 2000) to see whether cortical cells might have retained their cortical identity but differentiated into neurons. Again, ß-galactosidase containing cells in the GE of *Ngn2*^{LacZ}/*Ngn2*^{LacZ} did not express *Math2* (Fig. 14B). Similar results were also obtained with the riboprobe for *R-Cadherin* that is contained in both neurons and precursors in the cerebral cortex, but not in the GE (data not shown). Thus, cortical cells entering the GE loose their dorsal identity, raising the question of whether they instead acquire a ventral identity in their new environment?

Mash1 is a bHLH transcription factor expressed in the GE, but only at low levels in the cortex (Casarosa et al., 1999; Fode et al., 2000). However, in the absence of *Ngn2*, *Mash1* expression is up-regulated in the cortex (Fode et al. 2000). In the cortex of *Ngn2*^{LacZ}/*Ngn2*^{WT} mice most ß-galactosidase-positive cells in the cortex did not contain *Mash1* transcripts, suggesting that *Ngn2* and *Mash1* are expressed in different populations of cortical precursors (see also Nieto et al., 2001). In the cortex of *Ngn2*^{LacZ}/*Ngn2*^{LacZ} mice, however, most ß-galactosidase-positive cells also expressed *Mash1*, consistent with the notion that *Mash1* functionally replaces *Ngn2* and thereby misspecifies cortical precursors (Fig. 14C). Also most of the ectopic ß-galactosidase positive cells in the GE expressed *Mash1* (Fig. 14C). Although the endogenous expression pattern of *Mash1* in the GE is restricted to the VZ and SVZ (Bulfone et al., 1993), ectopic X-Gal-positive cells outside the VZ were clearly *Mash1* positive. Since, however, also cortical cells express *Mash1* in the absence of *Ngn2*, we examined other ventral markers, such as *Dlx5* that are not expressed by the ß-galactosidase-positive cells in the lateral cortex abutting the LGE (Fig. 14D). Interestingly, all ectopic ß-galactosidase positive cells in the GE contained *Dlx5* transcripts suggesting that they start to express *Dlx5* when they enter the GE (Fig.14D). Taken together, these results suggest that *Ngn2*-deficient cells migrating from the cortex into the GE lose their cortical identity and acquire the identity of their host region.

IV- COMPARISON BETWEEN THE PAX6 MUTANT AND THE NGN2 MUTANT

The results presented above show that in the absence of *Ngn2* in the cortex, the boundary becomes permeable in a dorsal to ventral direction and in the absence of *Pax6*, the boundary becomes permeable in both directions. Taking together the results of both studies, with the differences and similarities of both mutants, should help to clarify the molecular mechanisms acting in the restriction of migration at the cortico-striatal boundary. Table 9 summarizes the principle characteristics of both mutants and shows some molecules which could be involved in the altered cell migration at the boundary.

Table9: principle characteristics of the boundary in both mutants

	Pax6 mutant (*Sey/Sey*)	*Ngn2* mutant
PAX6	**non functional**	unaltered
NGN2	**absent**	**absent**
Ventral to dorsal migration	**increased**	unaltered
Dorsal to ventral migration	**increased**	**increased**
Boundary radial glia fascicle	**absent**	**defasciculated**
R-cadherin	**absent**	unaltered
Wnt7b	**absent**	unaltered
Sfrp2	**absent**	**increased in the cortex**
Slit2	**absent**	unaltered
EphrinB2	**decreased in the cortex**	unaltered

We examined by in-situ hybridization the expression pattern of further molecules known to play a role in the segregation of cells. The results of this study are summarized in table 10.

Table10: Expression patterns in WT, Small-eye and *Ngn2* mutant

	WT	SEY/SEY	*Ngn2*-/-
SFRP2	E14: in the VZ all around the ventricle, specially strong in the boundary region	Absent in the boundary	Boundary domain enlarged into dorsal direction
Wnt7b	E14: in cortex SVZ and CP, and in lateral cortex and boundary.	Absent in lateral cortex and boundary, still present in CP	No difference
Cadherin6	E14: in cortex VZ, IZ and CP. In GE VZ		No difference
Cadherin8	E14: in the cortex SVZ, stop at the boundary. In the GE mantle zone and weakly in VZ.	Absent in the cortex	No difference
Cadherin11	E14: in the CP, and in the GE mantle zone	Absent	No difference
EphrinB1	E14: in the VZ strongly in the cortex, weaker in the GE. Weak within the boundary	No difference	No difference
EphrinB2	E14: In the Cortex and GE VZ/SVZ, and in the CP of the lateral cortex.	Decrease in the lateral cortex	No difference
EphrinB3	E14: in the septum and ventrally in the GE	No difference	
EphrinA5	E14: in the cortex VZ	E16 No difference	
EphA5	E16: in the cortex SVZ and in boundary. E14 weak signal in boundary	No difference	No difference
EphA3	E14: in the GE VZ, in the cortex IZ with sharp border to the GE, and in lateral CP		No difference
Slit1	E14: in the GE VZ/SVZ and mantle zone. Cortex VZ only ventrally, and CP.	No difference	Caudally: increased expression in the cortex SVZ
Slit2	E14: in the cortexVZ/ SVZ; E16 within the boundary	E14: absent from the cortex	No difference
Slit3	E14: in the CP	absent	No difference
Robo1	E14: in the CP and in the GE mantle zone, boundary negative.	No clear border between positive GE and negative boundary	No difference
Robo2	E14: in cortex IZ and in GE mantle zone	Decrease in the cortex	No difference

VZ=ventricular zone; SVZ= subventricular zone; IZ= intermediate zone, CP= cortical plate

IV GAP JUNCTION UNCOUPLING AT THE CORTICO-STRIATAL BOUNDARY: ANOTHER ASPECT OF REGIONALIZATION

In the *Pax6* mutant, the patterning of the cortex and GE is distorted (Stoykova et al., 2000), the radial glia fascicle of the boundary is disrupted, and cell migration across the boundary is no longer restricted. Hence, *Pax6* regulates many features of the boundary delineating cortex and GE. We wanted to find out whether the loss of *Pax6* also influences a further characteristic of boundaries, concerning the coupling of cells via gap junctions. The uncoupling of gap junctional communication is a boundary feature found at the inter-rhombomeric boundaries (Martinez et al., 1992) and at drosophila compartmental boundaries (Blennerhasset and Caveney, 1884). Like the restricted cell migration, it is a mechanism that enables a distinct differentiation of adjacent regions, in this case by limiting the passage of small metabolites at the borders. Within the cortex, cells are connected via gap junctions (LoTurco et al., 1991), and we examined whether the cortico-striatal boundary interrupts this communication. We then examined the gap junctional coupling at the cortico striatal boundary in the Small-eye mutant. Using an electrophysiological method, we visualized gap junctional coupling of cells in the cortex, GE and cortico-striatal boundary in E14 telencephalic slices of wild type and Small-eye mutants.

IV-A Control experiments

As a measure of gap junctional coupling, we counted the number of cells labeled when single cells were filled with neurobiotin via a patch pipette in whole-cell recording configuration, as depicted schematically in Fig15A. Neurobiotin is a molecule small enough to pass through gap junctions and it allows the staining of the whole cell cluster (See also methods and Blanton et al., 1989). When a Gigaohm seal between patch pipette and cell surface was obtained the membrane was broken in order to be in contact with the cytoplasma, and the cell was filled through the patch electrode for 10 minutes. In about 60% of the cases, the patch was disrupted before this time. We therefore verified whether the number of cells labeled in a cluster was smaller when the time of patching was short. We found that the number of cells per cluster did not correlate with the duration of patching, as seen in the Fig 15B. Therefore we also included in the analysis clusters that were filled less than 10 minutes.

To control that we were filling cell clusters connected by gap junctions and not random groups of cells that were injured by the patch electrode, we put the electrode into the slice for 10 minutes, without making a patch onto a cell. In those cases, neither single cells nor clusters were visible after the DAB staining of the slice (n=10).

IV-B Uncoupling of cells within the cortico-striatal boundary

We first studied slices of embryonic day 14 wild type telencephali. In each slice, one cell in the cortex, one cell in the GE and one cell in the cortico-striatal boundary were filled with neurobiotin.

Clusters in the cortex revealed a columnar shape, extending from the ventricular zone in direction of the pial surface, as it has been also described by Lo Turco et al (1991). The mean cluster size consisted of 10 cells (see table 11). Fig. 15C a and b shows a large cortical cluster, containing 21 cells. In the GE, clusters had a triangular shape, being broad at the ventricular surface and thin in deeper positions, as can be seen in Fig. 15C. In almost all GE clusters, about one to three radial processes were visible, extending into the GE mantle zone. The mean cluster size was 10, the same as in the cortex. Clusters in the cortico-striatal boundary were much smaller, with a mean of 4.6 cells. In shape, they resembled the clusters of the GE, with cell somata at the ventricular surface only, and one, or few long radial processes extending to the pial surface.

The comparison of the cluster size distributions, depicted in Fig.16A, shows a significant difference between cortex, GE and boundary. While in the cortex and the GE, the cluster size is evenly distributed between 1 and 15 cells, 88% of the boundary clusters are clusters of 1 to 5 cells. The one to two-cells clusters represent already 41% of all boundary clusters, whereas they constitute only 10% and 14% of the cortex and GE clusters, respectively. Thus, the cortico-striatal boundary is a region where cells are less coupled, thereby disrupting communication of intracellular metabolites between the cortex and the GE.

Table 11:

Mean cluster size (number of cells)	Cortex	Boundary	GE
Wild type	**10.1± 1.3**; n=31	**4.6± 1.5**; n=17	**10.2± 1.5**; n=21
Small-eye	**8.1± 2.3**; n=19	**9.3± 2.3**; n=20	**13.3± 2.4**; n=16

IV-C No uncoupling in the Small-eye mutant boundary

As the cortico-striatal boundary is a region of uncoupling of cells, we were interested to study a case where the boundary is disrupted, as observed in the Small-eye mutant. We filled cells with neurobiotin in E14 small-eye telencephalic slices, and found several differences to the wild type.

We found cluster sizes within the *Sey/Sey* boundary that were clearly shifted towards bigger cell clusters. The one to two cell clusters represented only 15% of all clusters in *Sey/Sey*, compared to 41% in WT. The size of clusters in the *Sey/Sey* boundary was rather evenly distributed. Most of the clusters in the boundary had a shape resembling clusters of the WT GE, triangular with processes extending into the direction of the pial surface. Thus, in a mutant where the boundary region is disrupted, an uncoupling of cells does not take place.

In the *Sey/Sey* cortex, clusters were rarely organized in a columnar shape, as was the case in the wild type. Most of the clusters found in *Sey/Sey* cortex were small (53% of one to five cell clusters, compared to 35% in WT), and the bigger clusters did not extend so far in the direction of the pial surface, compared to the WT (see Fig. 15C). Thus, in correlation to the numerous other defects of the small-eye cortex, cells in the ventricular zone are not as highly connected as in they are in wild type. This may be related to a defect in synchronization of cell cycle events, as suggested by Bittman et al. (1997) and Owens and Kriegstein (1998), and may be in correlation to the excess of cells in S-phase in the *Sey/Sey* cortex (Götz et al., 1998).

In the Small-eye GE, we found a slightly increased cluster size compared to the WT (see Fig. 16D). The shape of the clusters was similar to that in the WT, with some radial processes extending out of the cluster. However, the percentage of big clusters (containing more than 15 cells) was higher in the *Sey/Sey* GE compared to the WT GE.

Although most defects of the Small-eye mutant are found in the cortex, the zone where *Pax6* is strongly expressed, the lateral GE also contains a very low level of *Pax6* expression and is also affected in several ways. For example, the expression territory of sonic hedgehog and Nkx2.1 are dorsally expanded from the medial GE to the lateral GE (Stoykova et al., 2000). Thus, other defects may be found in this territory.

In order to find the cause for the increased gap junctional communication at the *Sey/Sey* cortico-striatal boundary, we checked whether connexins are expressed differently in the mutant. We performed immunostainings for Connexin 26 and connexin43, both connexins expressed in the telencephalon at this developmental stage (Nadarajah et al., 1997). We could not find any difference in the immunoreactivity between WT and *Sey/Sey* slices. This result suggests that the increased coupling of cells in the *Sey/Sey* boundary is not due to a change in the gene expression of connexins but rather to a change in the regulation of the channel permeability.

Taken together, these results suggest a mechanism of uncoupling at the cortico-striatal boundary that would contribute to the delineation of the cortex and the GE. This mechanism is absent in the Small-eye muitant.

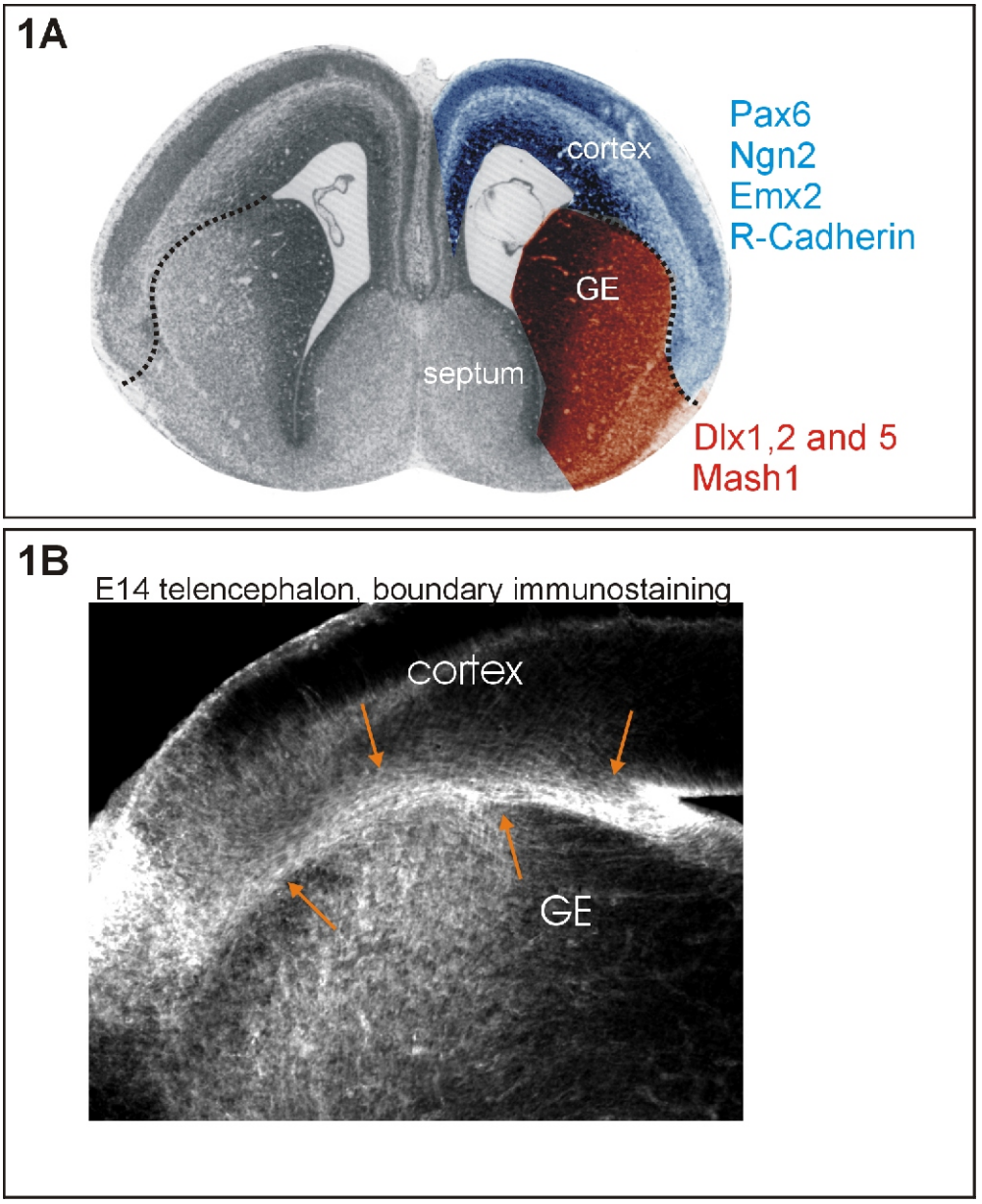

Figure1: Morphology of the telencephalon:
1A: Nissl staining (taken from the Atlas of the prenatal mouse brain, Schambra et al., Academic Press, 1992) of a coronal section of an embryonic day 14 (=E14) mouse telencephalon, depicting the dorsally located cortex, the ventrally located ganglionic eminence (GE), and the cortico-striatal boundary delineating both regions (represented by a doted line). The blue color represents the expression domain of dorsal transcription factors (i.e. Pax6, Ngn1 and 2, Emx2) and the brown colour the expression domain of ventral transcription factors (i.e. Mash1, Dlx1, -2 and -5).
1B: Immunhistochemistry with the monoclonal antibody 9-4 on a coronal section of an E14 mouse telencephalon, revealing the radial glia fascicle of the cortico-striatal boundary (pointed by the orange arrows).

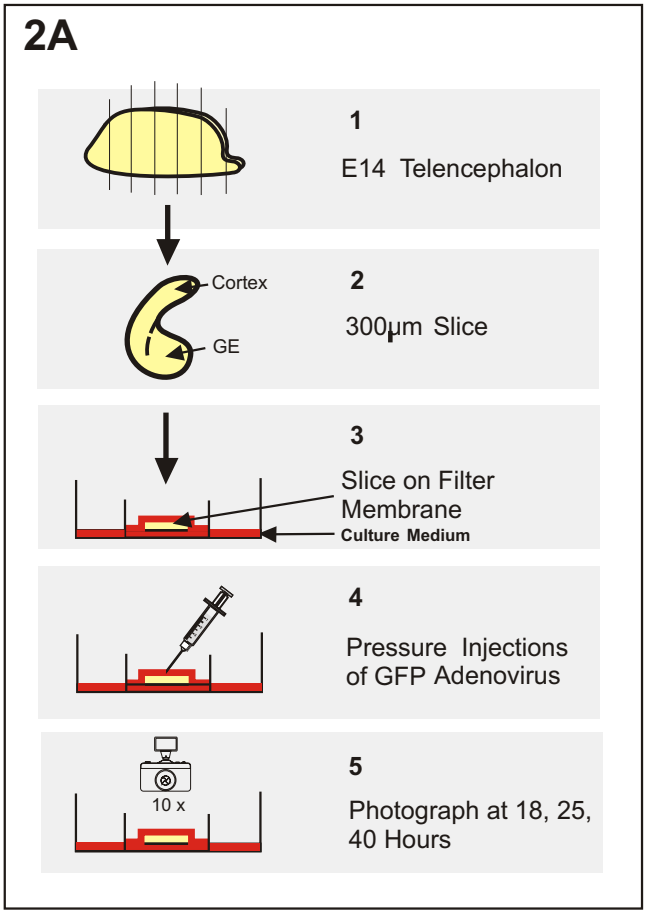

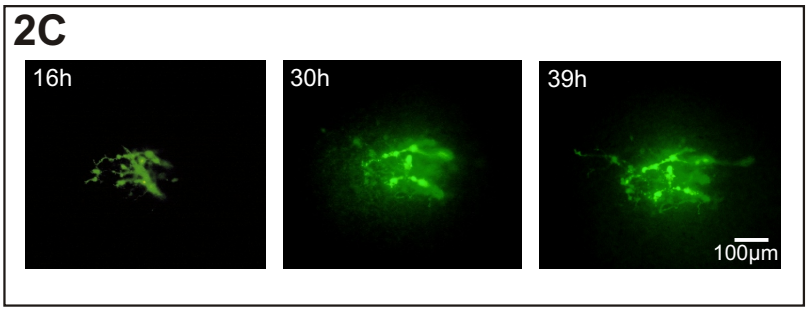

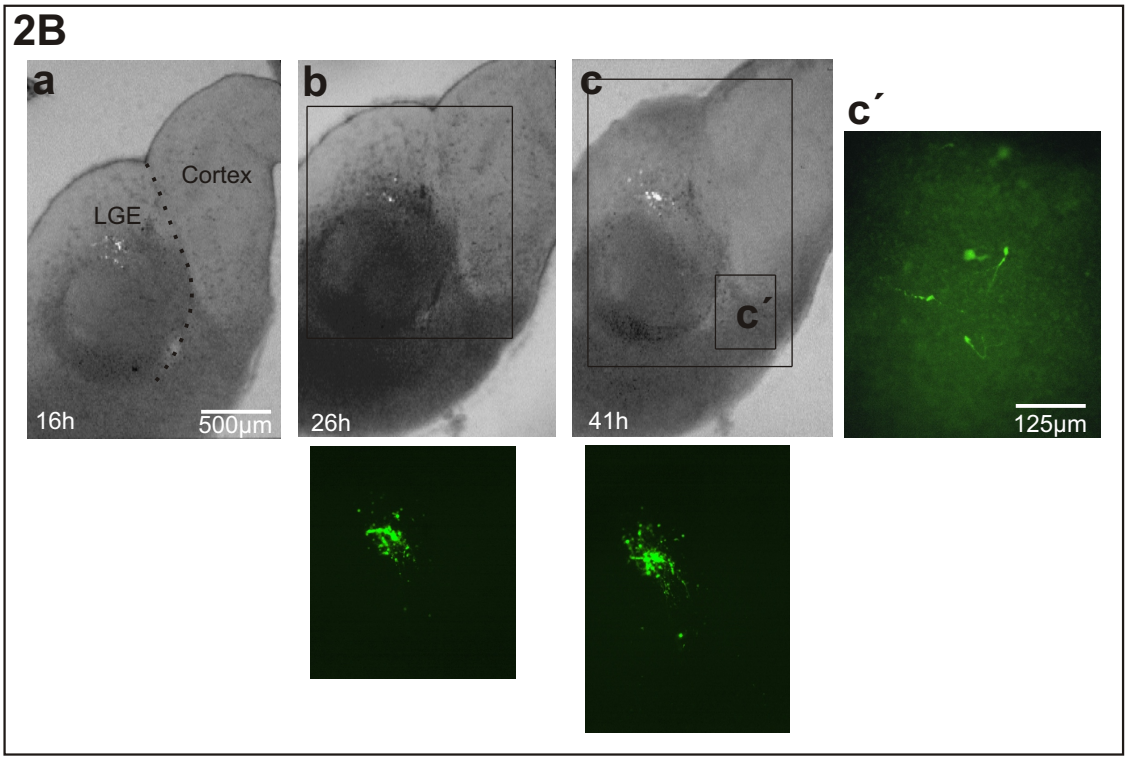

Figure 2: GFP-adenovirus injection experiments
2A: Schematic representation of the assay
2B: Frontal slice of embryonic day 14 telencephalon injected with GFP adenovirus. The slice was photographed under both phase contrast and fluorescence at a 5x magnification 16 hours (a), 26 hours (b) and 41 hours (c) after the injection of adenovirus encoding the enhanced green fluorescent protein (EGFP) into the GE. The GE and the cortex can be discerned in phase contrast and are indicated in a (slice orientation: medial is to the left, lateral to the right, ventral down and dorsal up). The cortico-striatal boundary is indicated in a as a dotted line. The green fluorescent cells are visible as white dots in a, b and c, and can be seen in the corresponding fluorescent micrographs shown below b and c, and indicated by black frames in b and c. c´ is a fluorescent micrograph taken at higher magnification in the lateral cortex depicting four green fluorescent cells that have migrated from the GE into the cortex after 41 hours.
2C: No diffusion of the GFP-adenovirus
In order to visualize the diffusion of adenovirus, cell migration was blocked by the addition of cytochalasin-D to the culture medium. Pictures were taken 16, 30 and 39 hours after injection into the GE. The green fluorescence increases during this time, but does not spread from the site of injection.

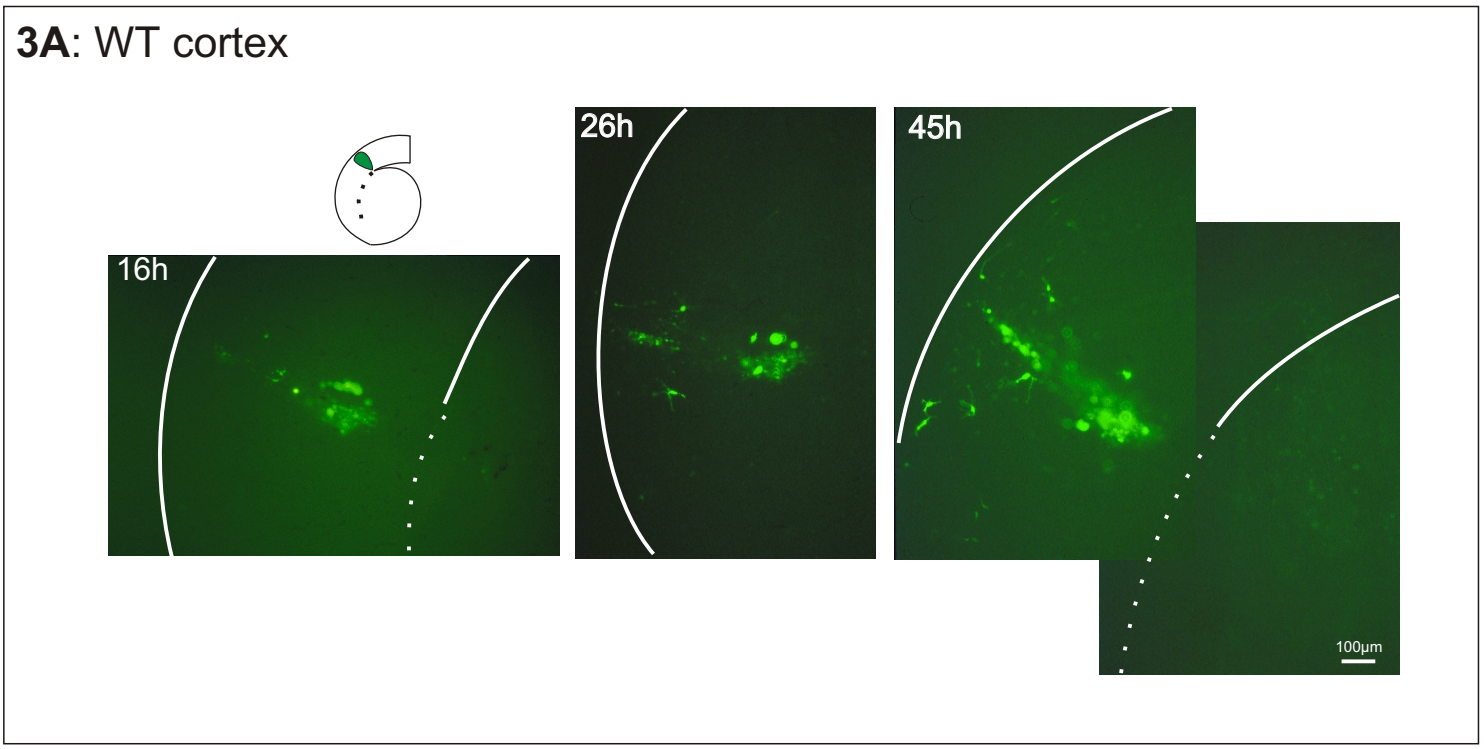

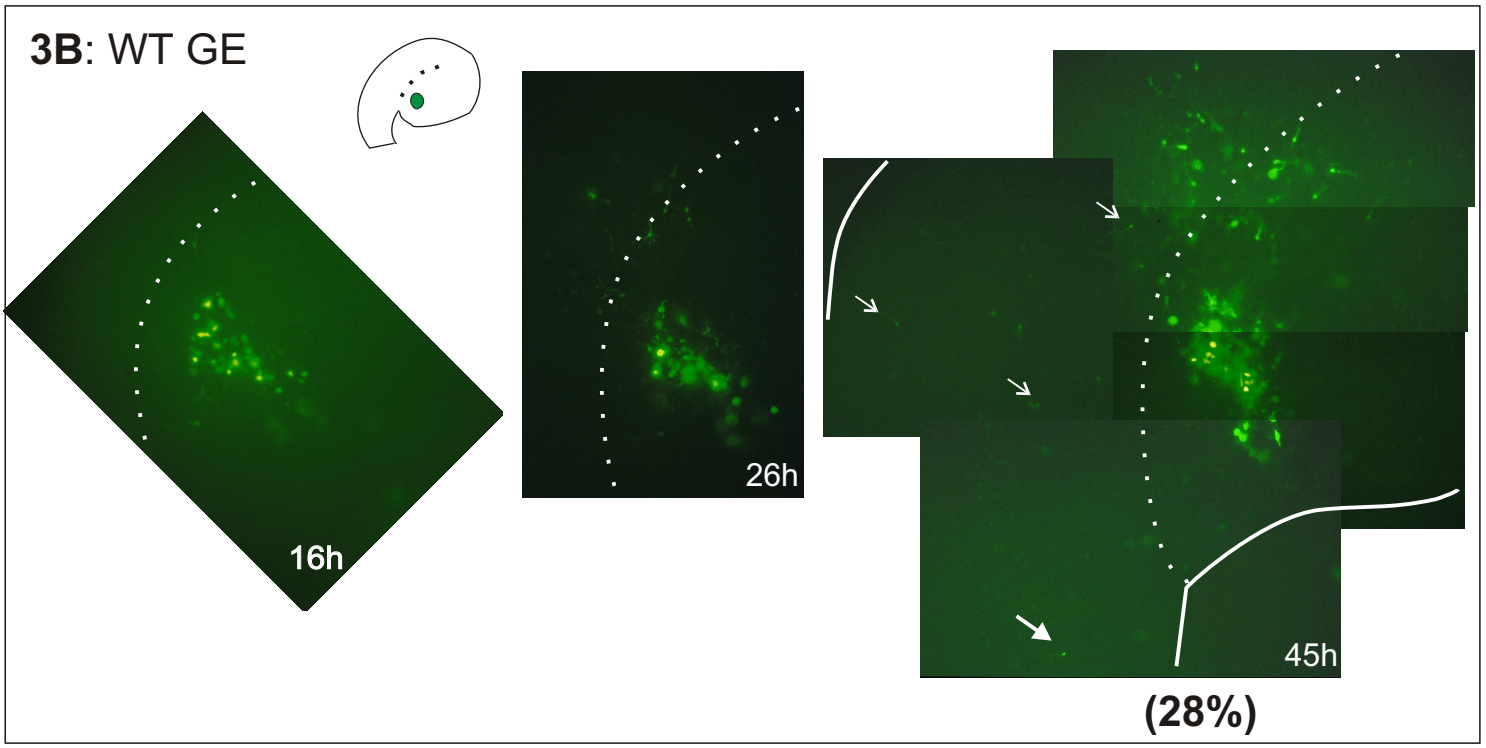

Figure 3: GFP-adenovirus injections into the cortical side or GE side of the boundary
Telencephalic slices from E14 wild-type mice were injected with EGFP-adenovirus in the cortex (A) or in the GE (B) and photographed at different times after the injections as indicated in the figure. The small drawings on top represent the telencephalic slice schematically.
A- Injection into the cortex: dorsal and medial is up, ventral down, and lateral to the left. The green spot indicates the location of the GFP cells and the dotted line shows the cortico-striatal boundary. The white line in the fluorescence micrographs depicts the pial (left) and the ventricular surface (upper right). Radial and tangential migration of the fluorescent cells within the cortex is visible after 26 and 45 hours. No cell has crossed the boundary into the GE (lower right corner).
B- Injection into the GE: Fluorescent cells have spread within the GE and have crossed the boundary into the cortex. After 26 hours, two GFP cells are already found in the cortex and after 45 hours about 15 cells (some are indicated by small arrows). Most of the cells that have migrated from the GE into the cortex are located in the lateral cortex, but one cell (indicated by a larger arrow) is located at a more dorsal position. 28% indicates the percentage of migrating cells that entered into the cortex, analyzed in 9 slices.

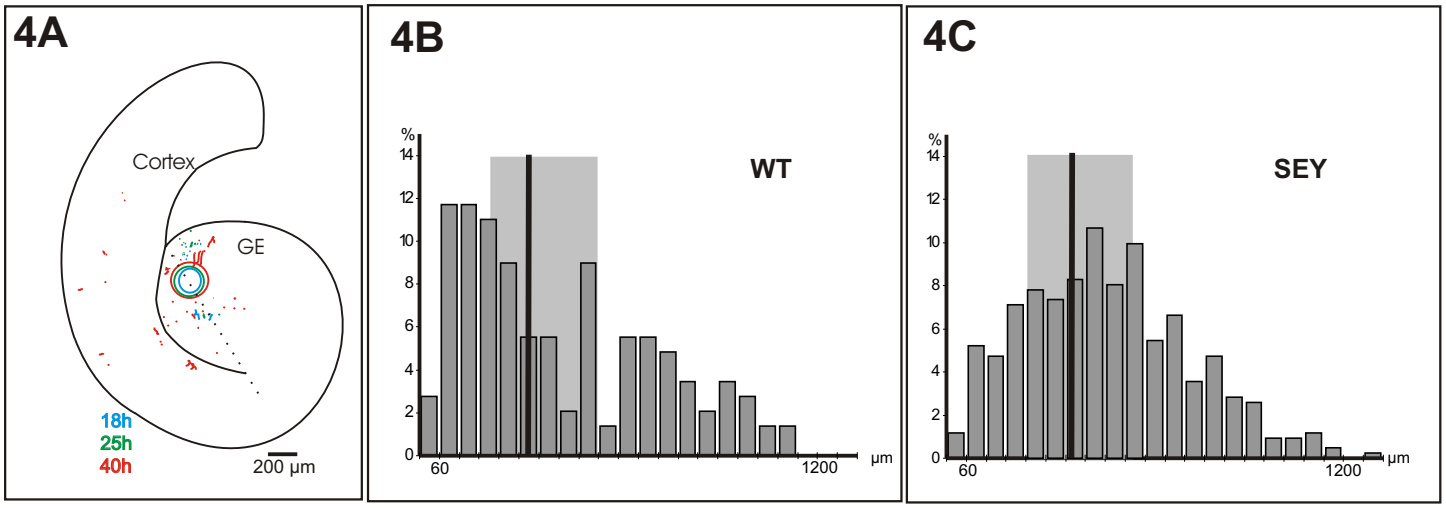

Figure 4: Analysis of cell migration

A- Schematic drawing of a telencephalic slice with cells as blue, green and red dots corresponding to their position at 18, 25 and 40 hours respectively after injection into the GE. The blue, green and red circles represent the site of injection, where many fluorescent cells are located. The dashed line divides the GE in two segments for the analysis of cells migrating towards and away from the boundary. The distances of migration were measured on such drawings as explained in the methods.

B, C Quantitative analysis of the migration distance of each GE cell migrating to or beyond the cortico-striatal boundary in slices from WT (A, n=7 slices) and Sey/Sey (B, n=7 slices). The maximum migratory distance was divided into 20 bins in order to determine the frequency of cells migrating for different distances. The X-axis depicts the distance of migration in µm (60 µm per bin) and the Y-axis the percentage of cells at this position. The position of the cortico-striatal boundary is indicated as a black line (mean from the different slices) and gray shading comprising the boundary location in the slices analyzed. Note the decrease in the number of cells at the distance of the boundary

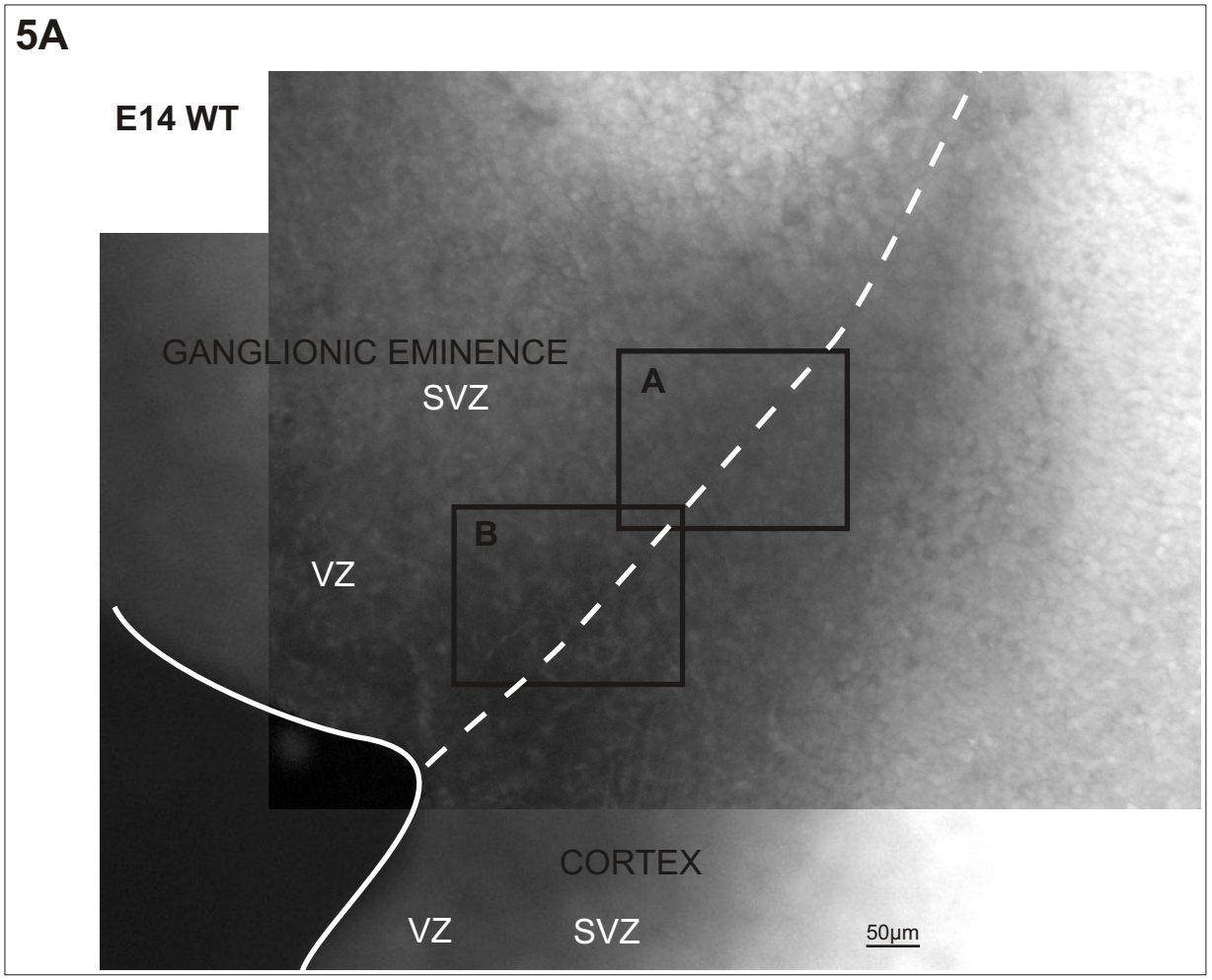

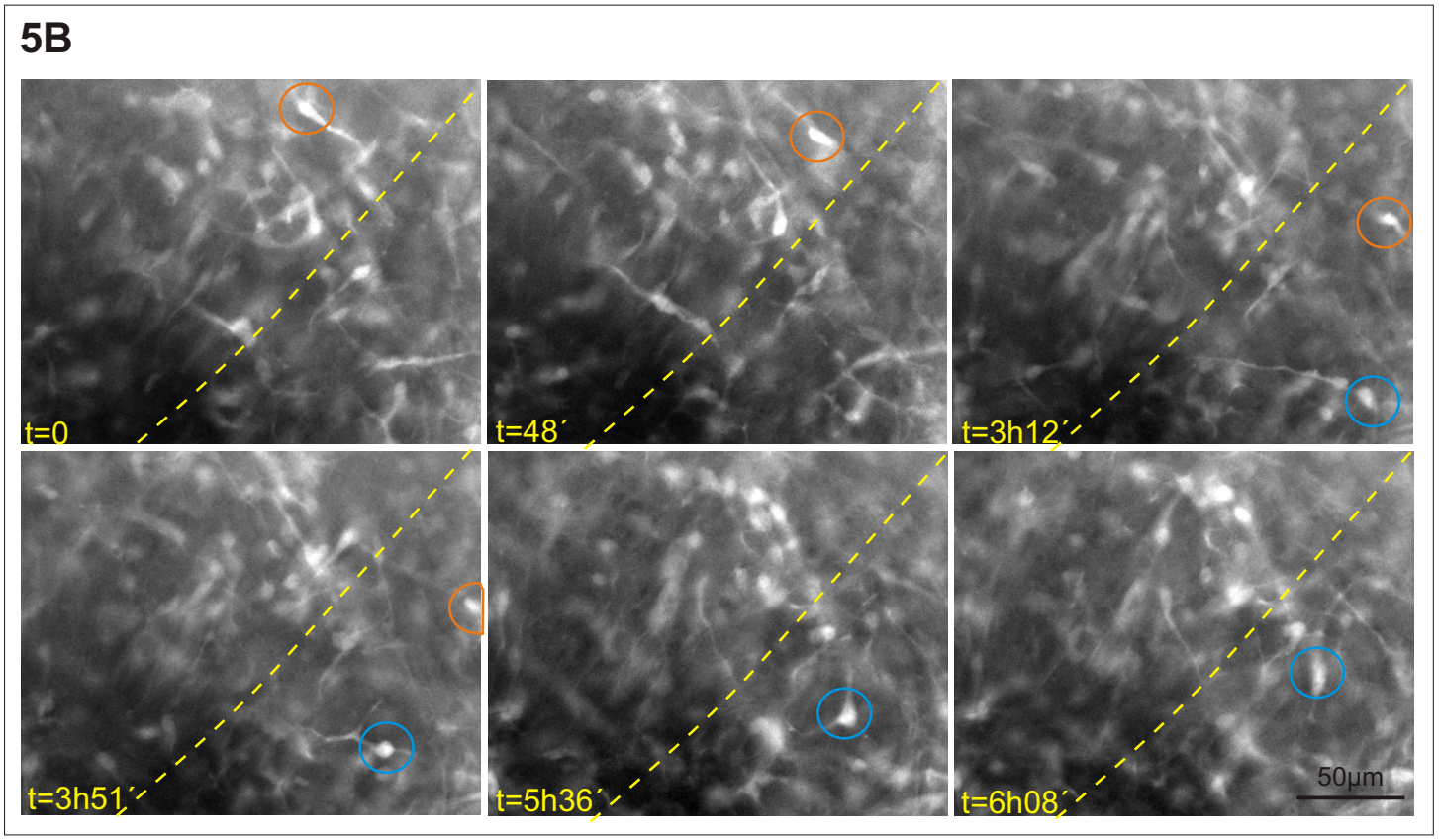

Figure 5: Time lapse recording of an E14 Tau^{GFPKI} telencephalic slice
A: Fluorescence micrograph of a frontal telencephalic slice depicting in the bright areas the GFP-expressing neurons in the differentiated zones of the cortex and GE. The frames A and B depict the regions recorded and the dashed line represents the cortico-striatal boundary. VZ= ventricular zone, SVZ= subventricular zone.
B: example of migrating cells: Two migrating cells in the field of view B are encircled in blue and orange respectively, and their position at 6 time points (indicated in the bottom left corner) reveals their migration path. The orange encircled cell crossed the boundary (represented by a dashed line) from the GE into the cortex. The blue encircled cell in the cortex made a 90° turn next to the boundary.

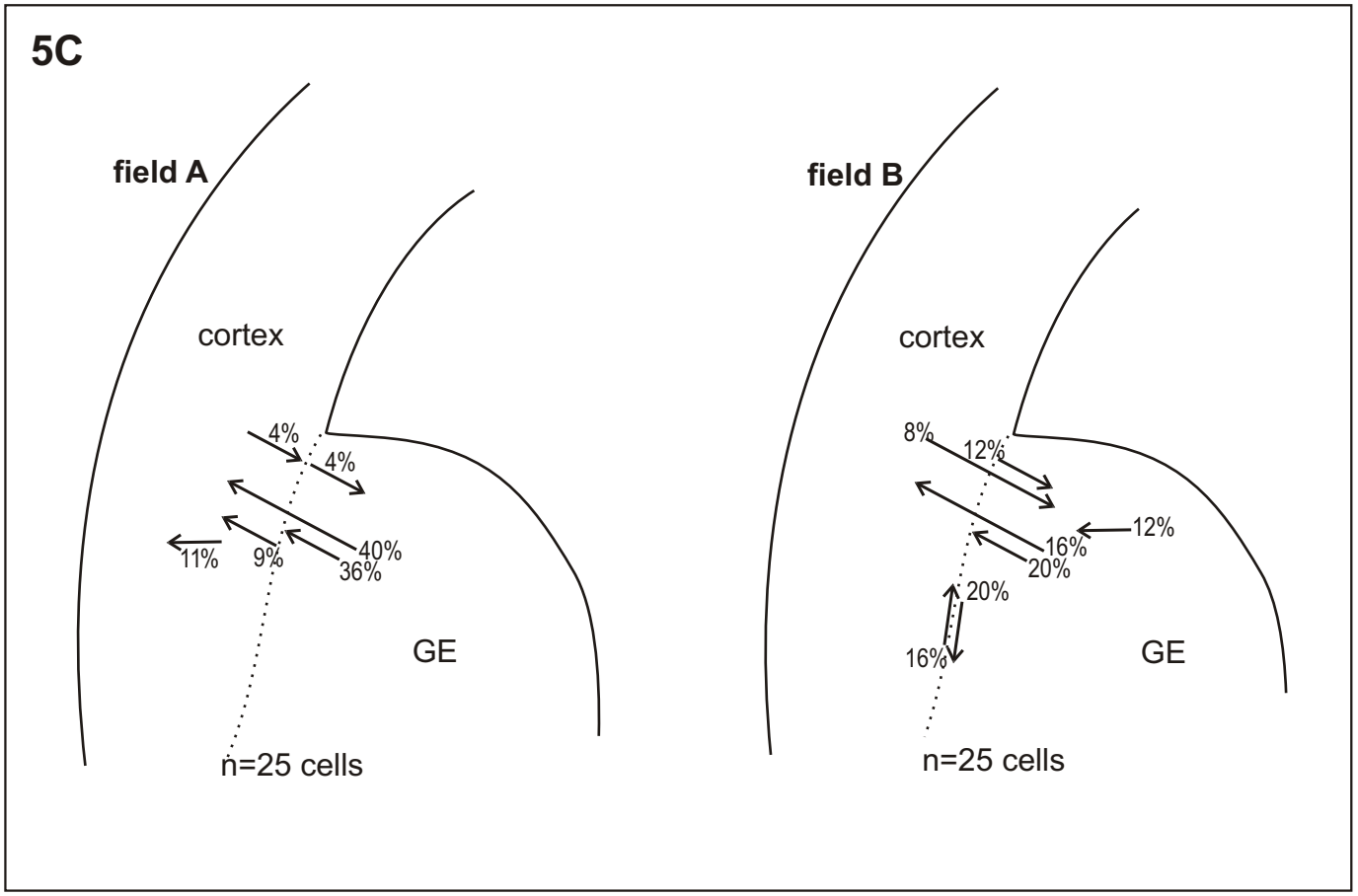

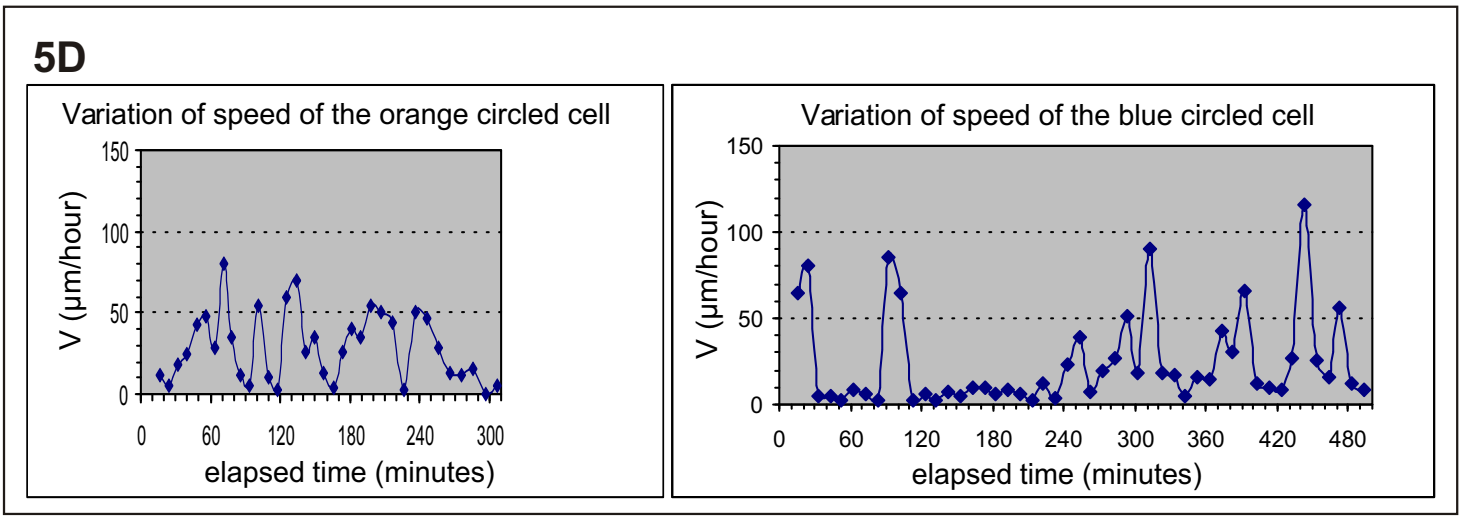

Figure 5C: classification of the directions of migration: The main migrating directions recorded around the cortico-striatal boundary are represented schematically. The arrows indicate the path of migration, and the numbers above the arrows indicate the proportion of cells migrating along this path.
5D: Variation of the speed of the migrating cells: The speed of migration of the two cells represented in C has been calculated at each recording point (every 10 minutes) and is shown in a graph, revealing the stop- and-go way of migration. Note that cell circled in blue remains in the same location for about 2 hours while searching for its new direction.

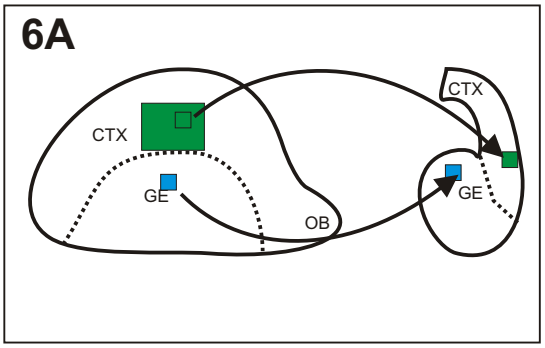

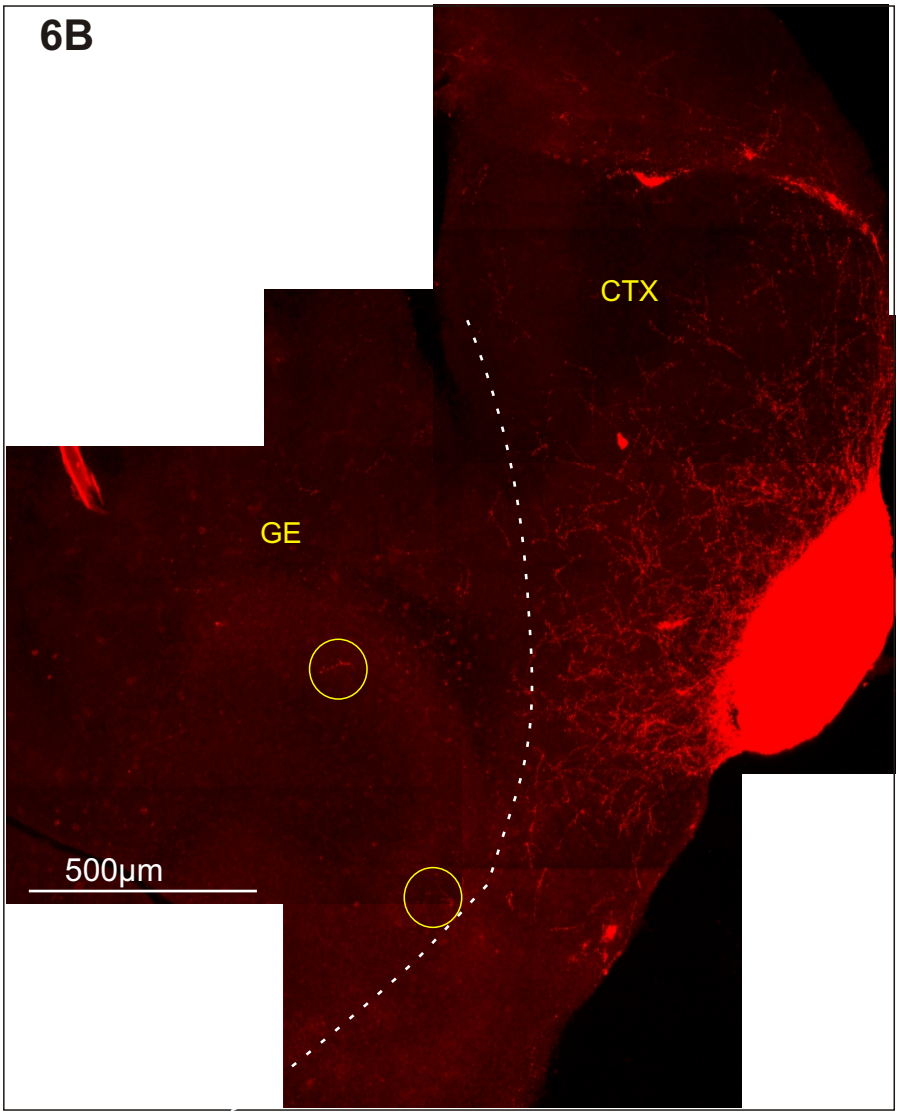

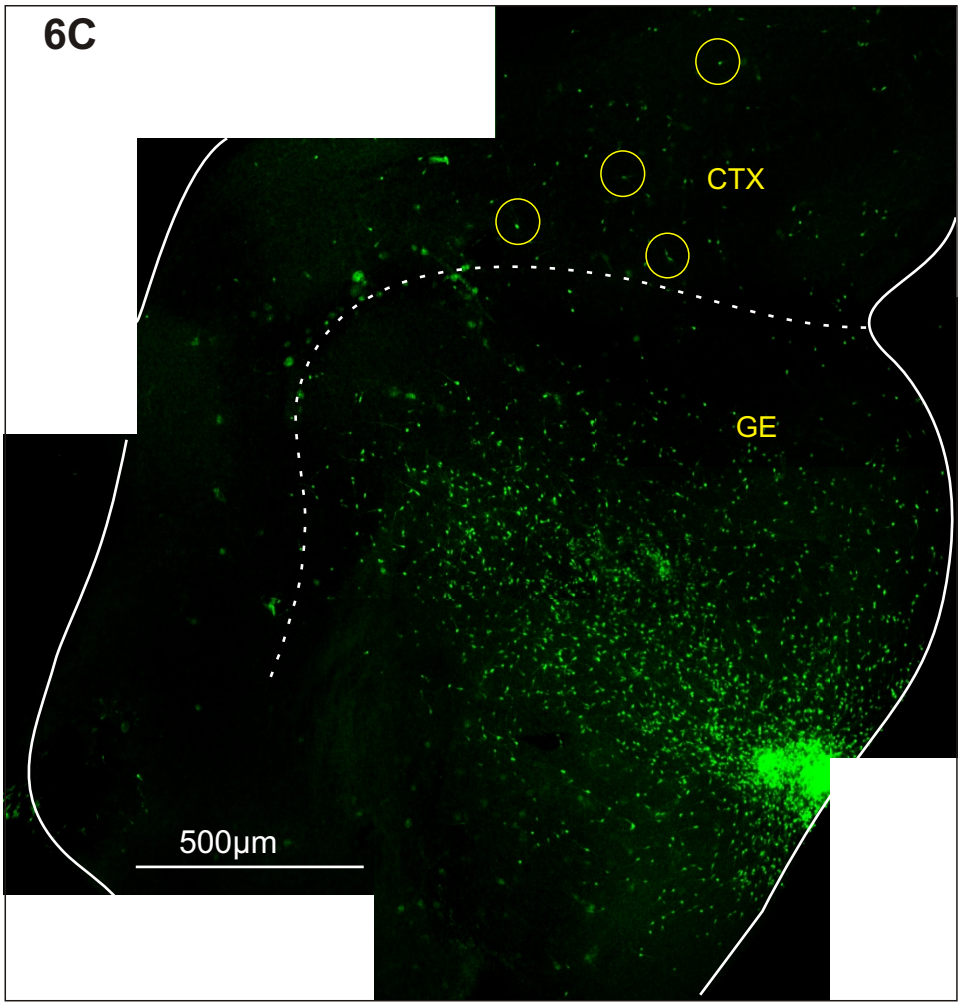

Figure 6: Transplantation in slice culture
A: Schematic representation of the experimental paradigm. A small piece of the donor telencephalon (either green mouse or WT mouse) is transplanted onto the host slice (either WT mouse or rat).Ctx= cortex, OB= olfactory bulb.
B: example of a mouse cortex transplant (E14) onto the cortex of a rat slice (E16). After two days in culture the slice has been stained with M2M6 antiserum, revealing the migrating mouse cells out of the transplant.
C: Example of a green mouse GE transplant (E14) onto the GE of a WT mouse slice (E14). The slice has been fixed after 2 days of culture. In B and C, a dotted white line depicts the boundary and yellow circles indicate cells that have migrated out of the transplant.

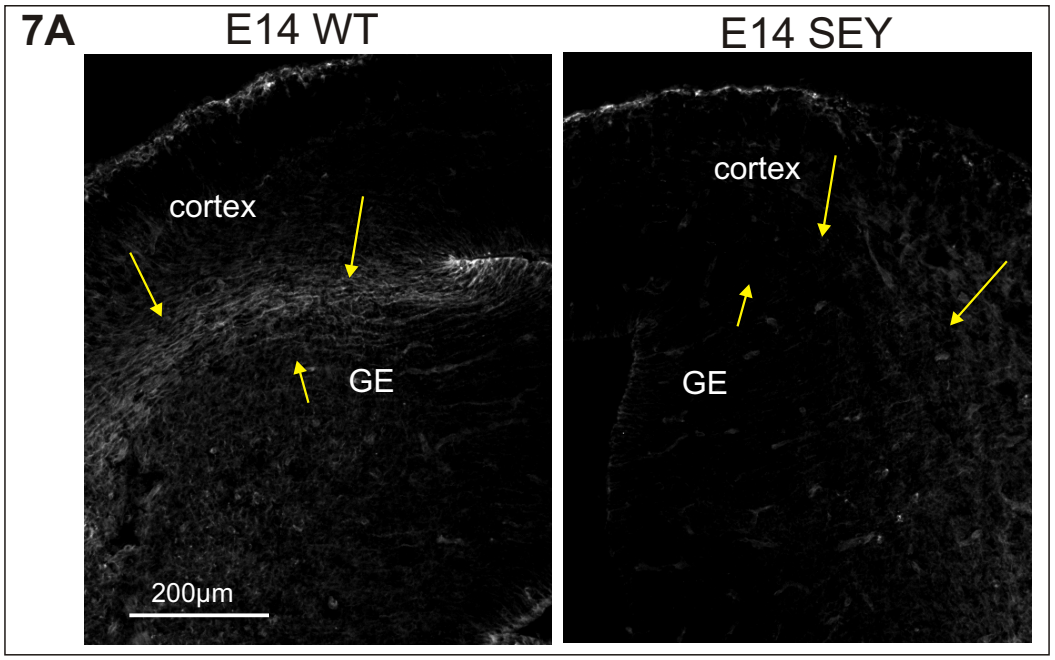

Figure 7A: absence of radial glia fascicle in *Sey/Sey*
E14 telencephalic WT and *Sey/Sey* slice that have been stained by the 9-4 antibody, revealing the absence of the radial fascicle in the *Sey/Sey* boundary region. The arrows point to the location of the fascicle.

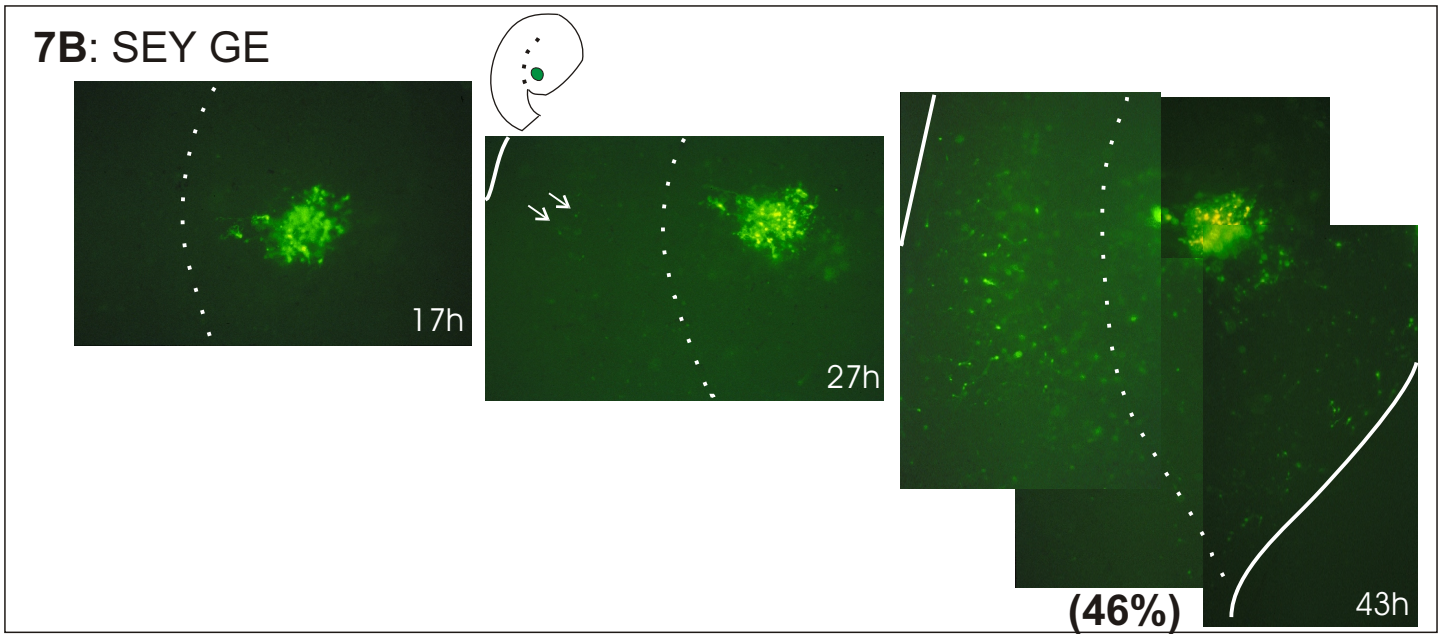

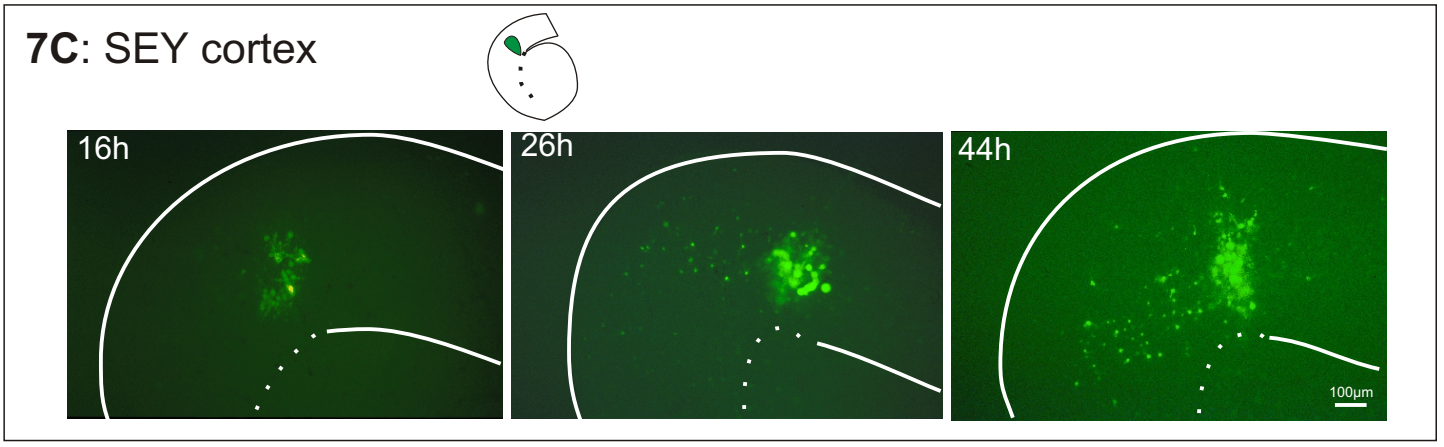

Figure 7B: Injections into the GE side of the boundary
Telencephalic slices from E14 *Sey/Sey* were injected with EGFP-adenovirus and photographed at the different times after injection as indicated in the figure. The schematic drawing indicates the injection site close to the boundary, as described in Fig. 3. The dotted line indicates the cortico-striatal boundary. Fluorescent cells have spread within the GE and have crossed the boundary into the cortex. Note the larger number of GFP-cells in the cortex of the *Sey/Sey* littermate. Small arrows indicate two of the three cells that have crossed the boundary into the cortex after 27 hours. After 43 hours, about 25 cells have migrated to the cortex. 46% indicates the percentage of migrating cells that entered into the cortex, counted in a total of 9 slices.

Figure 7C: Injections into the cortical side of the boundary
Telencephalic slices from E14 *Sey/Sey* were injected with EGFP-adenovirus in the cortex and photographed at different times after the injections as indicated in the figure. The small drawing on top schematically depicts the telencephalic slice. Dorsal and medial is up, ventral down, and lateral to the left. The green spot indicates the location of the GFP cells and the dotted line shows the cortico-striatal boundary. Dorsal and medial is up, ventral down, and lateral to the left. The white line in the fluorescent micrographs depicts the pial (lower left to right) and the ventricular surface (lower right). Radial and tangential migration of the fluorescent cells within the cortex is visible after 26 and 44 hours.

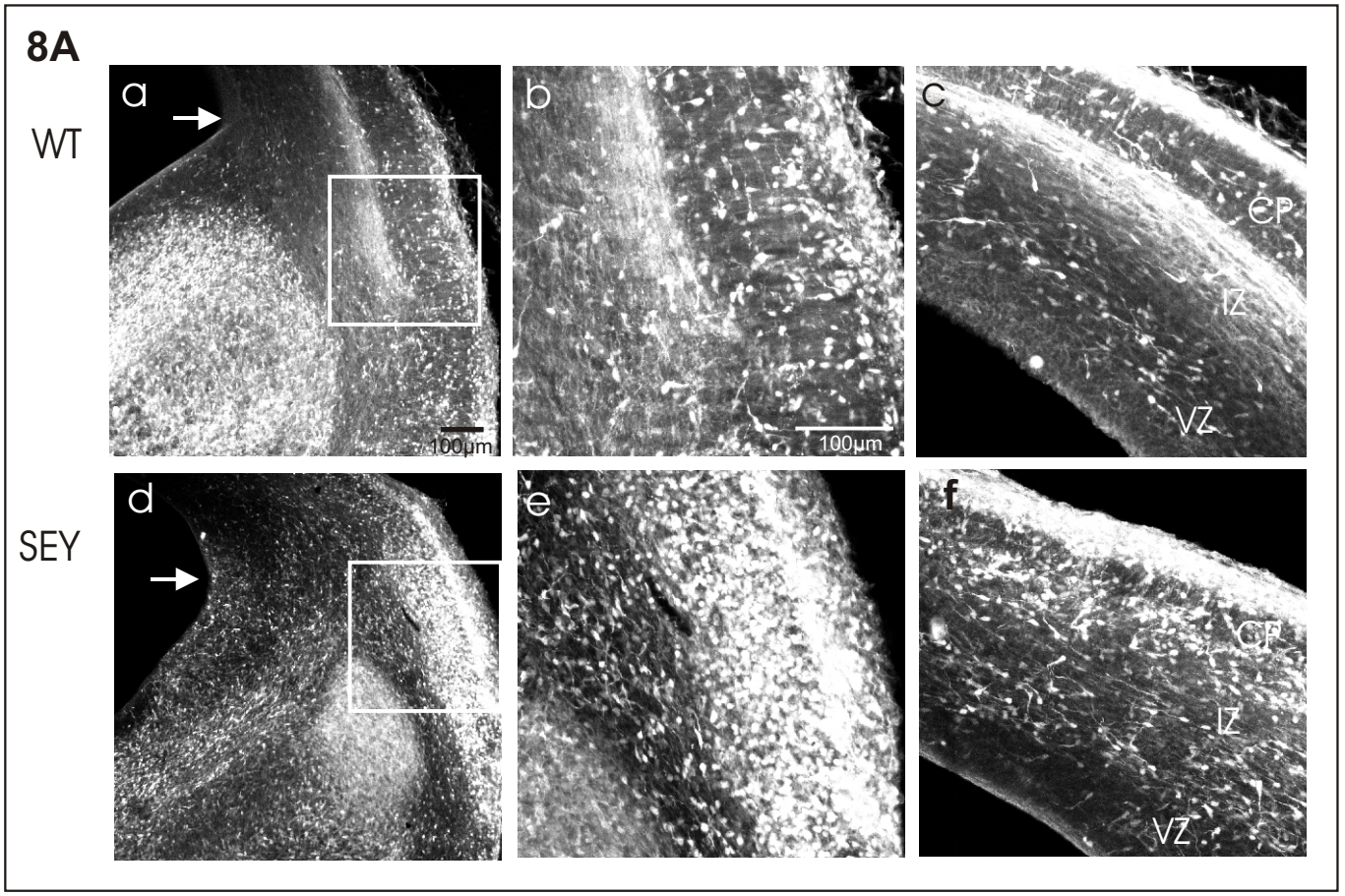

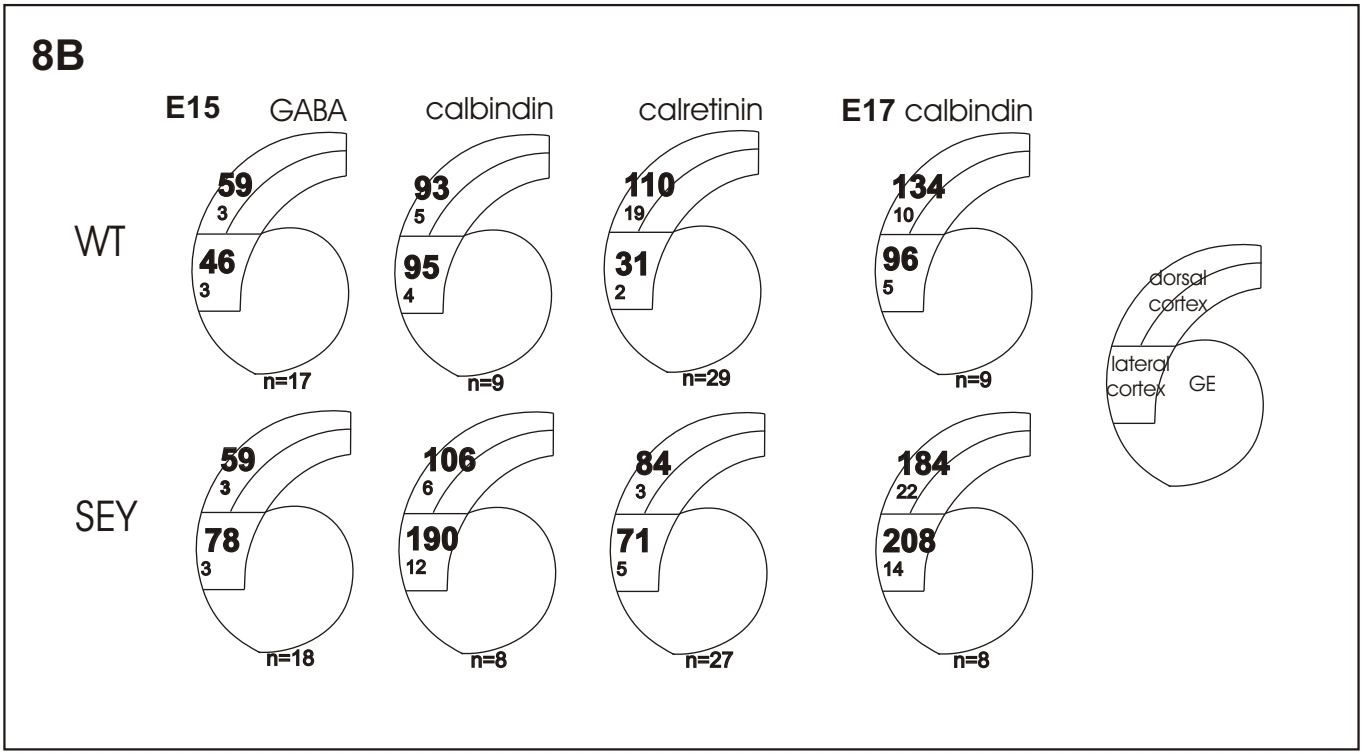

Figure 8A: Increase of calbindin-positive cells in the lateral cortex of *Pax6*-mutant mice
Fluorescent micrographs of 100 µm coronal sections of an embryonic day 15 telencephalon of wild-type (a-c) and *Sey/Sey* (d-f) littermates immunostained for calbindin. a and d depict a lower magnification, showing the pial surface on the right side and the ventricle as the dark part in the upper left corner. The sulcus separating the ventricular zone of the cortex (up) from the GE (down) is indicated by an arrow. The boxed areas in a and d depict the part of the lateral cortex shown in higher magnification in b and e, respectively. c and f are fluorescent micrographs of the dorsal cortex of the same sections at the same magnification as b and e. The layers of the developing cortex are indicated in c and f. VZ: ventricular zone, IZ: intermediate zone, CP: cortical plate. Note the higher number of calbindin-positive cells in the lateral cortex of *Sey/Sey* mice (e) as compared to WT (b).

Figure 8B: Quantitative analysis of GABAergic cells in WT and *Sey/Sey* telencephalon
The mean number of calbindin-, calretinin- and GABA-immuno-positive cells in the lateral and dorsal cortex are depicted in schematic drawings of sections from embryonic day 15 and 17 telencephalon. The standard error of the mean and the number of slices analysed are depicted in small print. For details of counting see Methods. Note the increase of GABA-, calbindin- and calretinin-positive cells in the lateral cortex of *Sey/Sey* littermates at E15/17 compared to WT. This increase extends into further dorsal regions by E17.

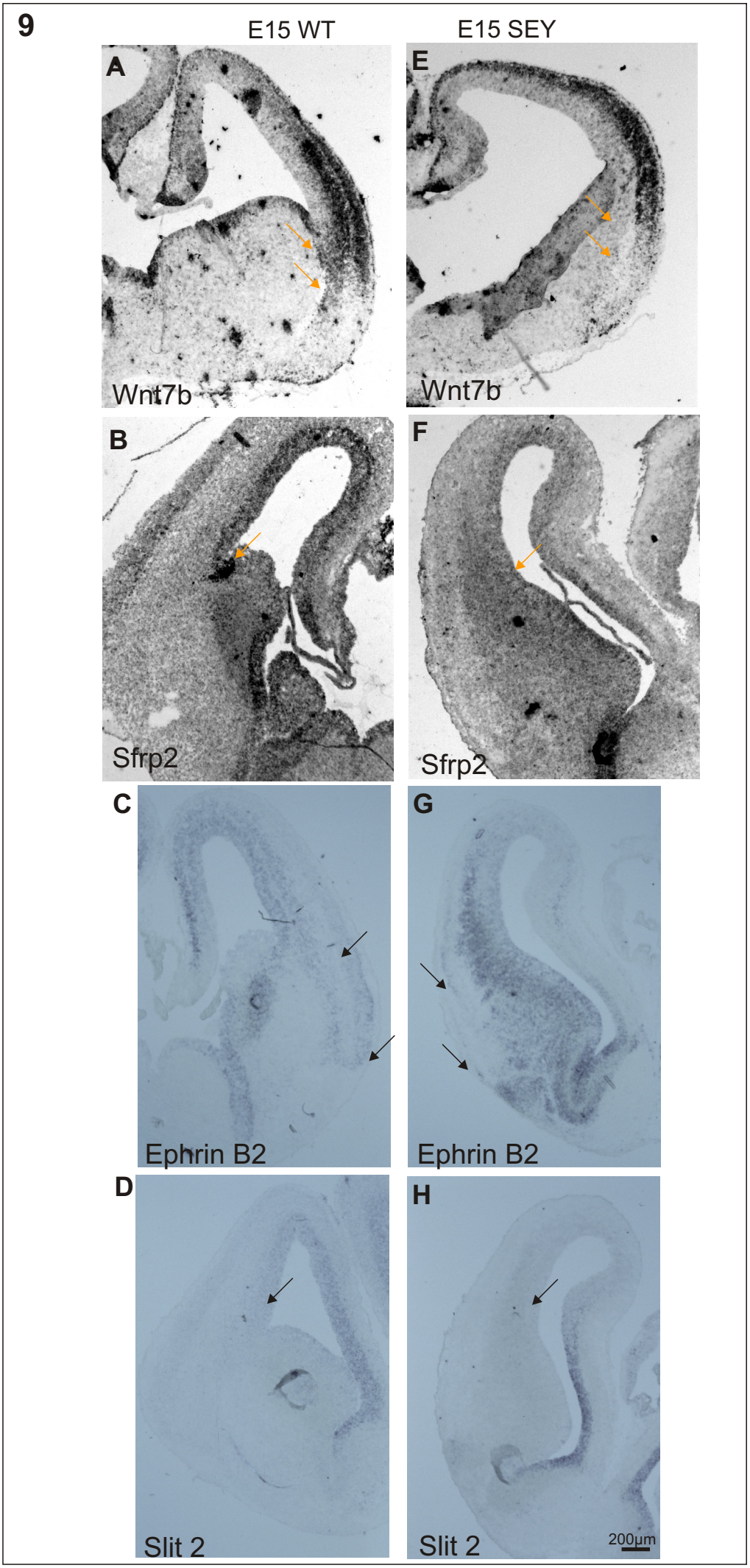

Figure 9: molecular changes affecting the Sey/Sey cortex and boundary
Non-radioactive in-situ hybridizations revealing the expression pattern of Wnt7b (A,E), Sfrp2 (B,F), Slit2 (C,G) and ephrin B2 (D,H) in WT (A-D) and *Sey/Sey* (E-H) telencephalic slices. The dark colour reveals the region of expression of the respective gene. The arrows point to regions where in Sey/Sey the gene expression is missing: Wnt7b and Sfrp2 are missing in the Sey/Sey boundary (A, E and B, F), Ephrin B2 is missing in the Sey/Sey lateral cortex (C, G) and Slit2 is missing in the Sey/Sey cortex (D, H). Scale bar in A-H: 200µm.

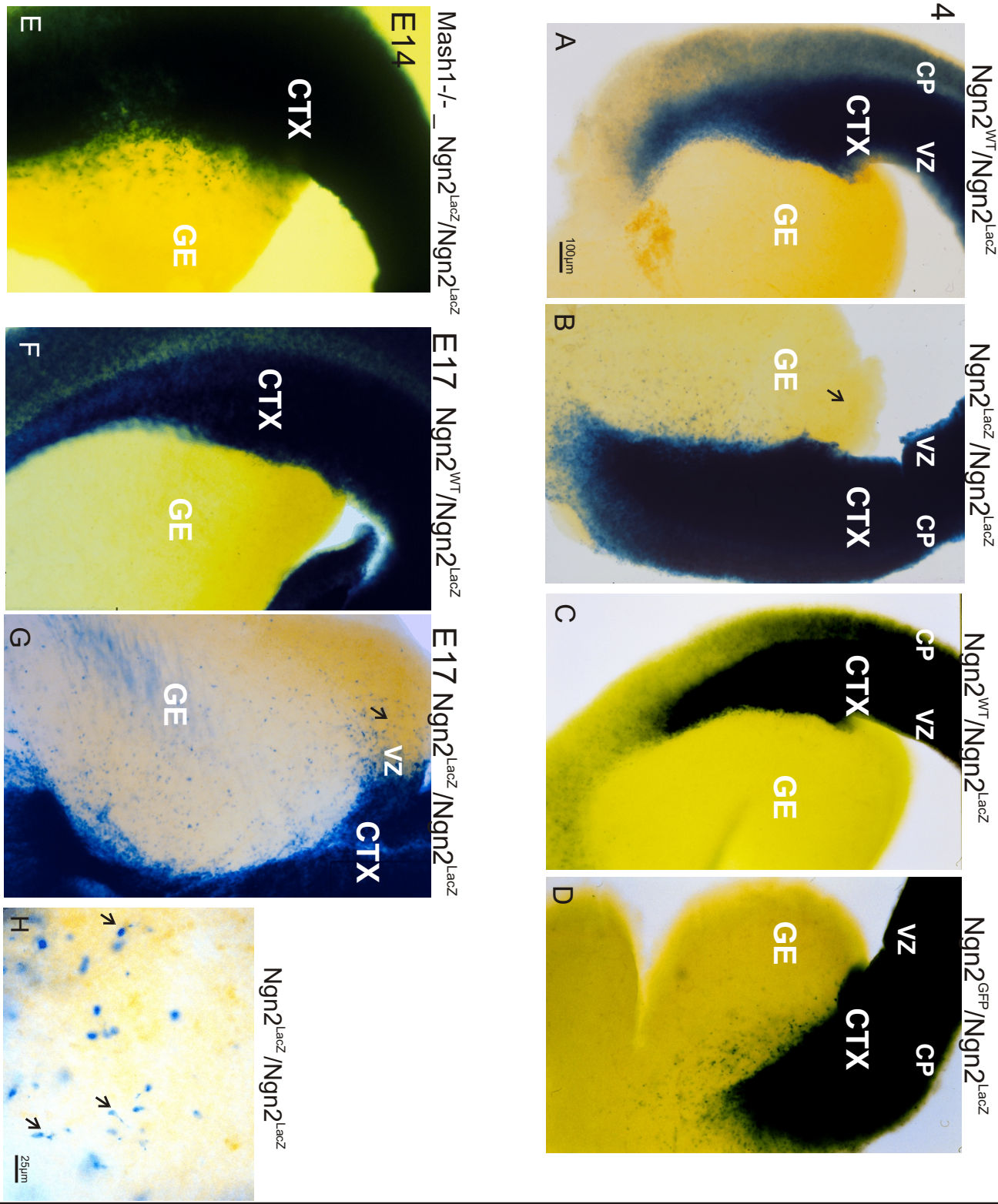

Figure 10: Ectopic ß-galactosidase containing cells in the ganglionic eminence of *Ngn2^{LacZ}/Ngn2^{LacZ} mice*
Sections of the telencephalon from *Ngn2^{LacZKI}* mice at E14 (A-E, H) and E17 (F, G) showing the expression pattern of ß-galactosidase in blue.
A: *Ngn2^{WT}/Ngn2^{LacZ}* heterozygous, and B: *Ngn2^{LacZ}/Ngn2^{LacZ}* homozygous littermates: The heterozygous mutant reveals a sharp boundary of ß-galactosidase staining between the positive cortex (CTX) and the negative ganglionic eminence (GE), whereas the homozygous mutant contains many ß-galactosidase positive cells scattered in the GE. The arrow in B indicates the absence of ectopic cells in the ventricular zone (VZ) of the GE, in contrast to later stages (E17, G). CP indicates the cortical plate containing postmitotic neurons.
C: *Ngn2^{WT}/Ngn2^{LacZ}* heterozygous, and D: *Ngn2^{GFP}/Ngn2^{LacZ}* homozygous mutant littermates: in the homozygous mutant carrying only one *LacZ* allele (D), ectopic cells are present in the GE, in a similar amount as in B.
E: *Ngn2^{LacZ}/Ngn2^{LacZ}* - Mash1-/- homozygous double mutant: In the absence of Mash1, ectopic ß-galactosidase positive cells are still present in the GE.
F *Ngn2^{WT}/Ngn2^{LacZ}* heterozygous, and G: *Ngn2^{LacZ}/Ngn2^{LacZ}* homozygous littermates at E17: The number of ectopic cells in the GE has increased compared to E14. The arrow in F indicates ectopic cells in the ventricular zone of the GE.
H: higher magnification of the ectopic cells in the GE of *Ngn2^{LacZ}/Ngn2^{LacZ}* homozygous mutants at E14. The arrows depict cells with morphologies characteristic of migratory neurons.
Scale bar in A-G: 100µm; in H: 25µm.

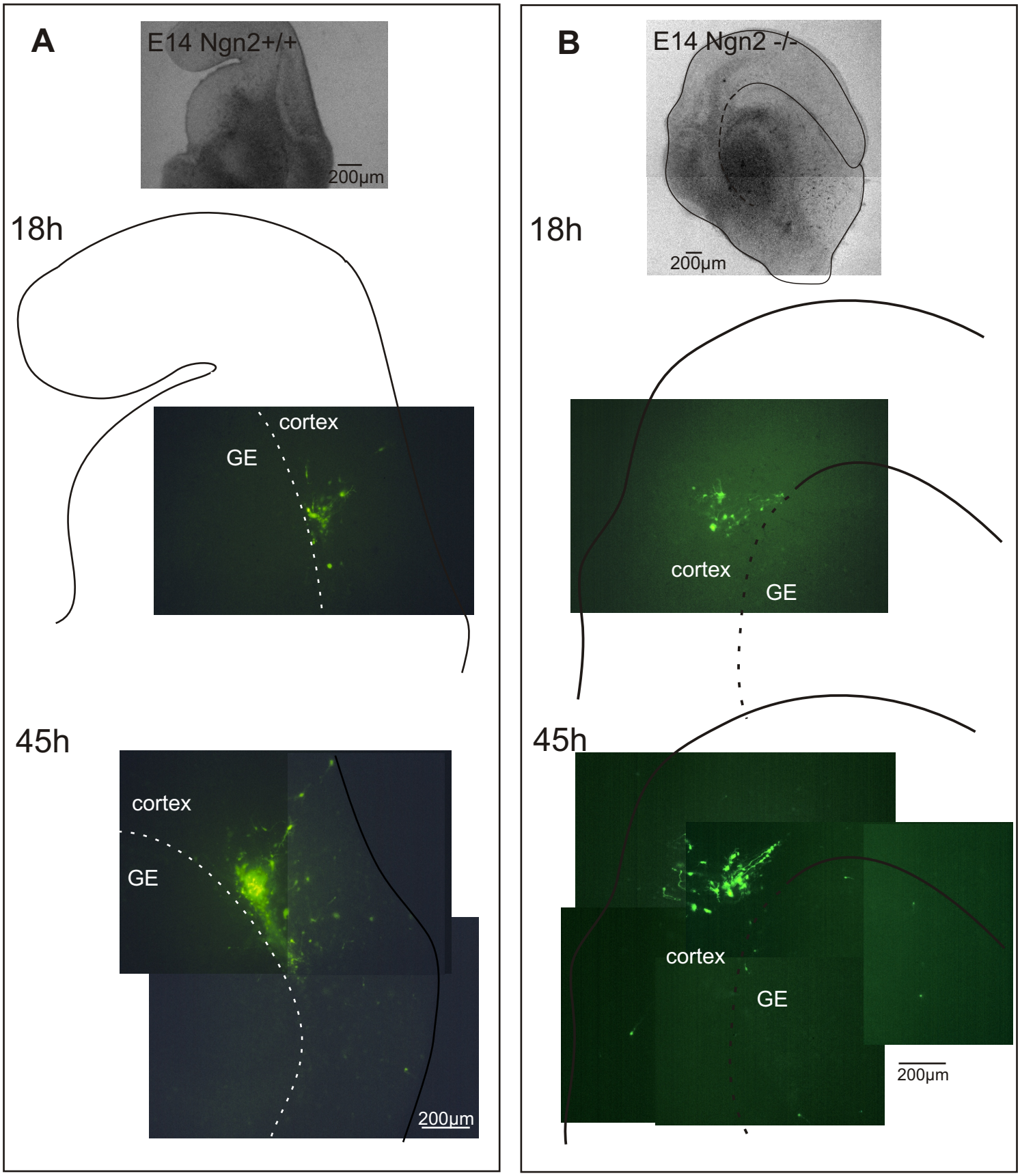

Figure 11: Cortico-striatal cell migration is increased in *Ngn2*^{LacZ}/*Ngn2*^{LacZ} mice
EGFP-adenovirus was injected focally in the cortex of a telencephalic slice from wild-type (WT=*Ngn*2+/+ in A) and a homozygous *Ngn*2-mutant littermate at E14. Micrographs of the injected sections were taken 18 hours and 45 hours after the virus injection as indicated in the figure. The phase contrast micrograph and fluorescence micrograph after 18 hours depict the position of the injection site, in the cortex, and the dashed line indicates the cortico-striatal boundary. Note that cells spread further away from the injection site after 45 hours. However, no cortical cell has migrated into the GE in the WT telencephalic slice, while 4 cortical cells have entered the GE of a *Ngn*2-/- mouse. Scale bars: 200µm.

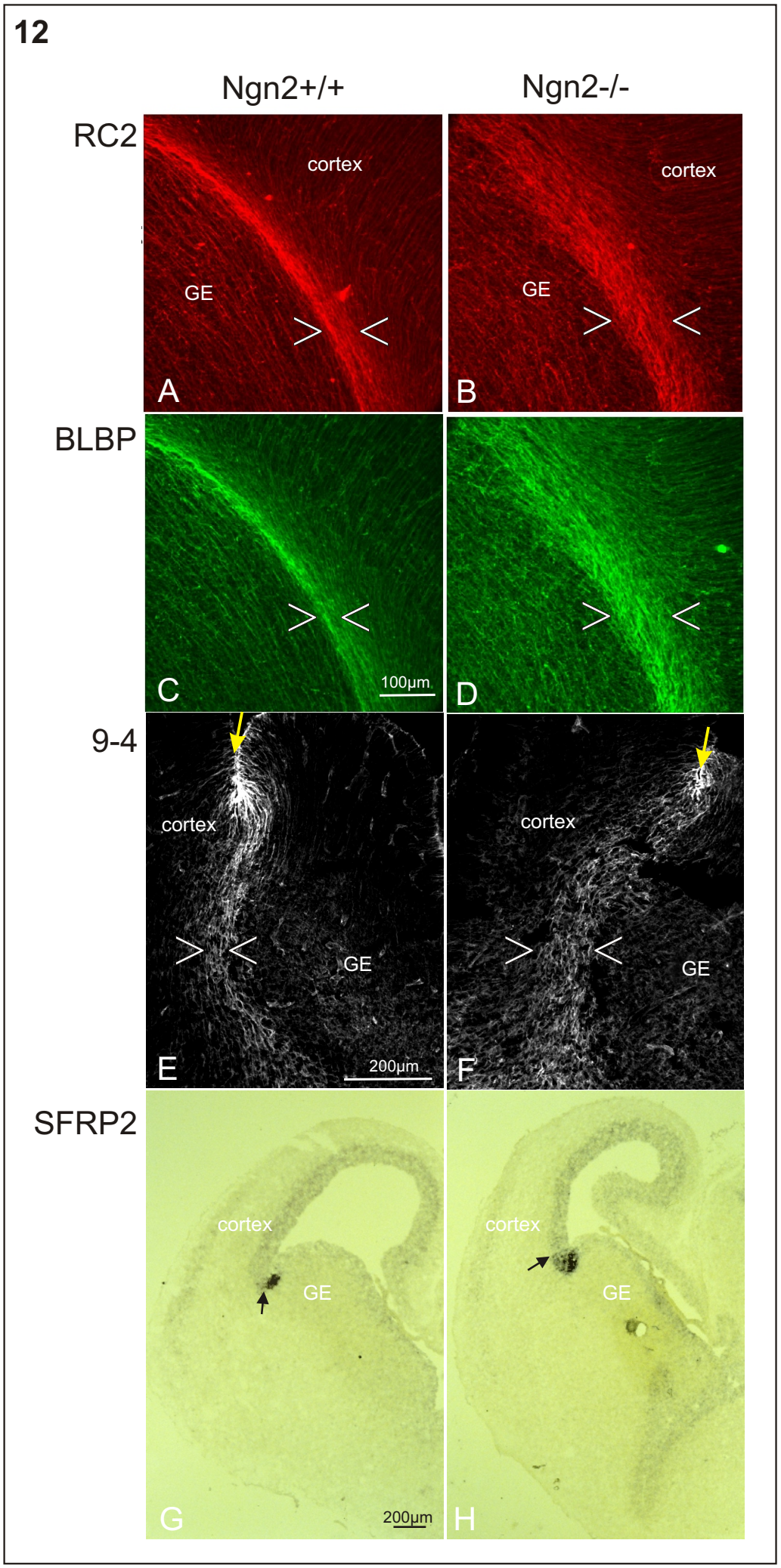

Figure 12: Broadening of the cortico-striatal boundary fascicle in *Ngn2*^{LacZ}/*Ngn2*^{LacZ} mice
Cortico-striatal boundary markers as indicated in the panel were detected in sections of telencephali at E16 (A-D) or E14 (E-H) in WT (A, C, E, G) and *Ngn2* homozygous mutant littermates (B, D, F, H). (A-F) show immunostainings for radial glia fibers. Note that the width of the radial glial fascicle indicated by triangles is prominently enlarged in the absence of *Ngn2*. The yellow arrow in (E,F) indicates the cortico-striatal sulcus.

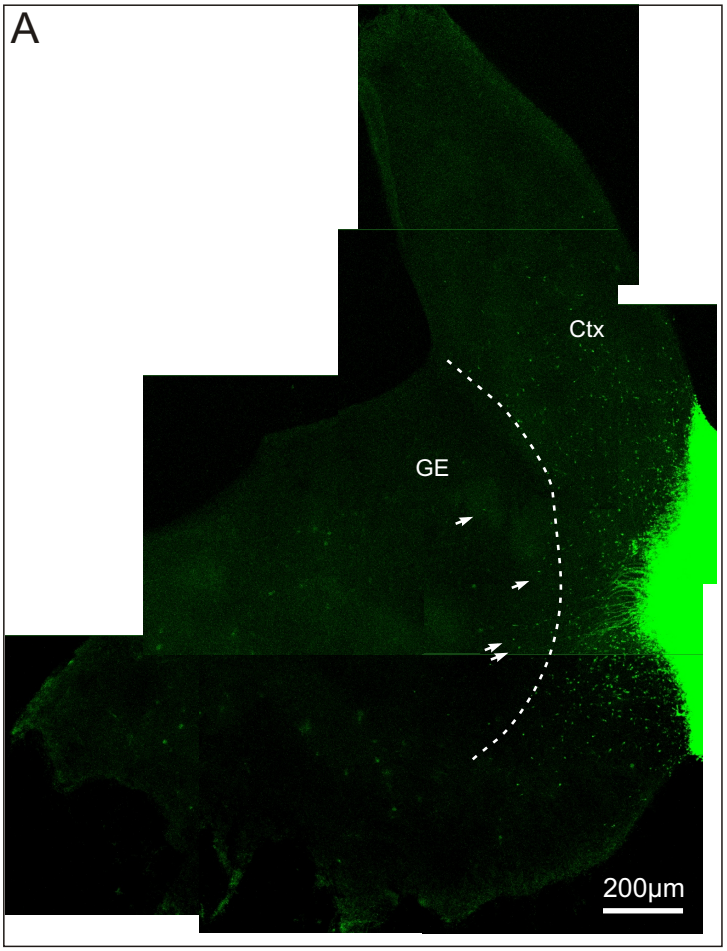

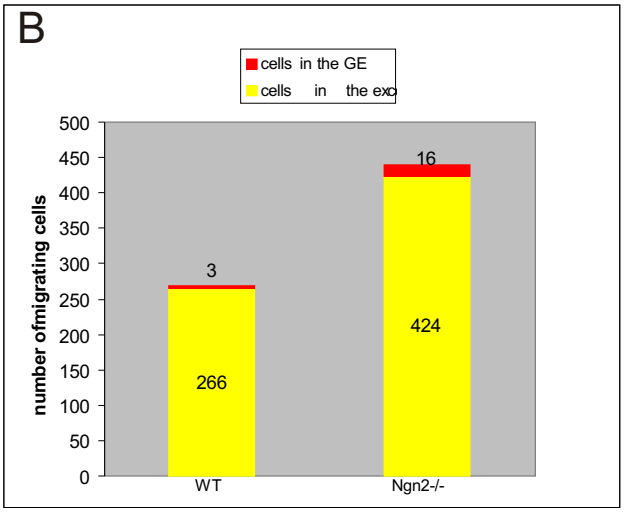

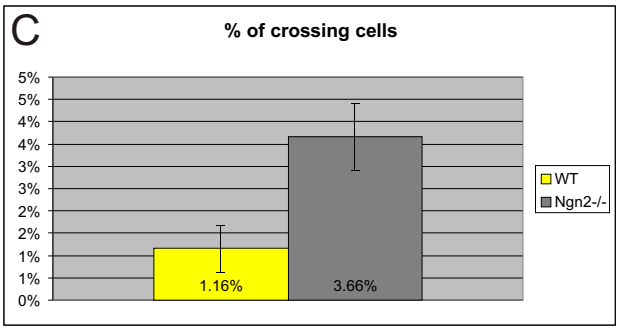

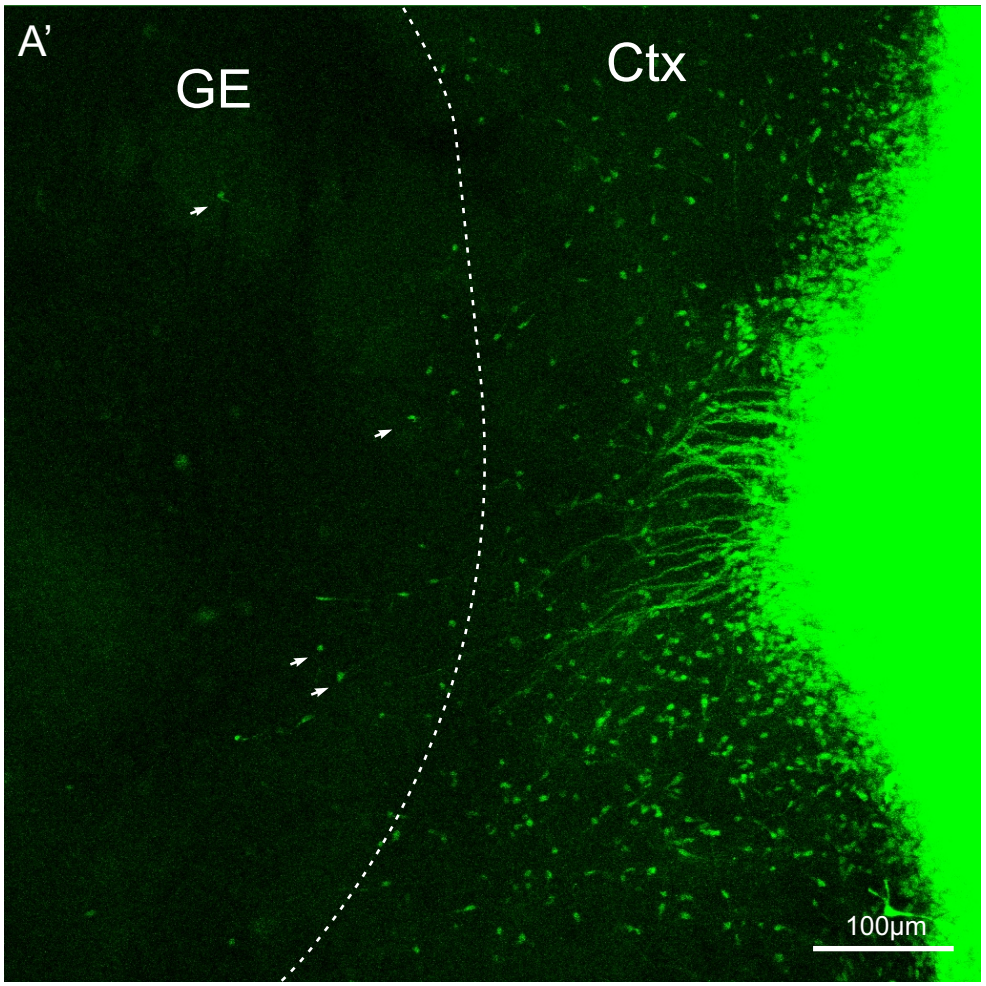

Figure 13: Non-cell-autonomous effect on cortico-striatal cell migration in *Ngn2*^{LacZ}/*Ngn2*^{LacZ} mice
A: Example of a homotypic transplantation of a small piece of cortex from the 'green mice' (Okabe et al., 1997) on a *Ngn2*-/- E14 cortex slice fixed after one day in vitro. Note that most GFP cells have migrated within the cortex and some of them have crossed the boundary (depicted by a dashed line) into the GE (depicted by arrows).
A': High power view of a part of the explant shown in A (see arrows for reference).
B: Quantification of the cells emigrating from transplants of WT cortex on slices from WT or *Ngn2*-/- littermates. Note that the overall number of migrating cells as well as the number of cortical cells entering the GE is higher on a *Ngn2*-/- substrate compared to WT.
C: The histogram depicts the proportion of cortical cells entering the GE amongst all cells emigrating from the cortex transplants (see B). Note that a 3x larger proportion of migrating cells cross the boundary into the GE on a *Ngn2*-/- than on a WT substrate.

14

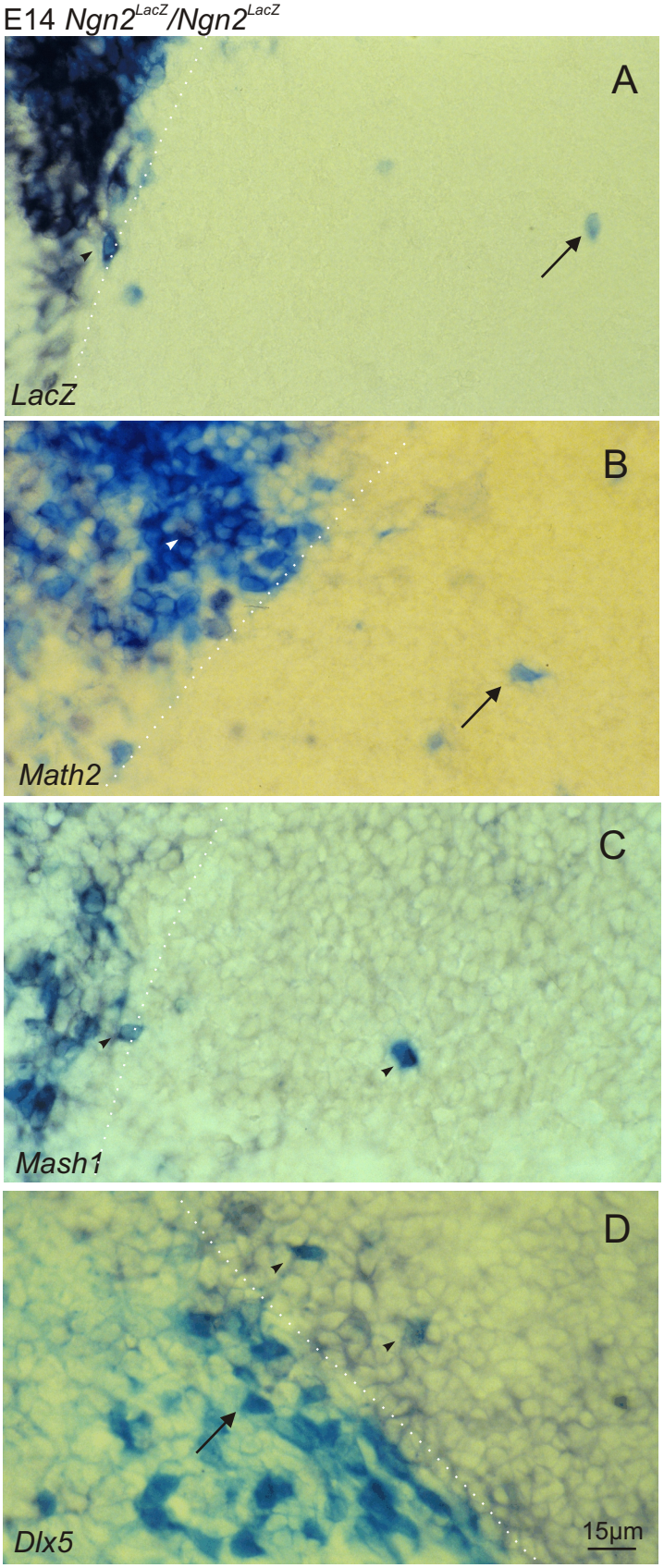

Figure 14: Cotrical cells entering the GE in *Ngn2^{LacZ}/Ngn2^{LacZ}* mice acquire a ventral identity
A-D depict the cortico-striatal border in sections of the telencephalon from E14 *Ngn2^{LacZ}/Ngn2^{LacZ}* mice stained for X-Gal (blue) and hybridized with the probes indicated in the panel (purple ring). Sections are oriented with the cortex to the left and the GE to the right. Double-positive cells are indicated by arrowheads, ß-galactosidase-positive cells negative for the respective transcripts are marked by an arrow. Note that ectopic cells loose expression of cortical genes (LacZ in the Ngn2-locus in A and Math2 in B), while they maintain (C) or acquire (D) expression of ventral genes such as Mash1 or Dlx5, respectively. The dotted white line represents the border between cortex and GE.

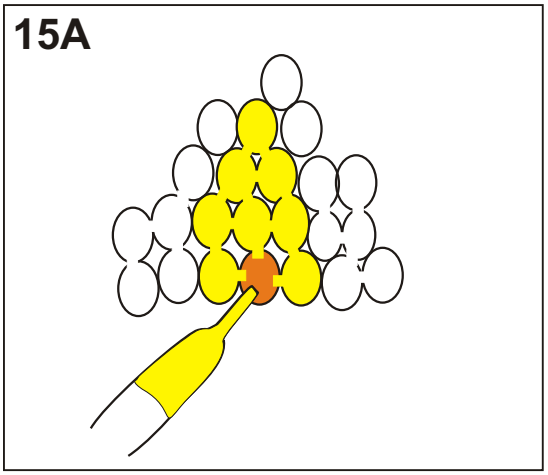

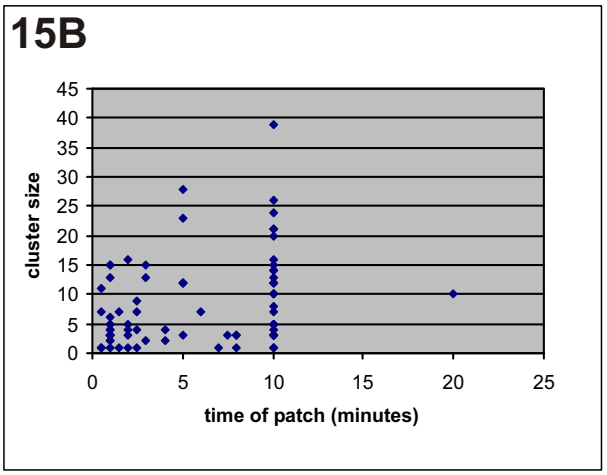

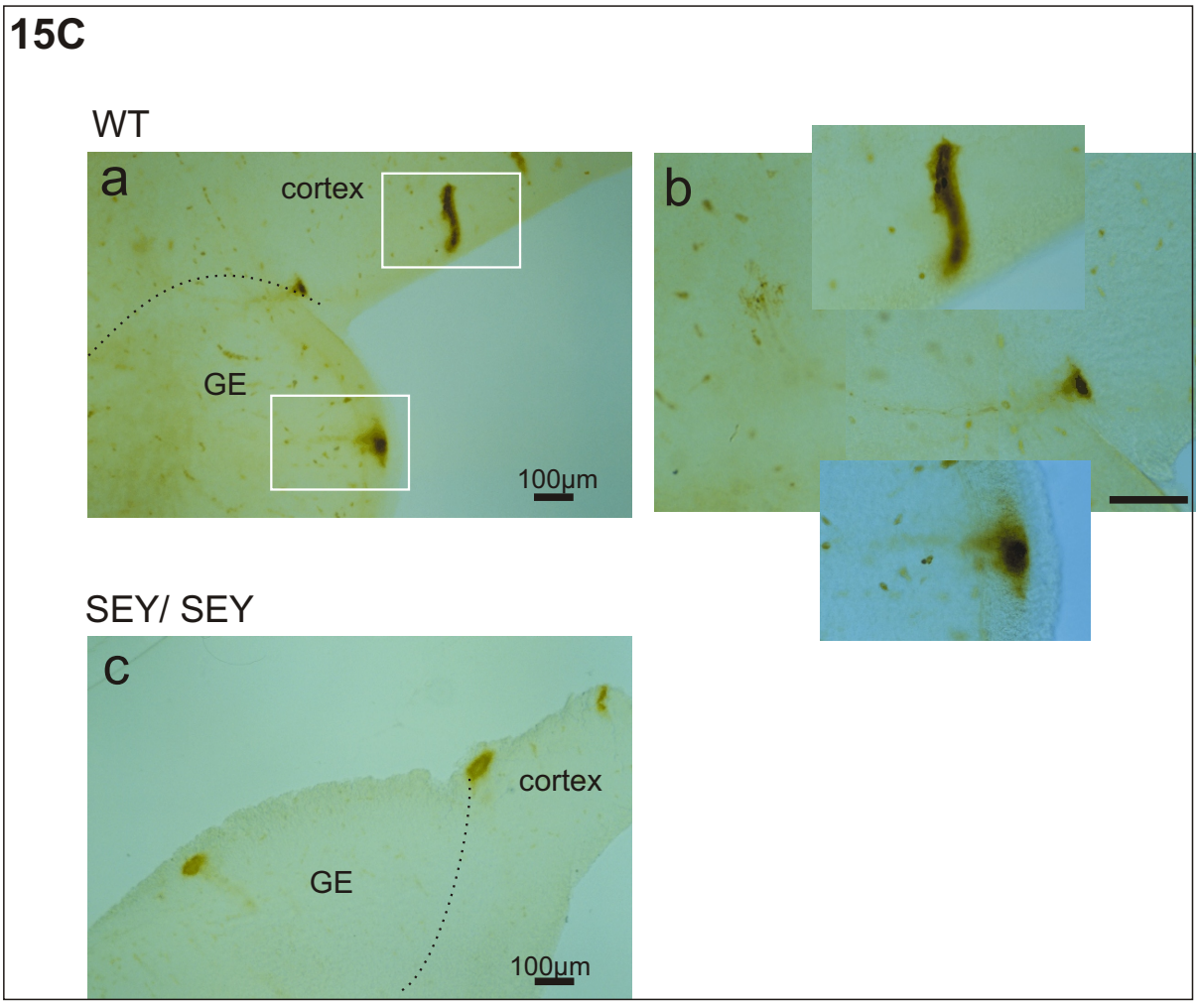

Figure 15A: Schematic representation of a cluster of cells connected via gap junctions. One cell within the cluster (represented in orange) is patched with an electrode containing neurobiotin (in the bottom left). Neurobiotin is small enough to pass through the gap junctions and enter into all the cells of the cluster.
Figure 15B: Graph depicting the number of cells contained in a cluster versus the respective duration of patch (=time of filling). Note that the dots are not arranged in a line, thus there is no correlation between cluster size and duration of patch.
Figure 15C: Examples of clusters filled with neurobiotin in the cortex, boundary and GE in WT (a, b) and Sey/Sey (c). The WT clusters in a are visible in b in a higher magnification. Scale bar in a, b and c: 100µm.

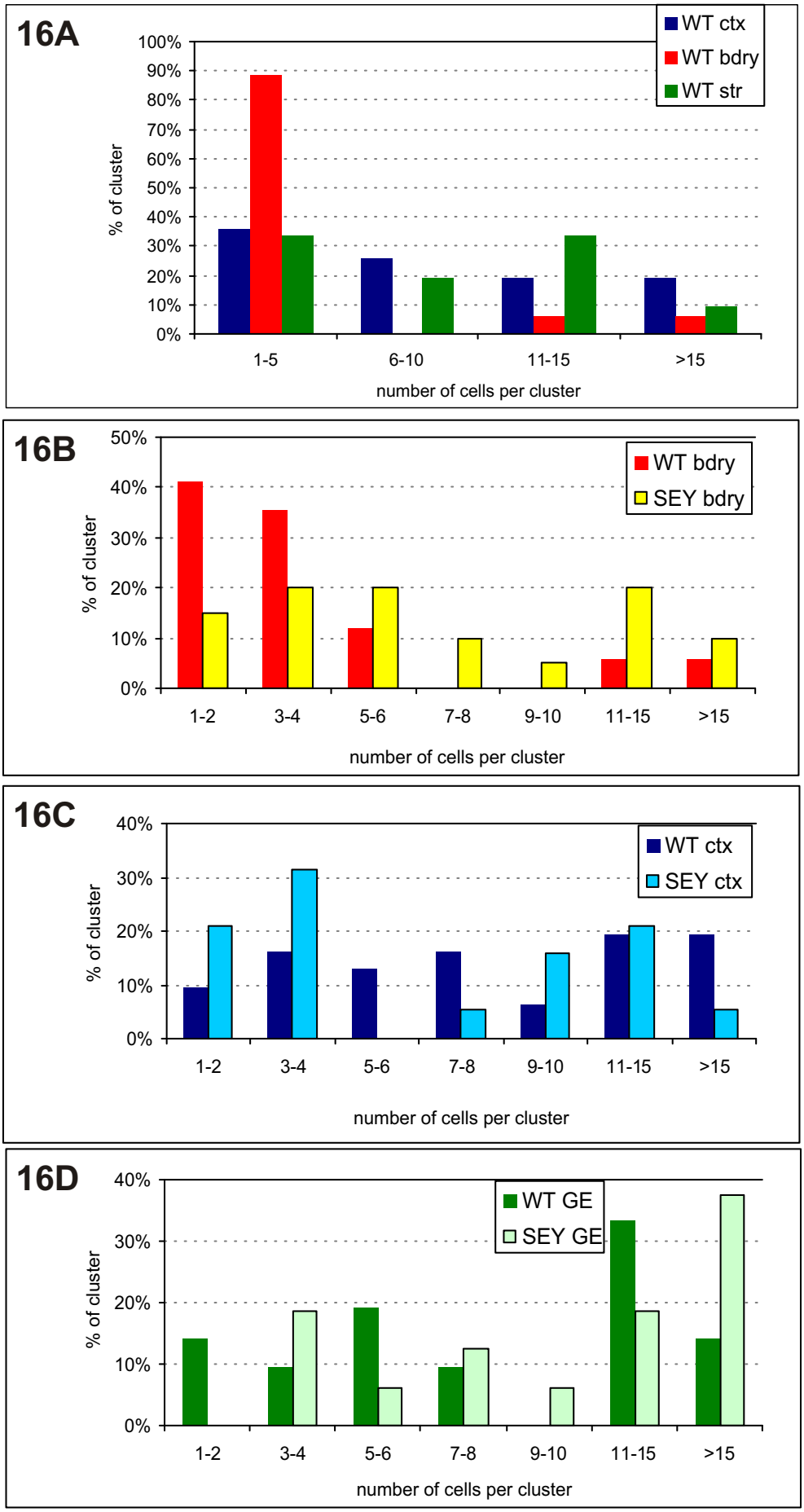

Figure 16: Distribution of the cluster size
The cluster size has been binned in 4 groups (A) or 7 groups (B-D) as indicated under the x axis, and the percentage of clusters belonging to the respective group are represented in y. The comparison between clusters of the cortex, boundary and GE in the WT is depicted in A, revealing the high proportion of small clusters in the boundary. Graphs B-D show the comparison between WT and Small-eye clusters in the boundary (B), cortex (C) and GE (D).

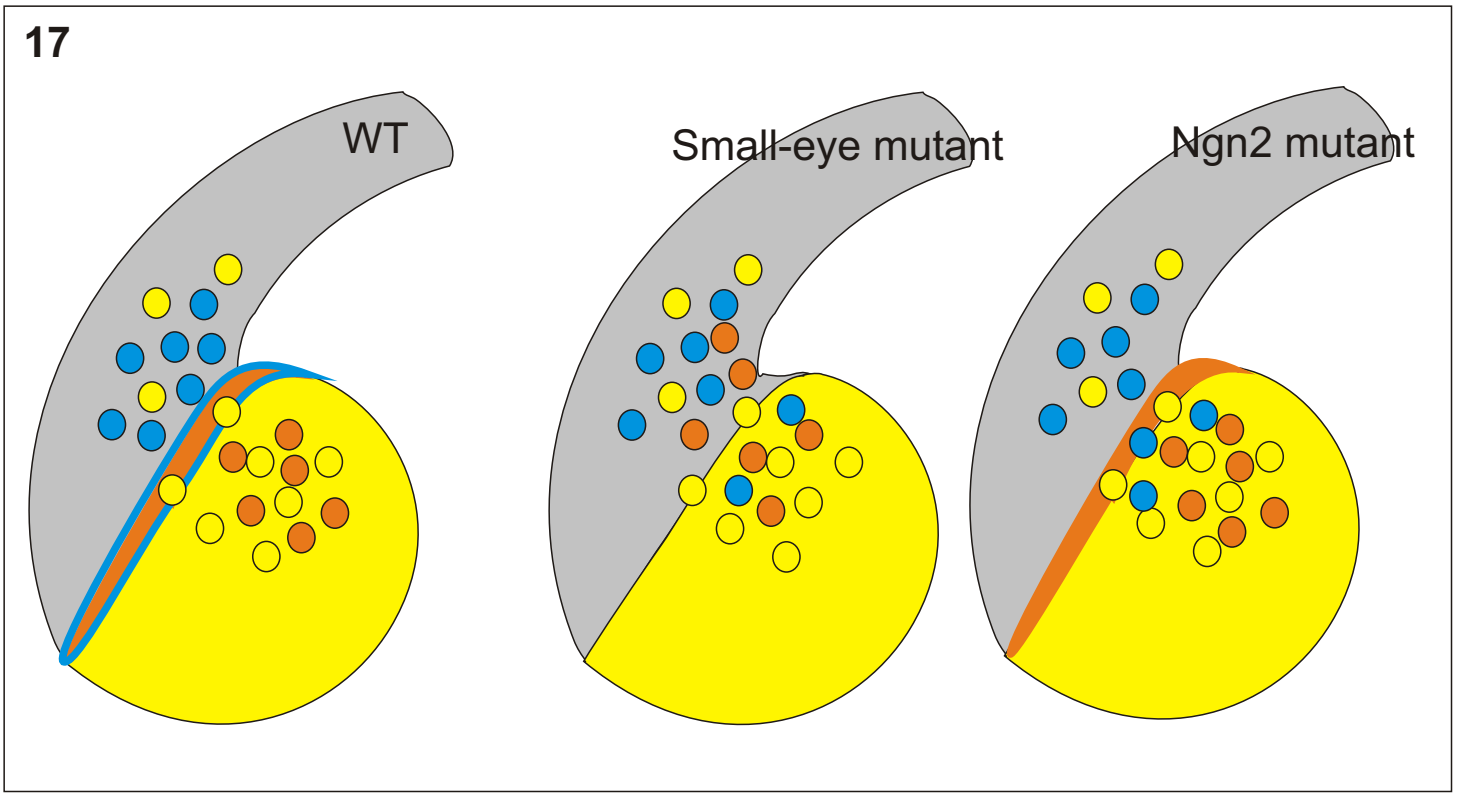

Figure 17: Model summarizing the results of this study
Schematic representation of a section of the embryonic telencephalon, with the cortex in gray, the GE in yellow, the boundary in blue and orange and the three cell populations encountered at the boundary. In WT, cortical cells (blue) recognize a stop signal in the boundary (blue) and remain in the cortex. A population of GE cells (orange) recognizes a different stop signal in the boundary (orange) and remains in the GE. Another GE cell population (yellow) is driven into boundary directions, where a permissive signal (or the absence of a stop signal) allows their migration into the cortex. In the Small-eye mutant, both inhibitory signals are lacking, provoking an increased migration in both directions across the boundary. In the Ngn2 mutant, only the signal restricting cortical cells is lacking.

DISCUSSION

The present study has revealed several characteristics of the complex mechanism driving delineation of cortex and GE during the embryonic development, the most striking feature being the asymmetry of migration across the cortico-striatal boundary. This asymmetry seems to be unique for the cortico-striatal boundary, as in almost all other developmental boundaries, cells have been shown to reduce their intermingling equally on both sides of the boundary. In contrast, the mechanisms acting at the cortico-striatal boundary allow a strong restriction of migration for cells coming from the cortex, opposed to a low level of restriction of cells coming from the GE. This asymmetry is also reflected in the distances of migration: while the few cells coming from the cortex migrate short distances into the GE, cells coming from the GE migrate far into the cortex. Previous data had left open the possibility that postmitotic neurons from both regions might be able to cross the cortico-striatal boundary, whereas precursor cells from both regions would be restrained from crossing into the adjacent territory (Lumsden and Gulisano, 1997). The results of this work now demonstrate a true asymmetry in the behavior of cortical and GE cells. The GFP-adenovirus labels both neurons and precursor cells. Since hardly any GFP-labeled cells migrated from the cortex into the GE, all cortical cells, both neurons and precursor cells, are restricted in their migration across the cortico-striatal boundary.

Which are the molecular mechanisms enabling the asymmetry of permeability across the cortico-striatal boundary?

The two mouse mutants we have studied have revealed that the transcription factors *Pax6* and *Ngn2* expressed in the cortex have a ditinct function in the restriction of migration at the boundary. While in the *Ngn2* mutant only the restriction of cortical cells was impaired, the absence of *Pax6* impaired the restriction of cells coming from both sides of the boundary. Both sets of data allowed us to shed light on the molecular mechanisms that could play a role in this asymmetrical migration.

Theoretically, in order to achieve different degrees of restriction on both sides of a boundary, two mechanisms would be possible:

First, the same molecular cue(s) could induce different responses from the two groups of cells. This signal could be an attractive or repulsive molecule, located in the appropriate position, driving the cells from ventral to dorsal territories, or it could be a

stop signal in the boundary, for which the two neighboring populations would carry different receptors. In this case, an alteration of the signal would affect both populations equally. This is the case for the *Pax6* mutant, but not for the *Ngn2* mutant.

Alternatively, the two cell populations could respond to distinct signals in the boundary. This model is consistent with the situation found in the *Ngn2* mutant where the migration of cortical cells is affected in a non-cell-autonomous manner, whereas the migration of GE cells is unaffected. There, only the signal for cortical restriction would be affected. In the Small-eye mutant, according to this model, both signals would be altered. Thus, a mechanism involving distinct molecular cues that regulates the migration on each side of the boundary is more likely.

The results we obtained in wild type and in the two mutant mice allow us to define candidate molecules that could regulate the migration on each side of the boundary.

Signal(s) regulating the restriction of cortical cells:

The mechanism preventing cortical cells from crossing the boundary has revealed a non-cell-autonomous character in several experiments. In the absence of *Ngn2*, the defect leading to an increased migration of cortical cells across the boundary was located in the substrate, as WT cortical cells were also able to cross the mutant boundary. Moreover, we could show that an alteration within the mutant cortical cells, their up-regulation of the ventral gene *Mash1* was not the cause for their abnormal migration into the GE. Indeed, removing *Mash1* did not rescue this phenotype, as the ectopically located cortical cells in the GE were still present in the *Mash1-Ngn2* double mutant. Heterotypic transplants in wild type slices have also suggested a cell non-autonomous component in the restriction of cortical cell migration, as cortical cells placed onto the GE were less restricted to cross the boundary than when they were placed onto the cortex (they crossed the boundary 4.5 times more). Thus, one signal responsible for the restricted cortical cell migration is not inherent to the cortical cells but is located in the environment. Neyt et al. (1997) have also suggested a non-cell-autonomous mechanism, involving the presence of a short-range signal in the boundary region that would hinder cortical cells from approaching this territory.

However, a substrate bound signal is probably not the only cue that restricts cortical cell migration within the cortex. In transplantation experiments we have also found that a cell-autonomous component should play a role in the restriction of cortical cells.

Indeed, cortical cells recognize a stop signal at the boundary that is not recognized by GE cells placed onto the cortex. In the opposite direction, cortical cells also recognize to a weaker degree a stop signal that is not recognized by GE cells.

A possible mechanism consistent with these results would be that a repressive signal in the boundary (the non-cell-autonomous component) would be specifically recognized by a receptor on cortical cells, which would provide the cell autonomous component. There could also be a signal within the cortex that would promote the affinity of cortical cells, keeping them together.

Another clue that we have about the nature of the restricting signals for cortex cells at the boundary comes from the comparison between the Small-eye and the *Ngn2* mutant. We know that the signal regulating the restriction of cortical cells should be altered in both mutants, as the cortical cell migration was increased in both mutants, and *Pax6* regulates the expression of *Ngn2* (Stoykova et al., 2000, Scardigli et al., 2000). In the Small-eye mutant, the increase of cells entering the GE was low compared to the increase of migration in the opposite direction. However the cortical cell migration was enhanced to a similar degree to that in the *Ngn2* mutant. Moreover, we have also found the presence of many X-gal positive ectopic cells in the GE of the *Pax6* ^{LacZ} knock-in mouse (data not shown), which ascertain the increase of migration from the cortex to the GE in the absence of *Pax6*.

As the cortex restricting cues should be changed in both the Small-eye and the *Ngn2* mutant, we have looked at the expression pattern of diverse molecules playing roles in cell migration and cell segregation at boundaries. One common defect in *Sey/Sey* and in *Ngn2* mutant was related to the Wnt signaling pathway: in the *Ngn2* mutant, the expression territory of Sfrp2 in the boundary was enlarged into the cortex, suggesting that cortical cells lack Wnt signaling, whereas Wnt is normally inhibited only within the boundary. In *Sey/Sey*, both Wnt7b and Sfrp2 were absent from the cortex and boundary, respectively (also in Kim et al., 2000), also suggesting a decrease of Wnt signaling in cortical cells. Thus, the Wnt signaling pathway is disturbed in both mutants and could be a factor normally acting at the cortico-striatal boundary in restricting cortical cell migration. As Wnt7b is a secreted molecule, it would provide the non-cell-autonomous mechanism to restrict cortical cells. Also in other boundaries, Wnt signaling plays a role in the delineation of adjacent regions. At the mid-hindbrain boundary Wnt1 is expressed in the midbrain in a stripe of cells aligning the border to

the hindbrain. It has been shown by Bally-cuif et al. (1995) to have a function in delineating the Otx2 positive cells of the midbrain. The Swaying mutant, where Wnt1 is non-functional, reveals clusters of Otx2 positive cells on the hindbrain side of the boundary, within a normally Otx2 negative territory. However, the authors have proposed that the presence of ectopic Otx2 positive cells in the hindbrain was caused by a lack of Otx2 down-regulation in the cells crossing the boundary, rather than by an increased migration across the mid-hindbrain boundary. An exact mechanism, involving directly Wnt signaling in the segregation of cells is not known.

Other molecules revealing an altered expression in both mutants could exist but have not been tested so far. Inoue et al. (2001) have proposed that the R-cadherin expression in the cortex opposed to the Cadherin6 expression in the GE would promote the cell segregation from both regions. However this study concerned earlier stages of development (E11). Moreover we found in the *Ngn2* mutant that the expression of R-cadherin was maintained (data not shown).

Signal(s) regulating migration and restriction of GE cells across the boundary

We have found that many cells from the GE migrate into the cortex. These cells entering the cortex have been shown to give rise to a population of gabaergic cells (Tamamaki et al.,1997, Anderson et al. 1997 and 2001, Wichterle et al.,1999; Pleasure et al., 2000) and to oligodendrocytes (He et al.,2001). However, not all GE cells are able to cross the boundary, some are still restricted within the GE, as shown by the trough around the boundary in the distribution of migrating cells. The increase in migration and the increase of GABA, calbindin and calretinin positive cells in the Small-eye mutant cortex support this conclusion. Thus, a certain population of cells in the GE is prevented from crossing the boundary, as it is the case for almost all cells at other boundaries. GE cells may thus respond to distinct signals, some of which promote their migration into the cortex and some of which prevent them from crossing the boundary. These contrary signals are probably detected by distinct groups of cells, fated to give rise to one or the other population. Marin et al (2001) have shown for example that within the gabaergic interneurons migrating from the medial ganglionic eminence, the expression of the transmembrane receptor Neuropilin in a subpopulation makes the cells avoid the lateral ganglionic eminence where the ligand semaphorin is expressed, and instead populate the cortex. Cells that do not express Neuropilin remain in the lateral ganglionic eminence. Our study in wild type and in the *Pax6* mutant revealed

several clues about the signals enabling both permeability and impermeability to GE cells.

Considering the capacity of GE cells to cross the boundary, several signals have been suggested to drive the migration of GE cells into the cortex. As mentioned above, Marin et al. have suggested that the repulsive molecule semaphorin in the GE forces the cells expressing Neuropilin to continue their migration into the cortex. Rao et al. (1999) have proposed that the repulsive secreted molecule Slit, expressed in the ventricular zone, directs migration of cells towards the boundary. The hepatocyte growth factor (HGF), expressed as well in the ventricular zone, has also been suggested to promote the migration of cells from the GE into the cortex (Powell et al., 2001). Our results rather suggest a migration of GE cells across the boundary driven by a cell autonomous mechanism, independently of directional cues. Indeed, transplantions in wild type show that the side of the boundary on which GE cells are placed does not make a major difference in the amount of cells that cross the boundary. Thus, repulsive molecules in the GE cannot be the only cue allowing GE cells to cross the boundary. There must be also an inherent property of the GE cells allowing them to migrate across the boundary. This is consistent with the observations of Wichterle et al. (1999) showing that LGE and MGE cells have a strong capacity to migrate, as compared to cortical cells.

On the other hand, we have shown that some GE cells encounter a barrier of migration at the boundary, and we have to consider which signal(s) mediate this restriction. The study of the two mutants allows two conclusions. First, the increased migration from the GE into the cortex in the Small-eye mutant implies that a signal in the boundary and/ or in the cortex promotes this restriction. *Pax6* being normally expressed in the cortex and in the boundary, most of the defects are located in this region in the Small-eye mutant, and the increase in GE cell migration is likely to be promoted by a defect there. Second, in the *Ngn2* mutant, the migration of GE cells was not affected. Thus, the signal responsible for GE cell restriction should be altered in the *Pax6* mutant and unchanged in the *Ngn2* mutant. We found several molecules which expression pattern was changed in the Small-eye mutant. The repellent molecule Slit2, which is normally expressed in the boundary and the cortex was missing in the Small-eye. The same was true for the ephrinB2 repellent molecule in the lateral part of the cortex. Ephrins and Eph receptors are known to mediate segregation of cells for example at rhombomere boundaries (Mellitzer et al., 1999). These two molecules are thus good candidates for the restriction of a subpopulation of GE cells at the boundary. The mechanism involving these molecules would cause GE cells expressing Robo, the receptor for Slit, or cells

expressing an Eph receptor for the ephrin B2 ligand to remain on their own side of the boundary. Furthermore, several other alterations in the Small-eye mutant could account for the increased migration of GE cells. The radial glia fascicle is missing, whereas it is only loosened in the *Ngn2* mutant. The cell adhesion molecule R-cadherin, expressed under the direct control of *Pax6*, is missing in the entire *Sey/Sey* cortex and in the boundary (Stoykova et al., 1997). Cadherins are known to mediate selective adhesion of cells. The expression of R-cadherin in the cortex, contiguous to cadherin6 in the GE has been indeed suggested to promote the restricted intermingling of cells at the boundary at earlier stages of development (E11; Inoue et al., 2001), and short-term aggregation assays have revealed a role for calcium-dependent adhesion molecules in the segregation of cortical cells from GE cells (Götz et al., 1996). A further defect in *Sey/Sey* concerns the expression of the extracellular matrix glycoprotein Reelin, known as a stop signal for the radial migration of cortical cells. This molecule is also expressed in the small GE territory lining the boundary, but is missing in this territory in *Sey/Sey*. The absence of reelin there could lead to the increased migration into the cortex. Thus, all these molecules altered in the Small-eye mutant cortex are likely to cause the restriction of migration of GE cells into the cortex.

A model summarizing these findings would propose that three different populations of cells meet at the cortico-striatal boundary (see Fig.17).

1- The cortical cell population encounters a stop signal within the boundary, which is not recognized by GE cells. The transition from a Wnt signaling territory to a territory without Wnt may play a role in this stop signal.

2- One population of GE cells has the capacity to cross the boundary and enters the cortex. This migration would be helped by repellent activities of the GE (mediated by Slit (Zhu et al., 1999), Semaphorin (Marin et al., 2000), HGF (Powell et al., 2000)) Repellent activity would be necessary because of the lack of other known substrate of migration, like radial glial cells in the cortex.

3- A second GE cell population expresses receptors for stop signals located in the boundary and/or in the cortex (which could be Slit2, ephrinB2, or reelin). These cells do not enter into the cortex.

<u>Change of fate of cells crossing the boundary</u>

Restriction of cell migration is a common mechanism that achieves the proper delineation of adjacent regions. However, when restriction is not observed, another mechanism allowing this delineation is a switch of fate when a cell enters into the

adjacent region, called the community effect (Gurdon, 1988). At the mid-hindbrain boundary for example, cells migrating into the neighboring region change their fate rapidly (Jungbluth et al., 2001, Bally-Cuif et al., 1995).

At the cortico-striatal boundary, change of fate seems to be different depending on the side of origin of the cells. Cells from the GE entering the cortex retain their identity (they express *Dlx*, *Lhx*6, Gaba, calbindin; Lavdas et al., 1999, Anderson et al, 1997, 2001), even over long distances of migration, like the cells that migrate to the hippocampus (Pleasure et al., 2000). In contrast we have shown that in the *Ngn2* mutant, cortical cells migrating across the boundary gradually acquired the fate of GE cells. Cells that were very close to the boundary still contained some mRNA for *Pax6* and R-cadherin but they lost this expression when they entered further into the GE, and started to express genes specific for the GE, such as *Dlx*5. In WT mice, there is a very low level of cell migration existing from the cortex into the GE, as revealed by the adenovirus injection experiments (see table 1 and 6). This leakage is reminiscent to the leakage of cells at the rhombomere boundaries (Birgbauer and Fraser, 1994). There, a mechanism involving signaling through ephrin ligands and Eph receptors promotes a change of fate when cells enter into the neighboring rhombomere (Xu et al., 1995). The cortical cells leaking into the GE probably also change their phenotype, as they do in the *Ngn2* mutant. Hamasaki et al. (2001) have also detected a population of cells that migrate from the piriform cortex (the ventro lateral part of the cortex) into the GE, and they have found that these cells undergo apoptosis after their migration across the boundary.

Thus, not only do the cells respond to a distinct permeability on each side of the cortico-striatal boundary, but also they behave differently when they enter the adjacent region. The few cortical cells entering the GE do not migrate far and seem to adopt the phenotype of GE cells, or disappear by apoptosis. On the other side of the boundary, GE cells entering the cortex migrate long distances and retain their phenotype. Overall, there seems to be a general dominance of the ventral side of the cortico-striatal boundary over the dorsal side. This dominance is also reflected by the alterations observed in mutants: when dorsal genes are mutated, the dorsal territory acquires a ventral fate (i.e. in the *Pax6* mutant and the *Ngn2* mutant), while in mutants for ventral genes (i.e. *Mash1*, *Dlx*1 and-2) no expression of dorsal genes in the ventral territory has been reported.

Hence, the boundary delineating the cortex and the GE is endowed with several very distinctive properties that are not found in the other studied developmental boundaries. The phylogenetically recent neocortex juxtaposed to the phylogenetically older structure of the basal ganglia may explain the unique properties found at the cortico-striatal boundary.

ACKNOLEDGMENTS

I would like to thank
first and mostly
Magdalena Götz, for the four years I spent in her lab, for everything I learned during this time, for the confidence she gave me, for our publications,
and especially for her amazing enthusiasm and vitality that made the work
a pleasure.

I would also like to thank all the other members of the lab,
Helga Zepter,
Mucella Öcalan, Eva
Hartfuss,
Nico Heins, Paolo Malatesta,
Julia von Frowein, Nicole Haubst,
Parvin Ghahraman and Michael Hack,
for being always ready to help, and being a joyful group.

I have a special thank you to
Volker Staiger,
who filled many cells with Neurobiotin and was always there to solve technical problems at the microscope.

Thank you also to Annette Gärtner who introduced me in the art of adenovirus construction, to Lothar Lindeman for showing me the cloning of in situ probes, and to Simona Casarosa in the Lab of François Guillemot who taught me the technique of in situ hybridization. For reading and correcting this manuscript, thank you to Martin Pool and Albrecht Kossel.

Finally, I am grateful to all the mice that contributed to this work.

REFERENCES

Altabef, M., Logan, C., Tickle, C and Lumsden, A. (2000). *Engrailed-1* Misexpression in Chick Embryos Prevents Apical Ridge Formation but Preserves Segregation of Dorsal and Ventral Ectodermal Compartments. *Dev. Biol*. **222**, 307-316.

Anderson, S.A., Marín, O., Horn, C., Jennings, K. and Rubenstein, J.L.R. (2001). Distinct cortical migrations from the medial and lateral ganglionic eminences. *Development* **128**, 353-363.

Anderson, S. A., Eisenstat, D. D., Shi, L. and Rubenstein, J. L. R. (1997). Interneuron migration from basal forebrain to neocortex: dependence on *Dlx* genes. *Science* **278**, 474-476.

Angevine, J.B. and Sidman, R.L. (1961). Autoradiographic study of cell migration during histogenesis of cerebral cortex in the mouse. *Nature* **192**, 766-768.

Bally-Cuif, L., Cholley, B.and Wassef, M. (1995). Involvment of Wnt1 in the formation of the mes/metencephalic boundary. *Mech. dev*. **53**, 23-34.

Barrantes, ID., Elia, AJ., Wunsch, K., De Angelis, MH., Mak, TW., Rossant, J., Conlon, RA., Gossler, A.and de la Pompa, JL. (1999). Interaction between Notch signalling and Lunatic fringe during somite boundary formation in the mouse. Curr. Biol. **9**, 470-480.

Bartholomä, A. and Nave, K.-A. (1994). NEX-1: A novel brain specific helix-loop-helix protein with autoregulation and sustained expression in mature cortical neurons. *Mech. Dev.* **48**, 217-228.

Birgbauer, E. and Fraser, S.E. (1994). Violation of cell lineage restriction compartments in the chick hindbrain. *Development* **120**, 1347-1356.

Bittman, K., Owens, D.F., Kriegstein, A.R. and LoTurco, J.J. (1997): Cell coupling and uncoupling in the ventricular zone of developing neocortex. *J. Neurosci*. (**18**): 7037-7044.

Blanton, M.G., LoTurco, J.J. and Kriegstein, A.R. (1989): Whole cell recording from neurons in slices of reptilian and mammalian cerebral cortex. *J Neurosci. Methods* (**30**) 203-210.

Blennerhasset, M.G. and Caveney, S. (1984). Separation of developmental compartments by a cell type with reduced junctional permeability. *Nature* **309**, 361-364.

Bulfone, A., Puelles, L., Porteus, M. H., Frohman, M. A., Martin, G. R. and Rubenstein, J. L. (1993). Spatially restricted expression of *Dlx*-1, *Dlx*-2 (Tes-1), Gbx-2, and Wnt-3 in the embryonic day 12.5 mouse forebrain defines potential transverse and longitudinal segmental boundaries. *Journal of Neuroscience* **13**, 3155-3172.

Bruckner, K., Perez, L., Clausen, H. and Cohen, S. (2000). Glycosyltransferase activity of Fringe modulates Notch-Delta interactions. *Nature* **406**, 411-415.

Caric, D., Gooday, D., Hill, R. E., McConnell, S. K. and Price, D. J. (1997). Determination of the migratory capacity of embryonic cortical cells lacking the transcription factor Pax-6. *Development* **124**, 5087-5096.

Casarosa, S., Fode, C. and Guillemot, F. (1999). *Mash1* regulates neurogenesis in the ventral telencephalon. *Development* **126**, 525-534.

Cau, E., Gradwohl, G., Fode, C. and Guillemot, F. (1997). *Mash*1 activates a cascade of bHLH regulators in olfactory neuron progenitors. *Development* **124**, 1611-1621.

Cooper, J. A. (1987). Effects of cytochalasin and phalloidin on actin. *J. Cell Biol.* **105**, 1473-1478.

Dahmann, C. and Basler, K. (2000). Opposing Transcriptional Outputs of Hedgehog Signaling and Engrailed Control Compartmental Cell Sorting at the *Drosophila* A/P Boundary. *Cell* **100**, 411-422.

DeCarlos, J. A., López-Mascaraque, L. and Valverde, F. (1996). Dynamics of cell migration from the lateral ganglionic eminence in the rat. *J. Neurosci.* **16**, 6146-6156.

DeDiego, I, Smith-Fernández, A. and Fairén, A. (1994). Cortical cells that migrate beyond area boundaries: characterization of an early neuronal population in the lower intermediate zone of prenatal rats. *Eur. J. Neurosci*. **6**, 983-997.

Durbin, L., Sordino, P., Barrios, A,. Gering, M., Thisse, C., Thisse, B., Brennan, C., Green, A., Wilson, S. and Holder, N. Anteroposterior patterning is required within segments for somite boundary formation in developing zebrafish. *Development* **127**(8),1703-1713.

Edwards, M.A., Yamamoto, M. and Caviness, V.S. Jr. (1990). Organisation of radial glia and related cells in the developing murine CNS. An analysis based upon a new monoclonal antibody marker. *Neuroscience* **36**, 121-144.

Figdor, M. C. and Stern, C. D. (1993). Segmental organisation of embryonic diencephalon. *Nature* **363**, 630-634.

Fishell, G., Mason, C. A. and Hatten, M. E. (1993) Dispersion of neural progenitors within the germinal zones of the forebrain. *Nature* **362**, 636-638.

Fode, C., Ma, Q., Casarosa, S., Ang, S.-L., Anderson, D.J. and Guillemot, F. (2000). A role for neural determination genes in specifying the dorsoventral identity of telencepalic neurons. *Genes & Dev.* **14**, 67-80.

Gerfen, C.R. (1992) The neostriatal mosaic: multiple levels of compartmental organization in the basal ganglia. *Annu. Rev. Neurosci***. 15,** 295-320.

Götz, M., Wizenmann, A., Reinhard, S., Lumsden, A. and Price, J. (1996). Selective adhesion of cells from different telencephalic regions. *Neuron* **16**, 551-564.

Götz, M., Stoykova, A. and Gruss, P. (1998). *Pax6* controls radial glia differentiation in the cerebral cortex. *Neuron* **21**, 1031-1044.

Gradwohl, G., Fode, C. and Guillemot, F. (1996). Restricted expression of a novel murine atonal-related bHLH protein in indifferentiated neural precursors. *Dev. Biol.* **180**, 227-241.

Graham, F. L. and Prevec, L. (1991). Manipulation of adenovirus vectors. In *Methods in Molecular Biology, Vol. 7: Gene Transfer and Expression Protocols* (ed. E. J. Murray), pp. 109-126. The Humana Press Inc., Clifton, NJ.

Gurdon, J.B. (1988). A community effect in animal development. *Nature* **336**, 772-774.

Guthrie, S., Butcher, M. and Lumsden,A. (1991). Petterns of cell division and interkinetic nuclear migration in the chick embryo hindbrain. *J. Neurobiol*. **22**, 742-754.

Hamasaki, T., Goto, S., Nishikawa, S. and Ushio, Y. (2001). Early-generated preplate neurons in the developing telencephalon: Inward migration into the developing striatum. *Cerebral Cortex* **11**, 474-484.

Harada, A et al., 1994. Altered microtubule organization in small calibre axons of mice lacking Tau protein. *Nature* **369**, 488-491.

Hartfuss, E., Galli, R., Heins, N. and Götz, M. (2001). Characterization of CNS precursor types and radial glia. *Dev. Biol*. **229**, 15-30.

He, W.L., Ingraham, C, rising, L., Goderie, S and Temple, S. (2001). Multipotent stem cells from the mouse basal forebrain contribute GABA ergic neurons and oligodendrocytes to the cerebral cortex during embryogenesis. *J. Neurosci*. **21**, 8854-8862.

Hill, R. E., Favor, J., Hogan, B. L. M., Ton, C. C. T., Saunders, G. F., Hanson, I. M., Prosser, J., Jordan, T., Hastie, N. D. and van Heyningen, V. (1991). Mouse *Small eye* results from mutations in a paired-like homeobox-containing gene. *Nature* **354**, 522-525.

Houzelstein, D. and Tajbakhsh, S. (1999). Increased *in situ* hybridization sensitivity using non-radioactive probes after staining for ß-galactosidase activity. *Techn. Tips Online*, 1999, **1**:*57*:T01600

Inoue, T., Tanaka, T., Takeichi, M., Chisaka, O., Nakamura, S. and Osumi, N. (2001). Role of cadherins in maintaining the compartment boundary between the cortex and striatum during development. *Development* **128**, 561-569.

Johnston S.H., Rauskolb, C., Wilson, R., Pabhakaran, B., Irvine K.D. Vogt T.H. (1997). A family of mammalian Fringe genes implicated in boundary determination and the Notch pathway. *Dev* **124,** 2245-2254.

Jungbluth, S., Larsen, C., Wizenmann, A. and Lumsden, A. (2001). Cell mixing between the embryonic midbrain and hindbrain. *Curr. Biol.* **11**, 204-207.

Kawano, H., Fukuda, T., Kubo, K., Horie, M., Uyemura, K., Takeuchi, K., Osumi, N., Eto, K. and Kawamura, K. (1999). *Pax6* is required for thalamocortical pathway formation in fetal rats. *JCN* **408**, 147-160.

Kim, SH., Jen, W., De Robertis, EM. and Kintner, C. (2000). The protocadherin PAPC establishes segmental boundaries during somitogenesis in Xenopus embryos. *Curr. Biol*. **10**(14), 821-830

Kim, A.S., Anderson, S.A., Rubenstein, J.L., Lowenstein, D.H. and Pleasure, S.J. (2001). Pax-6 regulates expression of SFRP-2 and Wnt-7b in the developing CNS. *J. Neurosci.* **21**, RC132.

Kimmel, R.A., Turnbull, D.H., Blanquet, V., Wurst, W., Loomis, C.A. and Joyner, A.L. (2000). Two lineage boundaries coordinate vertebrate apical ectodermal ridge formation. *Genes and dev*. **14**, 1377-1389.

Laird, P.W., Zijderveld, A., Linders, K., Rudnicki, M.A., Jaenisch, R. and Berns, A. (1991). Simplified mammalian DNA isolation procedure. *Nucleic Acids Res. 19*, 4293.

Lavdas, A.A., Grigoriou, M., Pachnis, V. and Parnavelas, J.G. (1999). The medial ganglionic eminence gives rise to a population of early neurons in the developing cerebral cortex. *J. Neurosci.* **19**, 7881-7888.

Laufer E., Dahn, R., Orozco, O., Yeo, C. Y., Pisenti, J., Henrique, D., Aqbbott, U. K., Fallon, J. F. and Tabin, C. (1997). Expression of radical fringe in Limb-bud ectoderm regulates apical ectodermal ridge formation. *Nature* **386** 366-373.

LoTurco J.J., and Kriegstein A.R. (1991). Clusters of coupled neuroblasts in embryonic neocortex. *Science* **252**, 563-566.

Lumsden, A. and Gulisano, M. (1997). Neocortical neurons: where do they come from? *Science* **278,** 402-404.

Ma, Q., Sommer, L., Cjerjesi, P. and Anderson, D.J. (1997). *Mash*1 and neurogenin1 expression patterns define complementary domains of neuroepithelium in the developing CNS and are correlated with regions expressing Notch ligands. *J. Neurosci.* **17**, 3644-3652.

Malatsesta, P., Hartfuss, E.and Götz, M (2000). Isolation of radial glial cells by fluorescence activated cell sorting reveals a neuronal lineage. *Development* **127**, 5253-5263.

Marin, O., Yaron, A., Bagri, A., Tessier-Lavigne, M. and Rubinstein, J.L.R. (2001). Sorting of striatal and cortical interneurons regulated by Semaphorin- Neuropilin interactions. *Science* **293**, 872-875.

Martinez, S., Geijo, E., Sanchez-Vives, M.V., Puelles, L. and Gallego, R. (1992): Reduced junctional permeability at interrhombomeric boundaries. *Dev*. **116,** 1069-1076.

Mellitzer, G., Xu, Q. and Wilkinson, D.G. (1999). Eph receptors and ephrins restrict cell intermingling and communication. *Nature* **400**, 77-81.

Milan M., Weihe, U., Perez, L. and Cohen, SM. (2001). The LRR proteins Capricious and Tartan mediate cell interactions during DV boundary formation in the drosophila wing. *Cell* **106**, 785-794.

Moloney, D.J., Panin, V.M., Johnston, S.H., Chen, J. Shao, L., Wilson, R., Wang, Y., Stanley, R., Irvine, K.D., Haltiwanger, R.S. and Vogt, T.F.(2000). Fringe is a glycosyltransferase that modifies Notch. *Nature* **386**, 369-375.

Nadarajah, B., Jones, E.M., Ewans, W.A. and Parnavelas, J.G. (1997). Differential expression of connexins during nocortical development and neuronal circuit formation. *J. Neurosci.* **17**, 3096-3111.

Neyt, C., Welch, M., Langston, A., Kohtz, J. and Fishell, G. (1997). A short-range signal restricts cell movement between telencephalic proliferative zones. *J. Neurosci.* **17**, 9194-9203.

Nieto, M., Schuurmans, C., Britz, O. and Guillemot, F. (2001). Neural bHLH genes control the neuronal versus glial fate decision in cortical progenitors. *Neuron* **29**, 401-413.

Nittenberg, R., Patel, K., Joshi, Y., Krumlauf, R., Wilkinson, D. G., Brickell, P. M., Tickle, C. and Clarke, J. D. W. (1997). Cell movements, neuronal organisation and gene expression in hindbrains lacking morphological boundaries. *Development* **124**, 2297-2306.

Okabe, M., Ikawa, M., Kominami, K., Nakanishi, T. and Nishimune, Y. (1997). 'Green mice' as a source of ubiquitous green cells. *FEBS Letters* **407**, 313-319.

Olsson, M., Campbell, K., Wictorin, K. and Björklund, A. (1995). Projection neurons in fetal striatal transplants are predominantly derived from the lateral ganglionic eminence. *Neurosci.* **69**, 1169-1182.

O'Rourke, N. A, Dailey, M.E., Smith S.J. and McConnel, S.K. (1992). Diverse migratory pathways in the developing cerebral cortex. *Science* **258**, 299-302.

O'Rourke, N. A., Chenn, A. and McConnell, S. K. (1997). Postmitotic neurons migrate tangentially in the cortical ventricular zone. *Development* **124**, 997-1005.

Owens, D.F. and Kriegstein, A.R. (1998). Patterns of intracellular calcium fluctuation in precursor cells of the neocortical ventricular zone. *J. Neurosci*. **18**, 5374-5388.

Panin, V.M., Papayannopoulos, V., Wilson, R. and Irvine K.D. (1997). Fringe modulates Notch-ligands interactions. *Nature* **387**, 908-912.

Peters, A. and Jones, E.G. (1984). Classification of cortical neurons. *Cerebr. Cortex* **1,** 107-121.

Pinto-Lord, M.C., Evrard, P. and Caviness, V.S. (1982). Obstructed neuronal migration along radial glial fibers in the neocortex of the reeler mouse: a Golgi-EM analysis. *Dev. Brain Res.* **4**, 379-393.

Pleasure, S.J., Anderson, S., Hevner, R., Bagri, A., Marin, O., Lowenstein, D.H. and Rubenstein, J.L.R. (2001). Cell migration from the ganglionic eminences is required for the development of hippocampal GABAergic interneurons. *Neuron* **28**, 727-740.

Powell, E.M., Mars, W.M. and Levitt, P. (2001). Hepatocyte growth factor/scatter factor is a motogen for interneurons migrating from the ventral to dorsal telencephalon. *Neuron* **30**, 79-89.

Rauskolb, C., Correia, T and Irvine, K.D. (1999). Fringe dependent separation of dorsal and ventral cells in the drosophila wing. *Nature*, **401**, 476-480.

Rhinn, M. and Brand, M. (2001). The midbrain-hindbrain boundary organizer. *Curr. Opin. Neurobio*l. **11**, 34–42.

Rodriguez-Esteban, C., Schwabe, J.W.R., De La Pena, J., Foys, B., Eshelman, B., and Belmonte, I.J.C. (1997). *Radical Fringe* positions the apical ectodermal ridge at the dorsoventral boundary of the vertebrate limb. *Nature* **386,** 360–366.

Scardigli, R., Schuurmans, C., Gradwohl, G. and Guillemot, F. (2001). Crossregulation between Neurogenin2 and pathways specifying neuronal identity in the spinal cord. *Neuron* **31**, 203-217.

Stoykova, A., Fritsch, R., Walther, C. and Gruss, P. (1996). Forebrain patterning defects in *Small eye* mutant mice. *Development* **122**, 3453-3465.

Stoykova, A., Götz, M., Gruss, P. and Price, J. (1997). *Pax6*-dependent regulation of adhesive patterning, *R-cadherin* expression and boundary formation in developing forebrain. *Development* **124**, 3765-3777.

Stoykova, A., Treichel, D., Hallonet, M. and Gruss, P. (2000). *Pax6* modulates the dorso-ventral patterning of the telencephalon. *J.Neurosci.* **20**, 8024-8050.

Stühmer, T., Puelles, L., Ekker, M. and Rubenstein, J.L.R. (2002). Expression from a *Dlx* gene enhancer marks adult mouse cortical gabaergic neurons. *Cereb. Cortex* **12**: 75-85.

Sussel, L., Marin, O., Kimura, S. and Rubenstein, J.L.R. (1999). Loss of Nkx2.1 homeobox gene function results in ventral to dorsal molecular respecification within the basal telencephalon: evidence for a transformation of the pallidum into the striatum. *Development* **126**, 3359-3370.

Takahashi, Y., Koizumi, K.I., Takagi, A., Kitajima, S., Inoue, T., Koseki, H. and Saga, Y. (2000). Mesp2 initiates somites segmentation through the Notch signalling pathway. *Nature genet*. **25**, 390-396

Tamamaki, N., Fujimori, K.E. and Takauji, R. (1997). Origin and route of tangentially migrating neurons in the developing neocortical intermediate zone. *J. Neurosci.* **17,** 8313-8323.

Theil, T., Frain, M., Gilardihebenstreit, P., Flenniken, A., Charnay, P. and Wilkinson, D.G. (1998). Segmental expression of the EphA4 (Sek1) receptor tyrosine kinase in the hindbrain is under direct transcriptional control of Krox20. *Dev*. **125**, 443-452.

Toresson, H., Potter, S.S. and Campbell, K. (2000). Genetic control of dorsal-ventral identity in the telencephalon: opposing roles for *Pax6* and Gsh2. *Development* **127**, 4361-4371.

Tucker, K.L. Meyer M. and Barde Y. A. (2001). Neurotrophins are required for nerve growth during development. *Nature Neurosci*. **4**, 29-37.

Weir, M.P. and Lo, C.W. (1985). An anterior/ posterior communication compartment border in engrailed wing discs: possible implication for drosophola pattern formation. *Dev. Biol* **110**, 84-90.

Wichterle, H., Garcia-Verdugo, J.M., Herrera, D.G. and Alvarez-Buylla, A. (1999). Young neurons from medial ganglionic eminence disperse in adult and embryonic brain. *Nature Neurosci.* **2**, 461-466.

Wurst, W. and Bally-Cuif, L. (2001). Neural plate patterning: upstream and downstream of the isthmic organizer. *Nature Rev. Neurosci.* **2,** 99-108.

Xu, Q., Alldus, G., Holder, N. and Wilkinson, D.G. (1995). Expression of truncated Sek-1 receptor tyrosine kinase disrupts the segmental restriction of gene expression in the Xenopus and zebrafish hindbrain. *Development* **121**, 4005-4016.

Xu, Q. and Wilkinson, D.G. (1997). Eph-related receptors and their ligands: mediators of contact-dependent cell interactions. *J.Mol.Med.* **75**, 576-586.

Xu, Q., Mellitzer, G., Robinson, V. and Wilkinson, D.G. (1999). *In vivo* cell sorting in complementary segmental domains mediated by Eph receptors and ephrins. *Nature* **399**, 267-271.

Zeltser, L.M., Larsen, C.W. and Lumsden, A. (2001). A new compartmental compartment in the forebrain regulated by lunatic fringe. *Nature Neurosci.* **4**, 683-684.

Zhang, N. and Gridley, T. (1998). Defects in somite formation in *lunatic fringe* deficient mice. *Nature* **394**, 374-377.

Zhu, Y., Li, H., Zhou, L., Wu, J.Y. and Rao, Y. (1999). Cellular and molecular guidance of GABAergic neuronal migration from an extracortical origin to the neocortex. *Neuron* **23**, 473-485.

CURRICULUM VITAE

Prisca Chapouton
Born on the 02.06.1972
Paris, France

School

1978-1982 Ecole primaire in Cadenet, Vaucluse
1982-1987 Collège in Cadenet, Vaucluse
1987-1989 Lycee in Pertuis, Vaucluse
Exam: June1989, Baccalaureat serie D (Sciences de la nature)

University

October 1989- June 1991: Faculte des sciences de Luminy, Marseille
Exam: Jume1991, DEUG (Diplome d´Etudes Universitaires Generales) des sciences de la nature et de la vie.

October 1991- December 1996: Freie Universität Berlin, Study of Biochemistry
Exam: Diploma in Biochemistry.
March1996-December1996: Diploma Thesis in the Laboratory of Dr. Fritz G. Rathjen at the Max-Delbrück-Center in Berlin-Buch. "*Biochemische und Zellbiologischen Untersuchungen zum Zelloberflächenmolekül CALEB*"
December1996- March1997: Continuation of the work of the diploma thesis.

September 1997-March 2002: PhD in the laboratory of Dr. Magdalena Götz at the Max-Planck-Institute of Neurobiology in Martinsried: "*Regionalization of the developing mouse telencephalon: cellular and molecular mechanisms*"

Publications

Chapouton, P., Gärtner, A. and Götz, M. (1999). The role of *Pax6* in restricting cell migration between developing cortex and basal ganglia. *Development* **126**, 5569-5579.

Chapouton, P., Schuurmans, C. Guillemot, F. and Götz, M. (2001). The transcription factor Neurogenin2 restricts cell migration from the cortex to the striatum. *Development* **128**, 5149-5159.

Heins, N., Malatesta, P., Cecconi, F., Nakafuku, M., Tucker, K. L., Hack, M.A., Chapouton, P., Barde, Y. and Götz, M. (2002). Glial cells generate neurons: the role of the transcription factor *Pax6*. *Nature Neuroscience* Online publication 18 March, 1-8.